SEMMELWEIS EGYETEM

DOKTORI ISKOLA

Ph.D. értekezések

3503.

SZÉLES ALIZ

Experimentális és klinikai farmakológia

című program

Programvezető: Dr. Szökő Éva, egyetemi tanár

Témavezető: Dr. Monostory Katalin, tudományos főmunkatárs

Konzulens: Dr. Renkecz Tibor, laborvezető

Bioanalytical Challenges in Toxicology:

Innovative Solutions for Bioanalysis of Xenobiotics and Their Metabolites

PhD thesis

Aliz Széles

Pharmaceutical Sciences and Health Technologies Division
Semmelweis University

Supervisor:	Katalin Monostory, DSc
Consultant / Corporate expert:	Tibor Renkecz, PhD
Official reviewers:	Pál Szabó, PhD
	László Tóthfalusi, DSc

Head of the Complex Examination Committee:
Zoltán Benyó, DSc

Members of the Complex Examination Committee:
Krisztina Ludányi, PhD; Blanka Tóth, PhD

Budapest
2026

TABLE OF CONTENTS

LIST OF ABBREVIATIONS

APCI	Atmospheric pressure chemical ionisation
AUC	Area under the curve
C_{max}	Maximum observed plasma concentration
CV	Coefficient of variation
ESI	Electrospray ionisation
hiFBS	Heat inactivated fetal bovine serum
HPLC	High-performance liquid chromatography
HPLC-ECD	HPLC with electrochemical detection
HPLC-FLD	HPLC with fluorescence detection
HPLC-UV	HPLC with ultraviolet detection
ICH	International Council for Harmonisation of Technical Requirements for Pharmaceuticals for Human Use
IPGE	Isopropyl glycidyl ether
IS	Internal standard
K3-EDTA	Ethylenediaminetetraacetic acid tripotassium salt
LC	Liquid chromatography
LLOQ	Lower limit of quantification
MRM	Multiple reaction monitoring
MS	Mass spectrometry
MS/MS	Tandem mass spectrometry
NAPQI	N-acetyl-p-benzoquinone imine
QC	Quality control
SIM	Selected ion monitoring
T_{max}	Time of maximum observed plasma concentration
ULOQ	Upper limit of quantification

1. INTRODUCTION

1.1. Chemical safety

Chemical safety assessment is a systematic process designed to evaluate the potential adverse health effects of substances on humans and other living organisms. (1, 2) It requires accurate information on systemic exposure to understand how different doses influence the toxicity levels of the chemicals of interest. (3) The toxicokinetic profile of these chemicals must be defined to evaluate the risks associated with chemical exposure. (4) Therefore, there is a need for appropriate bioanalytical methods capable of quantifying the compounds in question in biological samples.

1.1.1. The Role of bioanalysis in chemical safety

In a regulated environment (e.g. Good Laboratory Practice), bioanalytical method validation is critical for ensuring reliable results across all calibration ranges and biological sample types. As emphasized in current relevant guidelines, such as the "Bioanalytical Method Validation and Study Sample Analysis M10" issued by the International Council for Harmonisation of Technical Requirements for Pharmaceuticals for Human Use (ICH), accurate quantification can be challenging when dealing with complex biological matrices or unstable drugs with narrow therapeutic indices. (5) Current guidelines mandate the thorough investigation of all critical validation metrics, namely selectivity, specificity, matrix effects, calibration curve range, accuracy, precision, sensitivity, carry-over, dilution integrity, and stability. The need for such validated bioanalytical results arises in the following areas of research: preclinical safety assessments and therapeutic drug monitoring (TDM) for dose optimization and toxicity risk evaluation. (6)

1.2. "There is no royal road … " - *Euclid*

Because chemical entities differ substantially in structure and physicochemical properties, bioanalytical methods must be tailored not only to the analyte but also to the sample matrix. Therefore, there is no royal road to bioanalytical chemistry.

In industrial workplaces, protecting workers is essential; therefore, monitoring the effects of chemicals on humans and assessing bioaccumulation is inevitable. (7) Among

the wide variety of substances workers are exposed to, one of the most commonly used materials is epoxy resin systems. (8) The biomonitoring of specific components, such as reactive diluents like isopropyl glycidyl ether (IPGE), is challenging. (9, 10) These agents possess high reactivity and intrinsic instability, which require specialized derivatisation or stabilization methods to prevent their degradation during analytical investigation.

In clinical practice, it is not only necessary to analyse compounds that are introduced into the body externally (e.g. drugs), but also important to characterise endogenous substances. As the alterations in physiological concentrations of the endogenous substances (such as their unexpected appearance, elevation, or depletion) can reliably signal emerging toxic threats or metabolic imbalances, these compounds are referred to as biomarkers. They can be used to predict certain pathological or physiological processes and disease states before explicit clinical symptoms appear. One representative group among endogenous biomarkers is the group of porphyrins, where one encounters two primary obstacles: these compounds exhibit light sensitivity, and researchers must also work with alternative sample types, such as surrogate matrices.

Externally administered pharmaceuticals also exhibit diverse physicochemical properties which indicates that they have to be measured using different analytical strategies. For example, aminoglycoside antibiotics are monitored because of their potential multi-organ toxicity. (11) These substances lack strong chromophores and possess high polar properties. (12) Therefore, traditional analytical methods based on ultraviolet detection need to be modified or replaced. (13) Analytes that do not have a strong chromophore of their own require derivatization with reagents that introduce a chromophore group – such as aromatic rings, conjugated double bonds, or nitro groups – into the molecule, thereby enabling UV detection.

Due to the above-mentioned difficulties, most researchers in both industrial and clinical settings increasingly rely on liquid chromatography-tandem mass spectrometry (LC-MS/MS). (14) As a multifunctional detector, the mass spectrometer is a selective, specific and highly sensitive instrument. This technology enables the qualitative and quantitative determination of challenging analytes, thereby supporting e.g., pharmacokinetic studies and therapeutic drug monitoring in complex biological matrices. (15)

1.3. Specific challenges and solutions

The following sections will demonstrate bioanalytical method development and validation techniques applied to analytes (Table S 1.) from three different compound categories with diverse chemical and toxicological properties. In addition, a general overview of these classes is provided, including either their therapeutic benefits or toxicological effects, in order to highlight the current need for flexible safety testing methods. Furthermore, analytical solutions are presented which address three common challenges encountered during toxicological studies: insufficient analyte sensitivity, analyte instability and matrix-related issues.

1.3.1. Isopropyl Glycidyl Ether: A representative from the world of industrial chemicals

Glycidyl ethers represent a large family of reactive chemicals widely used in the chemical industry, primarily as reactive diluents in epoxy resin systems to reduce viscosity and improve processing characteristics. (8) In addition to epoxy formulations, they are employed as stabilizers for chlorinated compounds, in the manufacture of surface coatings and adhesives, and for chemically modifying decay resistance of wood products. (16) Isopropyl glycidyl ether, along with related alkyl glycidyl ethers (e.g., allyl, butyl, phenyl glycidyl ethers), contains a rigid oxirane (epoxide) ring structure. (17) The substantially strained ring makes epoxides highly reactive electrophilic species and contributes to their toxic properties. (10)

Toxicological studies have extensively documented the hazards of glycidyl ethers, highlighting the risks associated with occupational exposure through inhalation and dermal contact. These compounds act as direct-acting electrophilic alkylating agents, enabling them to attack nucleophilic sites on cellular macromolecules, including DNA and proteins, inducing mutations and genetic damage. (18) Experimental findings indicate that inhalation exposure can cause respiratory tract irritation and inflammation. (19) Acute toxicity studies in rats have reported an oral LD_{50} value of approximately 4200 mg/kg for IPGE. Studies investigating repeated-dose and subchronic exposure have shown that animals exhibit body weight loss, gastric alterations, and damage to reproductive organs, which leads to impaired fertility. (20)

Metabolically, the detoxification of glycidyl ethers primarily occurs *via* hydrolysis of the epoxide ring mediated by epoxide hydrolases or through conjugation with glutathione. For structurally related alkyl glycidyl ethers, such as *n*-butyl glycidyl ether, urinary

excretion of hydrolytic metabolites has been described as the predominant elimination pathway. (21, 22) The electrophilic properties of the epoxide group allow these compounds to form covalent bonds with proteins, including haemoglobin, through the formation of N-terminal valine adducts. These adducts can serve as biomarkers for monitoring occupational exposure to these reactive chemicals. (23)

Although information is available for bisphenol A diglycidyl ethers (BADGE), the toxicokinetics of isopropyl glycidyl ether and other aliphatic ethers remains insufficiently characterised because of the limited availability of detailed toxicokinetic data. (7, 24, 25) Only a few data are available for IPGE, including studies on acute toxicity, skin/eye irritation, and results from combined repeated dose toxicity studies (OECD Test No. 422). (26) However, the toxicokinetic knowledge is limited only to expert assessments derived from its chemical structure. (18) IPGE is a low molecular weight (Mw = 116.18) highly hydrophilic compound (estimated logP < 1), which partly explains the lack of bioanalytical methods for IPGE and related glycidyl ethers in blood plasma. (20) To determine systemic exposure levels for safety and risk assessments, alternative analytical strategies are often required, including chemical derivatisation or adduct formation, because the protonated molecule ion is not produced in high yield directly in the ion source. Related glycidyl ethers and compounds such as BADGE have been successfully evaluated *via* haemoglobin adducts or by monitoring ammonium adduct counterparts using multiple-reaction monitoring (MRM). (23, 27-30) Several specific epoxide derivatisation strategies have also been explored. These include derivatisation with 2,3,5,6-tetrafluorobenzenethiol for GC-EI-MS (31), dimethylamine in combination with coordination ion-spray spectrometry (32), benzylamine for LC-MS/MS (33), sodium diethyldithiocarbamate for LC-MS/MS (34), and 3-nitrobenzenesulphonic acid for UV detection (35).

1.3.2. Protoporphyrin IX: an endogenous biomarker

Biomarkers are measurable compounds that provide information about normal biological functions, disease-related processes, or the body's response to medical treatment and environmental influences. (36) In toxicology and clinical practice, monitoring endogenous biomarkers is important, because changes in their levels can

signal metabolic imbalances or toxic effects before explicit clinical symptoms appear. (37)

Protoporphyrin IX is a hydrophobic tetrapyrrole and the immediate precursor of heme in the biosynthetic pathway. (38) Under normal physiological conditions, its intracellular and circulating levels are tightly regulated; however, perturbations in this pathway can lead to pathological accumulation. (39, 40) Ferrochelatase deficiency causes erythropoietic protoporphyria, which results in the accumulation of protoporphyrin IX in erythrocytes, plasma, and skin, leading to severe cutaneous photosensitivity. (41-43)

Beyond its role in genetic metabolic disorders, protoporphyrin IX also has considerable importance in oncology, particularly in the context of photodynamic therapy and photodynamic diagnosis. (44) Administration of the exogenous precursor 5-aminolaevulinic acid bypasses physiological feedback regulation within the heme pathway, inducing preferential accumulation of fluorescent and photosensitizing protoporphyrin IX in malignant cells. (45, 46) This property enables the targeted destruction of tumour tissue upon light irradiation or the intraoperative visualization of tumour margins. (47) More recently, delayed fluorescence phenomena of protoporphyrin IX, including excimer formation, have been investigated as innovative tools to estimate local chromophore concentration and tissue oxygenation *in situ*. (48)

The endogenous presence of protoporphyrin IX complicates its quantitative determination in biological matrices. While recent advances in mass spectrometry (MS) and tandem mass spectrometry (MS/MS) provide high selectivity and detailed structural characterisation, their routine implementation is often hindered by substantial equipment costs, operational complexity, and the need for labour-intensive sample preparation (such as liquid-liquid or solid-phase extraction) that limits throughput in large-scale studies. (49-53) In contrast, high-performance liquid chromatography with fluorescence detection (HPLC-FLD) is a reliable, economical, and user-friendly analytical alternative. (54) It offers sufficient selectivity against structurally related porphyrins, and its streamlined sample preparation, combined with short analysis times, facilitates the efficient processing of large sample sets. (5, 55-59)

Unlike xenobiotics, protoporphyrin IX is inherently present in biological matrices at variable background levels, precluding the availability of a true analyte-free blank sample. Consequently, method development and validation require specialized

approaches in accordance with established bioanalytical guidelines, most notably the ICH M10 guideline finalized in 2022. This guideline delineates four acceptable strategies to address the endogenous background: the use of surrogate matrices devoid of the analyte, surrogate analytes, standard addition, and background subtraction. Among these, the surrogate matrix approach is highly effective, as the endogenous analyte should be selectively removed or degraded to generate a suitable blank matrix for calibration purposes. Porphyrins are intrinsically photosensitive and prone to rapid photodegradation; therefore, although they can be readily removed from the matrix, they require stringent light-protection throughout sample collection, processing, and analysis. The ICH M10 guideline highlights the necessity for accurate evaluation of selectivity, linearity, recovery, and stability of both native and spiked analytes, as well as matrix effects using individual and pooled matrices. (5)

Although several recent publications have explored method validation for endogenous analytes, none to date have applied the ICH M10 guideline specifically to protoporphyrin IX quantification. For instance, Walke et al. recently determined protoporphyrin IX levels with 87.0% accuracy, 90.5% positive predictive value, and 84.0% negative predictive value; however, their study did not incorporate the updated ICH recommendations. (52)

1.3.3. Pharmaceuticals

The evaluation of active pharmaceutical ingredients in safety/toxicology and clinical studies requires reliable bioanalytical techniques capable of measuring both drug levels in the body and active or toxic metabolites. Model compounds are used which demonstrate well-established toxicity patterns to study mechanisms of drug-induced damage and to validate new biomarkers. The present research has investigated bioanalytical challenges encountered during the analysis of six pharmaceutical compounds, which were selected by considering their organ targets and their potential to cause toxicity.

To represent nephrotoxicity and antibiotic-associated challenges, the aminoglycoside gentamicin —a classic nephrotoxicant—and the widely used combination of amoxicillin and clavulanic acid serve as appropriate models. (15, 60) Paracetamol (acetaminophen) functions as a paradigmatic model for drug-induced liver injury, given its predictable hepatotoxicity mediated by reactive metabolite formation. (11, 61) Finally, cardiotoxicity

is addressed using two distinct model drugs: isoprenaline, which induces myocardial infarction-like injury, and doxorubicin, a chemotherapeutic agent known for its cumulative cardiotoxic effects. (62) Each compound category is examined with respect to its characteristic bioanalytical challenges and toxicological relevance.

1.3.3.1. Gentamicin

Gentamicin is a broad-spectrum antibiotic belonging to the aminoglycoside class that physicians prescribe for the treatment of severe bacterial infections caused by Gram-negative aerobic bacteria, including *Pseudomonas aeruginosa,* as well as members of the *Enterobacteriaceae* family and *Staphylococcus* species. Gentamicin is produced by the fermentation of *Micromonospora purpurea* and exists as a complex multicomponent system rather than a single molecular structure. The major components of this complex include gentamicin C1 and C1a (no methyl group on 2-amino-hexose ring) as well as the epimeric C2 and C2a, together with multiple additional minor components. (13, 63) Gentamicin exerts its antibacterial effect by binding the 30S subunit of bacterial ribosomes, thereby inhibiting protein synthesis and causing translation errors. Because gentamicin has a narrow therapeutic window and patient responses vary depending on age, renal function and underlying medical conditions, careful therapeutic monitoring is required. (6, 64, 65)

The therapeutic use of gentamicin is limited by two major adverse effects, nephrotoxicity and ototoxicity. The primary dose-related side effect, nephrotoxicity, occurs when the drug accumulates in the renal cortex, where it damages proximal tubular epithelial cells leading to acute tubular necrosis that may progress to acute renal failure. (6, 64) Experimental studies have shown that gentamicin can accumulate in the renal cortex at concentrations several times higher than those observed in plasma and other tissues. (66) In addition, its elimination from kidney tissue is unusually slow, with a reported half-life of 109 hours in rat studies. (67, 68) The selective renal uptake and prolonged retention of gentamicin are key factors contributing to kidney injury through mechanisms involving oxidative stress, mitochondrial dysfunction, and metabolic disturbances. Metabolomic studies have demonstrated characteristic alterations in urinary biomarkers, including glucose, amino acids, and the tubular enzyme N-acetyl-β-D-glucosaminidase. (11, 69)

The bioanalytical approach of gentamicin detection in biological samples requires special analytical methods due to its unfavourable physicochemical properties. The individual gentamicin components are highly polar, water-soluble and non-volatile basic compounds which lack strong UV-absorbing chromophore or intrinsic fluorophore. (12) The conventional methods of HPLC with UV or FLD are not directly applicable and require complex pre- or post-column derivatisation procedures, for example with 1-fluoro-2,4-dinitrobenzene. (13, 63) Furthermore, the C1, C1a, C2 and C2a components exhibit strong structural similarity, which makes their chromatographic separation challenging. Specific conditions, including high-pH mobile phases and ion-pairing reagents, are often required to achieve adequate separation while minimizing peak broadening caused by interactions with silanol groups. (70)

Traditional clinical monitoring of gentamicin using microbiological assays or immunoassays has important limitations, including the inability to distinguish individual gentamicin components and susceptibility to false results due to interfering substances or sample contaminants. In contrast, the LC-MS/MS system enables the direct and selective quantification of gentamicin components without the need for derivatisation. Lecároz et al. compared the results of their new LC-MS/MS method with those of a traditional bioassay (71), demonstrating improved accuracy (5.59% versus 14%) and precision (6.13% versus 15%). Since gentamicin is a highly polar ($\log P \sim -3.1$) compound, conventional reversed-phase chromatography often struggles with its poor retention. To address this challenge, modern bioanalytical approaches have increasingly utilized Hydrophilic Interaction Liquid Chromatography (HILIC), which has proven to be a powerful separation technique for highly polar antibiotics. (72, 73) HILIC is an analytical separation technique that isolates polar compounds based on their differential partitioning between an organic-rich mobile phase and a water-enriched layer immobilized on a hydrophilic stationary phase. (72) Oertel et al. used a HILIC analytical column to simultaneously determine six aminoglycosides in human serum without the need for signal-suppressing ion-pairing reagents. (74) Alternatively, specialized stationary phases such as porous graphitic carbon columns (e.g., Hypercarb) have been used to strongly retain and separate individual gentamicin C components, even in complex matrices such as fish tissues. (75) After solid-phase extraction, Zhang et al. performed LC-MS/MS analysis on an HPH C8 (high pH stability octyl silica) column using a highly alkaline

mobile phase (0.2% formic acid, 50 mmol/L ammonium acetate, and 2% ammonia in water), enabling the determination of gentamicin in animal tissues while avoiding fluorinated ion-pairing reagents. (76) Heller et al. developed an HPLC-MS/MS method using a Waters ODS-AM (octadecyl silica) column with a mobile phase containing trifluoroacetic acid. This approach enabled gentamicin quantification across diverse biological matrices, including bovine plasma, urine, milk, and biopsy samples. (77) Modern applications also strongly support the clinical monitoring of polypharmacy and the evaluation of potential synergistic nephrotoxicity. This is illustrated by multianalyte procedures developed for the simultaneous extraction and quantification of complex drug combinations in human plasma, including daptomycin, amikacin, gentamicin, and rifampicin. Similar simultaneous approaches have proven essential for measuring amikacin, gentamicin, and vancomycin in vulnerable populations like newborns, as well as for evaluating the co-administration of nephrotoxic agents in rat experimental models using eco-friendly LC-MS/MS strategies. (78)

1.3.3.2. Amoxicillin and clavulanic acid

The combination of the β-lactam type amoxicillin and clavulanic acid is a commonly used antibacterial therapy prescribed for treatment of bacterial infections. Amoxicillin, a semi-synthetic penicillin derivative, exerts its antibacterial activity by inhibiting bacterial cell wall synthesis. However, the efficacy of amoxicillin is frequently compromised by the production of β-lactamase enzymes by resistant bacteria, which hydrolyse the β-lactam ring. Bacterial resistance to amoxicillin often develops through this mechanism; therefore, physicians commonly prescribe this antibiotic in combination with clavulanic acid, a potent β-lactamase inhibitor (typically administered as potassium clavulanate; e.g., Augmentin Duo). Clavulanic acid expands the antibacterial spectrum of amoxicillin by irreversibly binding to β-lactamases which prevents enzymatic degradation of the antibiotic. (60, 79)

Attempting to quantify amoxicillin and clavulanic acid simultaneously in biological samples, however, raises significant analytical challenges. (80) Clavulanic acid is a chemically unstable compound that is highly susceptible to degradation under acidic or alkaline conditions and at elevated temperatures. (81) In addition, it lacks a strong UV-absorbing chromophore, which limits the sensitivity of conventional HPLC-UV methods.

Consequently, complex pre- or post-column modification procedures (e.g., imidazole derivatisation) are often required to reach suitable detection sensitivity. (82) In contrast, amoxicillin is chemically more stable but exhibits an amphoteric and highly polar nature, which complicates its extraction from biological fluids using conventional liquid–liquid extraction methods because of its high water solubility. (80-84)

The substantial differences in stability (85) and polarity (amoxicillin logP ~ 0.87 vs. clavulanic acid logP ~ -2.3) make it difficult to develop a single analytical method capable of quantifying both analytes simultaneously. Understanding the solution stability of amoxicillin, clavulanic acid, and their impurities, as demonstrated by Atici et al. (86), is a prerequisite for bioanalytical method development. Their study evaluated these compounds under various stress conditions, including thermal, hydrolytic, pH-induced, photolytic (UV), and oxidative degradation. Previously reported HPLC-UV methods (e.g., described by Hoizey, Matar and Foroutan) exhibit concentration range limitations that restrict their applicability in pharmacokinetic studies. For instance, Hoizey et al. (60) utilized a reversed-phase C8 column, achieving linear ranges of 0.625–20 mg/L for amoxicillin and 0.3125–10 mg/L for clavulanic acid in plasma. Matar reported separate UV methods: one for amoxicillin using a Symmetry C18 column over a range of 0.5–12 µg/mL (87), and another for clavulanic acid utilizing a Nova-Pak C18 column with a lower limit of quantification (LLOQ) of 0.1 µg/mL (88). Meanwhile, Foroutan et al. (89) achieved LLOQs of 15 and 30 ng/mL for amoxicillin and clavulanic acid respectively, utilizing a Chromolith Performance column. These methods lack sufficient sensitivity and selectivity and typically require large sample volumes, making them less suitable for pharmacokinetic studies where small amounts of analytes may be available for analysis. In addition, the selectivity of UV-based detection can be compromised by endogenous components present in biological matrices such as plasma or urine. (79) To address these challenges, Xi et al. (90) developed an LC-MS/MS method for dog plasma featuring a Phenomenex Luna C8 column, achieving a linear range of 0.5–500 ng/mL. Similarly, Reyns et al. (81) and Yoon et al. (91) employed LC-MS/MS with negative electrospray ionisation and selected ion monitoring for calf and human plasma analyses. LC-MS/MS has therefore become the preferred analytical approach, as it provides superior sensitivity and specific molecular detection, in order to accommodate both analytes within a single analytical run.

1.3.3.3. Paracetamol

Paracetamol is one of the most frequently used analgesic and antipyretic drugs worldwide, and is widely available as an over-the-counter medication. It is considered safe when taken at recommended doses; however, overdose can result in acute liver failure which occurs in numerous cases. (92-94) Due to its well-documented hepatotoxic potential, paracetamol is frequently used as a model hepatotoxicant in toxicological research to investigate the mechanisms of drug-induced liver injury. (95)

The hepatotoxicity of paracetamol is closely related to its metabolism which depends on the administered dose and follows well-defined metabolic pathways. Approximately 80–90% of the drug is eliminated *via* phase II conjugation reactions, forming non-toxic metabolites, such as paracetamol-glucuronide and paracetamol-sulphate, which are excreted in the urine. A minor fraction (5–10%) undergoes oxidative metabolism mediated by cytochrome P450 enzymes, predominantly CYP2E1, leading to the formation of the highly reactive and toxic intermediate N-acetyl-p-benzoquinone imine (NAPQI). Under normal conditions, NAPQI is detoxified in the liver through glutathione conjugation, forming paracetamol-glutathione, which is subsequently converted to paracetamol-cysteine and paracetamol-N-acetylcysteine before excretion. (96) During overdose, excessive NAPQI is produced because the sulphation and glucuronidation pathways become saturated, while hepatic glutathione stores are depleted. The resulting accumulation of NAPQI leads to covalent binding to cellular proteins, causing oxidative stress, mitochondrial damage, and ultimately hepatocellular necrosis. (97, 98)

The safety assessment of paracetamol requires the measurement of both the parent compound and its metabolites formed through conjugation and oxidative pathways due to its complex metabolism. (97) The risk of liver injury depends on the balance between detoxification and bioactivation processes; therefore, the simultaneous quantification of paracetamol, and its metabolites is essential in toxicokinetic and pharmacokinetic studies. Historically, standard HPLC methods with UV or photodiode array detection are routinely used for the quality control and quantification of the parent drug in multi-component pharmaceutical formulations. For example, Brunner et al. reported a detection range of 1.56–200 µg/mL for paracetamol, and quantified two metabolites, paracetamol-sulphate and paracetamol-glucuronide. (99) Over two decades later, reflecting advancements in column technologies and UV detector sensitivity the method developed

by Pereira et al. resulted in an approximately 8-fold improvement in a limit of detection (LOD) of 0.2 μg/mL for paracetamol. (100) Both of these HPLC-UV methods employed isocratic elution. However, when applied to biological samples, such approach failed to adequately resolve and distinguish structurally similar metabolites.

Therefore, LC-MS/MS has become the preferred technique for the accurate quantification of paracetamol and its metabolites in complex biological matrices such as plasma and urine. For instance, Delahaye et al. developed an LC-MS/MS method to measure paracetamol and four of its metabolites in plasma, whole blood, and dried blood microsamples, with a linear range of 0.10-50.0 μg/mL for paracetamol. (15) Other studies by Dargue, An, and Tan employed gradient elution with mobile phases containing formic acid to investigate various matrices, including rat, pig, and human plasma, as well as urine. In these studies, Dargue and An identified 7 and 6 metabolites, respectively, in addition to paracetamol. (61, 101, 102) Furthermore, Cook et al. detected paracetamol and 5 of its metabolites in human plasma and urine using an Agilent Poroshell 120 EC-C18 column with a gradient elution consisting of 10 mM aqueous ammonium acetate (pH 3.5) and methanol. (103) The development of fast and sensitive LC-MS/MS methods holds significant importance for the comprehensive evaluation of paracetamol-induced liver injury, enabling the simultaneous quantification of analytes from extremely small plasma volumes and complex tissues. For example, Gicquel et al. quantified paracetamol, paracetamol-glutathione, and paracetamol-sulphate with a linear range between 0.25–20 mg/L using only a 25 μL (human and mouse) plasma sample volume. (104) Additionally, Pietruk et al. successfully determined paracetamol and its metabolites (paracetamol-glutathione, paracetamol-sulphate) in muscle, liver, lung, and kidney samples from various animal species within a rapid, 8-min analytical run. (105)

1.3.3.4. Doxorubicin

Doxorubicin, an anthracycline glycoside antibiotic originally isolated from *Streptomyces peucetius var. caesius*, is one of the most effective and widely used antineoplastic agents. It exhibits broad antitumor activity and is used to treat various malignancies, including breast, lung, ovarian, and thyroid cancers, as well as leukaemia, lymphoma and sarcoma. (106) Doxorubicin exerts its cytotoxic effects through multiple mechanisms, including DNA intercalation, topoisomerase II inhibition, and generation of

reactive oxygen species, resulting in impaired DNA replication and tumour cell death. However, the clinical use of doxorubicin is limited by dose-dependent cardiotoxicity, which can lead to irreversible cardiac damage and heart failure following repeated doses. (62, 107)

The mechanisms underlying doxorubicin-induced cardiotoxicity are not yet fully understood. A widely accepted hypothesis implicates doxorubicinol, a major metabolite formed *via* two-electron reduction of the C-13 carbonyl group in the side chain of doxorubicin. This biotransformation is primarily mediated by cytosolic NADPH-dependent aldo-keto reductases and carbonyl reductases. Doxorubicin undergoes extensive hepatic metabolism *via* two main pathways, producing doxorubicinol as the primary alcohol metabolite and several aglycone metabolites, including doxorubicinone and 7-deoxydoxorubicinone. The studies by Zeng (108), Mross (109), Wang (110) and Beijnen (111) have demonstrated that doxorubicinol disrupts intracellular iron and calcium homeostasis and inhibits key ion transporters, including Na^+/K^+-ATPase and Ca^{2+}-ATPase in sarcoplasmic reticulum and mitochondria. In addition, doxorubicinol contributes to increased oxidative stress due to its redox cycling properties. Although doxorubicinol is generally less cytotoxic toward tumour cells than the parent compound, it is considered more cardiotoxic and preferentially accumulates in cardiac tissue, where it may persist longer than doxorubicin itself. (112) Accurate measurement of systemic doxorubicin levels remains essential for understanding toxicokinetic relationships and determining exposure in safety studies, given the complex interplay between the parent drug and its metabolite.

The bioanalytical quantification of doxorubicin in biological samples presents several challenges due to its structural similarity to its metabolites, as well as its polarity and instability. High-performance liquid chromatography with fluorescence detection has been the standard method for analysis, taking advantage of the intrinsic fluorescence of the anthracycline moiety. However, these methods often require extended chromatographic run times (22 to 25 minutes) to achieve adequate separation, and may be less effective when analysing complex biological matrices. (111, 113)

LC-MS/MS is widely used for the bioanalytical quantification of doxorubicin. The development of robust LC-MS/MS methods requires optimized sample preparation techniques, such as protein precipitation and solid-phase extraction, to ensure efficient

recovery of doxorubicin and doxorubicinol from plasma and tissue homogenates. (114) For preclinical applications, studies by Arnold (107), Liu (115), and Zhou (116) have reported robust LC-MS/MS methods capable of simultaneous measurement of doxorubicin and doxorubicinol in *in vivo* rat plasma and tissue samples. Chromatographic separation must effectively resolve doxorubicin from structurally related compounds (e.g. doxorubicinol), which have similar mass values differing by only 2 Da; otherwise, insufficient separation may lead to inaccurate quantification. Transitioning to clinical and *in vitro* applications, researchers such as Xu (117), Sottani (118), and Semreen (119) have successfully utilized sensitive LC-MS/MS methods for quantification in human plasma, as well as subcellular and exosomal fractions of leukemic cell cultures.

1.3.3.5. Isoprenaline

The synthetic catecholamine isoprenaline (also known as isoproterenol) is a potent non-selective β-adrenoceptor agonist with no significant affinity for α-adrenergic receptors. Its chemical structure, 3,4-dihydroxy-α-[(isopropylamino)methyl]benzyl alcohol, is structurally similar to epinephrine and norepinephrine but contains an N-isopropyl group. (120) Clinically, it is used in aerosol form for the treatment of bradycardia, heart block and bronchial asthma due to its positive chronotropic and inotropic effects, as well as its strong bronchodilator properties. (121) Although its medical application has significantly declined, it remains widely employed in experimental studies to induce myocardial infarction and cardiac hypertrophy in laboratory animals. (122) High doses of isoprenaline trigger severe oxidative stress, leading to calcium overload and myocardial tissue damage that resembles the pathological features of ischemic heart disease. (123, 124)

The bioanalytical quantification of isoprenaline in biological samples is challenging due to its fast elimination and extensive metabolism. Following administration, isoprenaline is rapidly metabolized *via* two main metabolic pathways, catechol-O-methyltransferase-mediated O-methylation and sulphate conjugation. As a result, isoprenaline exhibits a short plasma half-life, ranging from 2 to 5 minutes in both humans and laboratory animals. (125, 126) This rapid clearance results in very low circulating concentrations of the parent compound, necessitating highly sensitive analytical methods for reliable quantification in low concentration range. (127)

The short half-life of isoprenaline, combined with its instability when exposed to light, oxygen, and high pH further complicates bioanalytical measurements. Oxidative degradation results in the formation of three types of compounds, quinones, aminochromes and polymeric pigments, leading to underestimation of plasma concentrations during sample collection and processing. (120, 128)

Various analytical methods have been developed for determination of catecholamines (including isoprenaline), using techniques such as high-performance liquid chromatography with electrochemical detection (HPLC-ECD) (129), spectrophotometry (130), capillary electrophoresis (131) and chemiluminescence-based (132, 133) assays. While HPLC-ECD offers good sensitivity for catecholamines, its applicability is often limited by labour-intensive sample preparation procedures (e.g., alumina extraction), and relatively long analysis times.(134, 135)

Currently, LC-MS/MS is the preferred method for isoprenaline quantification in complex biological matrices, offering better selectivity and sensitivity than previous methods. (136, 137) Reported LC-MS/MS methods vary widely in terms of sample preparation, stabilization strategies and analytical performance. Careful optimization is required to reduce matrix effects, and to achieve proper retention and separation of this highly polar compound.

2. OBJECTIVES

This thesis addresses bioanalytical challenges encountered in chemical safety assessment and related studies through the development and validation of „fit-for-purpose" analytical methods. The work focuses on three distinct classes of compounds that present different analytical difficulties: reactive industrial chemicals, endogenous biomarkers, and pharmaceuticals.

Specific objectives were defined as follows:

1. Toxicokinetic characterisation of an industrial chemical: isopropyl glycidyl ether

- To develop and validate a sensitive LC-MS/MS method for the quantification of isopropyl glycidyl ether in rat plasma,
- To characterise the toxicokinetic profile of isopropyl glycidyl ether and to identify its potential metabolites.

2. Elaboration of a validated bioanalytical protocol for an endogenous biomarker: protoporphyrin IX

- To establish a selective and sensitive HPLC-FLD method for the quantification of protoporphyrin IX in biological samples, addressing the analytical challenge arising from the endogenous presence of protoporphyrin IX in plasma.
- To demonstrate the applicability of the method in monitoring the kinetics of 5-aminolaevulinic acid induced protoporphyrin IX formation in rats.

3. Bioanalytical support for toxicity studies

- To develop and validate analytical methods of various pharmaceutical compounds for the determination of model compounds in organ-specific toxicity studies (gentamicin, amoxicillin and clavulanic acid, paracetamol, doxorubicin, isoprenaline).

3. METHODS

3.1 Chemicals and reagents

Isopropyl glycidyl ether (99.7%), *tert*-butyl glycidyl ether (99.8%), neopentyl glycol diglycidyl ether (technical grade), trifluoroacetic acid (99.0%), protoporphyrin IX (95.0%), mesoporphyrin IX dihydrochloride (94.0%), aminolaevulinic acid (97.0%), doxorubicin (97.8%), daunorubicin (98.8%), isoprenaline (85.3%), paracetamol (~100%), paracetamol-d3 (100%), gentamicin (92.85%), kanamycin (99.3%), amoxicillin (~100%), clavulanic acid (~100%), trichloroacetic acid (99.5%), nutrient mixture F-12 ham, Williams' medium E, D-(+)-glucose, sodium bicarbonate and 4-(2-hydroxyethyl)piperazine-1-ethanesulfonic acid (HEPES) were obtained from Sigma-Aldrich (St. Louis, MO, USA).

LC-MS grade solvents and additives, specifically acetonitrile, 2-propanol, dimethylformamide, formic acid, acetic acid, ammonium formate, ammonium acetate and 25% ammonium solution were supplied by VWR International (Leuven, Belgium). Methanol suitable for HPLC gradient analysis was purchased from Carlo Erba Reagents S.A.S. (Val de Reuil, France). For the preparation of ultrapure water, an ELGA Veolia PURELAB Chorus water purification system (High Wycombe, UK) was used. Heat inactivated fetal bovine serum (hiFBS) was bought from Euroclone (Via Figino, Italy).

Rat primary hepatocytes were prepared at HUN-REN Research Centre for Natural Sciences (Hungary). Blank rat plasma and urine (Toxi-Coop Toxicological Research Centre, Hungary), used for matrix-matched calibration, was prepared with K3-EDTA anticoagulant and kept frozen at - 20 ± 5°C.

3.2. Analytical method for isopropyl glycidyl ether

3.2.1. Preparation of calibration standards and quality control samples

Primary stock solutions of both IPGE and the internal standard (IS), *tert*-butyl glycidyl ether (TBGE), were prepared in methanol at a concentration of 1 mg/mL. Working solutions were obtained by serial dilution with methanol, resulting in concentrations ranging from 0.05 to 50 µg/mL for the calibration curve and from 0.05 to 40 µg/mL for quality control purposes. The IS working solution was further diluted in

acetonitrile to a final concentration of 1 µg/mL. All solutions were stored at -20 ± 5 °C. The calibration curve consisted of ten nominal concentration levels: 0.01, 0.02, 0.05, 0.1, 0.2, 0.5, 1, 2, 5, and 10 µg/mL. Quality control samples were prepared at four concentration levels: 0.01, 0.03, 3, and 8 µg/mL. Sample preparation involved spiking 50 µL of blank rat plasma with 10 µL of the appropriate working solution, followed by the addition of 150 µL of the IS solution.

3.2.2. Sample preparation protocol

Prior to processing, plasma samples (described in section 3.2.5.) were allowed to thaw at ambient temperature. A 50 µL aliquot of rat plasma was pipetted into a 1.5-mL microcentrifuge tube, followed by the addition of 10 µL of methanol (used to replace the spiking working solution matrix). Protein precipitation was initiated by adding 150 µL of the IS working solution (1 µg/mL in acetonitrile). The mixture was vortexed thoroughly to ensure homogeneity and then centrifuged at 6596 × *g* for 10 minutes at room temperature. Finally, at least 100 µL of the clear supernatant was transferred into vials and placed in the autosampler, maintained at 10 °C.

3.2.3. LC-MS/MS conditions

Analyses were performed using a Shimadzu Nexera X2 liquid chromatography system coupled to a Shimadzu LCMS-8060 triple quadrupole tandem mass spectrometer, supplied with nitrogen and air by a Peak Scientific Genius 1051 generator. Chromatographic separation was performed on a YMC-Triart C18 column (3 µm, 2.1 × 75 mm) equipped with a YMC-Triart C18 guard column (3 µm, 2.1 × 10 mm), both maintained at 30 °C. The injection volume was set to 10 µL. A gradient elution method was applied with a flow rate of 0.4 mL/min, using 0.5% formic acid in ultrapure water as Mobile Phase A and 0.5% formic acid in acetonitrile as Mobile Phase B. The gradient program began at 10% B for 0.5 min, increased linearly to 90% B by 3.5 min, was held at 90% B for 0.5 min, and subsequently returned to 10% B for column re-equilibration. The total run time was 5 min. Atmospheric pressure chemical ionisation (APCI) was operated in positive mode. The ion source parameters were optimized as follows: interface temperature, 350 °C; desolvation line temperature, 300 °C; and heat block temperature, 300 °C. Gas flow rates were set to 3 L/min for the nebulizing gas and

5 L/min for the drying gas. Quantification was conducted using multiple reaction monitoring (MRM) transitions of 157.90 → 116.10 *m/z* for the analyte (IPGE) and 172.00 → 116.10 *m/z* for the IS (*tert*-butyl glycidyl ether). (Table S 2)

3.2.4. Validation procedures

Method validation was performed in accordance with the ICH M10 guidelines. Selectivity was evaluated using blank plasma obtained from six individual rats. Linearity was demonstrated across the concentration range of 0.01–10 µg/mL, applying a weighted ($1/x^2$) least-squares linear regression model. Precision and accuracy (both intra-day and inter-day) were assessed at four quality control concentration levels. Carry-over was checked by injecting blank samples immediately after the highest calibration standard. Stability was assessed under various conditions, including short-term stability at room temperature, long-term storage at -75 ± 10 °C, freeze-thaw stability over three cycles, and autosampler stability.

3.2.5. Toxicokinetic study

A single-dose oral toxicity study was conducted using Han-Wistar rats (Toxi-Coop Toxicological Research Centre, Budapest, Hungary). Three groups were included (receiving IPGE doses of 1000, 1500, and 2000 mg/kg), each comprising nine animals per sex. Blood samples were collected *via* the retro-orbital venous plexus at scheduled time points: pre-dose, 0.5, 1, 2, 4, 6, 8, 12, and 24 hours after administration. Samples were drawn into K3-EDTA tubes, centrifuged to obtain plasma, and stored at -75 ± 10 °C until bioanalysis.

3.2.6. Qualitative identification of IPGE metabolites

For metabolite profiling of IPGE, a dedicated qualitative method was developed distinct from the quantitative APCI protocol. For the investigation, the ion source was switched to electrospray ionisation (ESI), operated in both positive and negative modes to cover a broad range of potential metabolites. Chromatographic separation was performed using the same column type, but with a modified gradient program to ensure adequate separation of polar metabolites. The mobile phases consisted of 0.1% formic acid in water (A) and 0.1% formic acid in acetonitrile (B). The gradient started at 0% B,

increased linearly to 100% B over 10 min, was held for 0.5 min, and then returned to initial conditions, resulting in a total run time of 12 minutes. Detection was carried out in selected ion monitoring (SIM) mode, targeting the predicted precursor ions of potential metabolites. The search strategy focused on identifying products arising from epoxide hydrolysis, oxidation, and conjugation reactions (e.g., with glutathione, sulphate, or glucuronic acid). The target mass-to-charge ratios (*m/z*) included 135, 151, 231, 309, 149, 190, 206, 165, 119, 296, 424, and 280, along with the Meerwein-derivative of the parent compound at 158 *m/z*.

3.3. Analytical method for protoporphyrin IX

3.3.1. Preparation of calibrators and quality control samples

Stock solutions containing protoporphyrin IX (200 µg/mL) and the internal standard, mesoporphyrin IX dihydrochloride (200 µg/mL), were prepared in a solvent mixture of dimethylformamide and methanol (1:1, v/v). Working solutions were prepared by serial dilution using the same solvent system. Eight nominal concentration levels were established for the calibration standards: 10, 20, 50, 100, 200, 400, 500, and 700 ng/mL. Quality control samples were prepared at four concentration levels: 10, 30, 150, and 550 ng/mL. To prevent photodegradation, all solutions and samples were handled and stored in amber glass vials.

3.3.2. Preparation of surrogate matrix

Given that protoporphyrin IX is an endogenous compound, a surrogate matrix strategy was adopted. This matrix was produced in-house by exposing authentic rat plasma to visible light from a desk lamp (IKEA-SOLHETTA LED light bulb, 2700 K, 470 lm) for a duration of at least four hours. This illumination procedure effectively decomposed the endogenous protoporphyrin IX, resulting in an analyte-free matrix that retained a composition comparable to the original biological fluid.

3.3.3. Sample preparation

A 50 µL volume of rat plasma was transferred into a 1.5-mL amber centrifuge tube. Subsequently, 10 µL of a dimethylformamide/methanol (1:1) mixture, 10 µL of the IS

working solution (2 µg/mL), and 150 µL of acetonitrile were added. The mixture was vortexed and then centrifuged at 6596 × *g* for 10 min at ambient temperature. From the resulting supernatant, an aliquot of at least 100 µL was transferred to autosampler vials and maintained at 10 °C, ensuring protection from light throughout the process.

Calibration and LLOQ QC samples were prepared in the surrogate matrix. Low, medium high and endogenous quality control samples were made in the authentic matrix.

3.3.4. HPLC-FLD conditions

Chromatographic analysis was performed using a Shimadzu Prominence system equipped with a Shimadzu RF-20 A XS fluorescence detector. Separation was achieved using an ACE Ultracore SuperC18 column (2.5 µm, 2.1 × 75 mm) protected by an Inertsil ODS-4guard column (3 µm, 1.5 × 10 mm), with the column temperature maintained at 30 °C. The mobile phase consisted of ultrapure water containing 0.05% trifluoroacetic acid (Eluent A) and acetonitrile containing 0.05% trifluoroacetic acid (Eluent B). A gradient elution program was applied at a flow rate of 0.5 mL/min starting at 40% B, increasing to 70% B over 5.0 min, then to 100% B by 5.5 min, held for 1.0 min, and finally re-equilibrated to 40% B. The total run time was 8 min. Fluorescence detection was performed using an excitation wavelength of 405 nm and an emission wavelength of 630 nm. (Table S 3)

3.3.5. Method validation

The method validation was conducted in full accordance with the ICH M10 guideline, employing the surrogate matrix approach. Selectivity was confirmed by analysing six individual blank surrogate and authentic plasma samples, along with haemolyzed and lipemic plasma pools. Linearity was verified across the concentration range of 10–700 ng/mL. Parallelism between the surrogate and authentic matrices was assessed by comparing the slopes of their respective calibration curves. Stability studies evaluated freeze-thaw cycles, short-term and long-term stability, as well as autosampler stability for both the analyte and the IS.

3.3.6. *In vivo* study

To demonstrate the practical applicability of the method, an *in vivo* experiment was performed using male Wistar rats treated with 5-aminolaevulinic acid to stimulate protoporphyrin IX production. A single oral dose of 100 mg/kg 5-aminolaevulinic acid or vehicle was administered to the animals. Blood samples were collected at pre-dose, 1, 2, 4, 7, and 24 hours following administration. To prevent photodegradation, samples were processed under dim light conditions and stored at -75 ± 10 °C until analysis.

3.4. Analytical methods for pharmaceuticals in toxicity studies

3.4.1. Instrumentation

Liquid chromatography-tandem mass spectrometry analyses were conducted using a Shimadzu LCMS-8060 triple quadrupole mass spectrometer equipped with a Nexera X2 UHPLC system (Shimadzu, Japan). The system configuration included LC-30AD pumps, a SIL-30AC autosampler, a CTO-20AC column oven, and a DGU-20A5R degassing unit. Nitrogen for the MS system was supplied by a Genius 1051 nitrogen generator (Peak Scientific).

3.4.2. Chromatographic and mass spectrometric conditions

3.4.2.1. Gentamicin assay

For both plasma and urine matrices, separation was performed on a Supel^{TM} Carbon LC (2.7µm, 2.1 x 100 mm) column with Supel^{TM} Carbon LC (2.7µm, 2.1 x 20 mm) guard column, maintained at 60°C. The mobile phase consisted of a 5% ammonium solution in ultrapure water (Eluent A) and acetonitrile (Eluent B) delivered at a flow rate of 0.35 mL/min. Gradient elution was used as follows: 5% B (0–0.5 min), increased to 40% B (1.0–3.5 min), then to 90% B (4.0–5.0 min), followed by re-equilibration. The total run time was 7 min.

Detection was performed in positive ESI mode. Gentamicin components were monitored individually: C1a (450.10 → 322.10 m/z), C1 (478.10 322.20 m/z), and C2/C2a (464.1 → 322.30 m/z). Kanamycin served as the internal standard (485.00 → 163.15 m/z). (Table S 4)

3.4.2.2. Amoxicillin and clavulanic acid assay

Analytes were separated on an InertSustain C18 column (3µm, 2.1x75 mm) with an Inertsil ODS-4 (3µm, 1.5x10 mm) guard column at 25°C. The mobile phase consisted of 0.1% formic acid in ultrapure water (A) and 0.1% formic acid in acetonitrile (B). The gradient started at 5% B, increased to 100% B at 2.0 min, was held until 3.0 min, and re-equilibrated, resulting in a total run time of 4.0 min.

The MS operated in negative ESI mode. MRM transitions were 363.90 → 223.10 m/z for amoxicillin and 197.90 → 82.10 m/z for clavulanic acid. (Table S 5)

3.4.2.3. Paracetamol assay

An InertSustain C18 column (3µm, 2.1x75 mm) with an Inertsil ODS-4 (3µm, 1.5x10 mm) guard column was used for separation at 30°C. The mobile phases were 0.1% formic acid in ultrapure water (A) and 0.1% formic acid in methanol (B). The gradient began at 5% B, increased to 40% B at 4.5 min, ramped to 95% B at 5.0 min, was held it for 1 min, and then re-equilibrated to 5% B, resulting in a total run time of 8.0 min.

Positive ESI was used, monitoring 152.10 → 110.15 m/z for paracetamol and 155.10 → 110.15 m/z for the internal standard, paracetamol-d3. (Table S 6)

Metabolites also were monitored for semiquantitative purposes. Positive ESI was used to monitor 271.00 → 139.90 m/z for paracetamol-cysteine, 328.10 → 152.10 m/z for paracetamol-glucuronide, 457.20 → 139.90 m/z for paracetamol-glutathione. Negative ESI was used to monitor 230.00 → 150.00 m/z for paracetamol-sulphate, 311.04 → 182.00 m/z for paracetamol-N-acetylcysteine.

3.4.2.4. Doxorubicin assay

Chromatographic separation was achieved on a YMC-Triart C18 (3µm, 2.1x75 mm) with a YMC-Triart C18 (3µm, 2.1x10 mm) guard column, maintained at 30°C. The mobile phase consisted of 10 mM ammonium acetate with 0.1% formic acid in ultrapure water (Eluent A) and acetonitrile (Eluent B). Gradient elution was applied at a flow rate of 0.4 mL/min, starting at 30% B, increasing to 90% B by 2.0 min, being held until 3.5 min, and re-equilibrated to 30% B for a total run time of 5.0 minutes.

The mass spectrometer operated in positive electrospray ionisation (ESI) mode with multiple reaction monitoring (MRM) mode. The monitored transitions were 544.20 → 397.05 m/z for doxorubicin and 528.30 → 321.05 m/z for the internal standard (IS), daunorubicin. (Table S 7)

3.4.2.5. Isoprenaline assay

Isoprenaline was analysed using a Kinetex-EVO C18 (2.6µm, 3x50 mm) with an InertSustain C18 (3µm, 1.5x10 mm) guard column, maintained at either 30 °C or 25 °C. The mobile phase comprised 0.1% trifluoroacetic acid in ultrapure water (Eluent A) and methanol (Eluent B), delivered at a flow rate of 0.4 mL/min. The gradient program began at 5% B, increased to 70% B between 1.5 and 2.5 min, then to 90% B between 2.5 and 3.5 min, and returned to initial conditions within a total run time of 6.0 min.

Quantification was performed in positive ESI mode, monitoring the transition 211.90 → 194.20 m/z for isoprenaline. Paracetamol was used as the internal standard, monitoring the transition 151.90 → 110.10 m/z. (Table S 8)

3.4.3. Preparation of standard and working solutions

For gentamicin, primary stock solutions of the analyte and the internal standard, kanamycin, were prepared by dissolving 3.0 mg of the reference substance in ultrapure water to obtain a concentration of 1000 µg/mL. These solutions were stored in plastic containers, protected from light at - 20 ± 5°C. Working solutions for calibration standards and quality control samples were prepared by serial dilution of the stock solutions with ultrapure water, covering a concentration range of 0.1 - 100 µg/mL for the analyte, while the kanamycin working solution was diluted to 1 µg/mL.

For the amoxicillin and clavulanic acid method, separate stock solutions were prepared for each analyte by dissolving the reference standards in ultrapure water to obtain a final concentration of 500 µg/mL. Due to the instability of clavulanic acid, this stock solution was aliquoted and stored frozen at - 20 ± 5°C. Working solutions were freshly prepared by serial dilution with ultrapure water on each day of use, yielding intermediate solutions of 5 µg/mL and 50 µg/mL, which were further diluted to generate calibration levels ranging from 0.05 µg/mL to 2.5 µg/mL.

In the case of paracetamol, the stock solution of the analyte was prepared in methanol at a concentration of 1000 µg/mL, while the stock solution of the internal standard (paracetamol-d3) at 500 µg/mL. Working solutions for the calibration curve (0.5–500 µg/mL) were prepared by serial dilution using methanol, whereas the internal standard was diluted with acetonitrile to obtain a working concentration of 1 µg/mL. All solutions were stored at - 20 ± 5°C.

For doxorubicin, the stock solution was prepared in ultrapure water at a concentration of 1000 µg/mL and stored at 2–8 °C. The internal standard, daunorubicin, was dissolved in methanol to obtain a concentration of 1000 µg/mL and stored at - 20 ± 5°C. Working solutions of doxorubicin were prepared by serial dilution with ultrapure water to cover a concentration range of 5 ng/mL to 100 µg/mL. The internal standard working solution was prepared by diluting the stock with methanol to 1 µg/mL, followed by a final dilution with ultrapure water to 10 ng/mL prior to use.

For isoprenaline, stock solutions of the analyte and the internal standard (paracetamol) were prepared in ultrapure water at a concentration of 1000 µg/mL. To minimize oxidative degradation, the isoprenaline stock solution was stored in amber glass vials at 2–8 °C. Working solutions of isoprenaline were prepared by serial dilution with ultrapure water, spanning a concentration range of 25 ng/mL to 100 µg/mL. The internal standard working solution was similarly diluted with ultrapure water to concentration of 3 µg/mL.

3.4.4. Sample preparation

3.4.4.1. Plasma sample preparation (protein precipitation)

For gentamicin, 50 µL of plasma was treated with 10 µL of ultrapure water, 150 µL of 0.1 g/mL trichloroacetic acid solution and 10 µL of internal standard working solution (kanamycin). Samples were centrifuged twice at 14841 × *g* at 5°C (10 min and 5 min) to ensure clear supernatants.

For paracetamol, 50 µL of plasma was spiked with 10 µL of methanol and 150 µL of internal standard working solution (paracetamol-d3). Following vortex mixing and centrifugation at 6596 × *g* for 10 min, 10 µL of the supernatant was diluted with 90 µL ultrapure water – methanol (1:1 v/v) mixture, homogenised and analysed.

For doxorubicin quantification, 50 µL of rat plasma was spiked with 10 µL ultrapure water and 150 µL of internal standard working solution (daunorubicin). Samples were vortexed, centrifuged at 6596 × *g* for 10 min, and the supernatant was injected.

For isoprenaline, 50 µL of plasma was mixed with 10 µL of ultrapure water, 40 µL of internal standard working solution (paracetamol), and 20 µL of 0.1 g/mL trichloroacetic acid solution for protein precipitation. Samples were centrifuged at 6596 × *g* at 4 °C for 10 min before being transferred into autosampler vials.

3.4.4.2. Preparation of urine and cell culture medium samples

Sample preparation for alternative matrices was adapted to the specific properties of the samples.

For gentamicin, 50 µL of rat urine was mixed with 10 µL of ultrapure water, 10 µL of internal standard (kanamycin) working solution, and 150 µL of 0.1 g/mL trichloroacetic acid solution. Prior to this spiking, urine samples were centrifuged twice (10 min and 5 min) at 14841 × *g* at room temperature to remove particulate matter, if necessary.

For paracetamol, 10 µL of cell culture medium sample was diluted with ultrapure water – methanol (1:1 v/v) mixture (990 µL) and homogenised. After that, the sample preparation process was the same as for plasma samples.

For amoxicillin and clavulanic acid, 100 µL of cell culture medium sample was diluted with 900 µL of ultrapure water, and vortexed in an autoinjector vial.

3.5. *In vitro* studies in hepatocyte model

Primary hepatocytes were isolated from male Wistar rats weighing approximately 200-250 g. The isolated cells were cultured in collagen-precoated plates using a 1:1 mixture of Williams' medium E and Ham's F-12 nutrient mixture. This basal medium was supplemented with other additives (10 mM HEPES, 2.2 g/L NaHCO3, 6.9 mM glucose, and 1.25 mL/L gentamicin).

During the cell-attachment phase, the culture medium was further supplemented with 5 % heat inactivated fetal bovine serum. The hepatocyte cultures were maintained at 37 °C and 5% of CO_2. Following an overnight incubation to facilitate cell attachment, the hiFBS-containing medium was replaced with an hiFBS-free complete medium for a 24-hour acclimatization period.

The hepatocytes in monolayer were exposed to 1) paracetamol or 2) amoxicillin and clavulanic acid, which were formulated in 7.5 mL of the hiFBS-free complete medium. To analyse the effect of paracetamol, cells were exposed to concentrations of 1 mM and 10 mM. To evaluate the combination of amoxicillin and clavulanic acid, cells were treated with amoxicillin at 15 µg/mL and clavulanic acid at 5 µg/mL alone or in combination. A control group was incubated with drug-free complete medium.

In parallel with the cellular experiments, cell-free stability controls (incubation of the treatment medium without cells) were maintained under identical conditions to assess the spontaneous degradation of the compounds in the culture medium. Paracetamol was evaluated in these cell-free systems at concentrations of 1 mM and 10 mM, along with amoxicillin (15 µg/mL) and clavulanic acid (5 µg/mL) were tested both individually and in combination.

Both the hepatocyte cultures and the cell-free samples were incubated with their respective treatments at 37 °C for 24 hours. At the end of the 24-hour treatment period, the culture media from all Petri dishes (including the cell-free controls) were collected into 50-mL sterile centrifuge tubes. To prepare the samples for further investigation, the collected media were centrifuged at 2500 × *g* for 15 minutes at 4 °C, and the resulting supernatants were carefully removed and stored at -75 ± 10 °C.

3.6. *In vivo* toxicity studies

In vivo experiments were performed using male Han-Wistar rats across all study groups (Toxi-Coop Toxicological Research Centre). The animals weighed approximately 200-250 g at the beginning of the study. The administration volume was maintained at 2 mL/kg for both intraperitoneal and intravenous routes and 20 mL/kg for oral dosing. Blood samples were drawn from the retroorbital plexus. Urine samples were collected using individual metabolic cages.

In the gentamicin toxicity study, animals (N=5 per group) received intraperitoneal injections of gentamicin sulphate (daily dose of 120 mg/kg) or physiological saline for nine consecutive days. Blood and urine samples were collected pre-dose, on days 5, and 10.

For the paracetamol toxicity study, animals (N=5 per group) were administered a single oral dose of 500 or 1000 mg/kg *via* gavage, with the vehicle control group

receiving 0.5 % methyl-cellulose in distilled water. Blood was collected pre-dose, as well as at 8-, 24-, and 48-hours post-administration, coinciding with study termination.

In the doxorubicin cardiotoxicity model, intravenous injections of doxorubicin (3 or 6 mg/kg) were administered on days 0, 4, and 8, compared against an untreated control group (N=3 per group). Following pre-dose blood sampling on day 0, the study was terminated on day 12, four days after the final dose, with the collection of terminal blood.

Prior to the main isoprenaline toxicity study, a pharmacokinetic pilot experiment was conducted. The animals (N=3) received a single intravenous injection of isoprenaline hydrochloride at a dose of 50 mg/kg. Blood samples were collected into K3-EDTA tubes at 0, 5, 10, 20, 30, 60, and 120 minutes, as well as 4 hours post-treatment. To prevent degradation, the samples were centrifuged at 4 °C, and the isolated plasma was transferred into amber Eppendorf tubes and immediately placed on dry ice.

3.7. Data analysis

Instrument control, data acquisition, and chromatographic peak integration for both the LC-MS/MS and HPLC-FLD systems were performed using the Shimadzu LabSolutions software. Calibration curves were generated using a weighted ($1/x^2$) least-squares linear regression model in most of the experiments, with the exception of isoprenaline, where an unweighted exponential curve fitting was used. Bioanalytical method validation, including the assessment of accuracy, precision (CV%), recovery and stability (expressed as deviation under different storage conditions) was conducted in accordance with the ICH M10 guideline (Equations 1-4). For the quantification of the endogenous biomarker protoporphyrin IX, the validity of the surrogate matrix approach was confirmed by evaluating the parallelism between the calibration curves (Equation 5). (55)

Accuracy (%) = [(measured conc.-nominal conc.)/nominal conc.] ×100 (Eq. 1.)

Precision (CV%) = (standard deviation/mean conc.) ×100 (Eq. 2.)

Recovery (%) = (processed peak area/post-spiked peak area) ×100 (Eq. 3.)

Deviation (%) = [(stored peak area /freshly prepared peak area) ×100]-100 (Eq. 4.)

Slope Difference (%) = $\left(\frac{1}{1+B} - 1\right) \times 100$ (Eq. 5.)

(Where B is the ± % bias accuracy acceptance criterion for the assay.)

The toxicokinetic parameters from the *in vivo* IPGE study were determined using non-compartmental analysis. Calculations were performed with Phoenix WinNonlin software (version 8.1), yielding pharmacokinetic parameters such as maximum plasma concentration (C_{max}), time to maximum concentration (T_{max}), area under the curve (AUC_{last}, AUC_{inf}), and elimination half-life ($t_{1/2}$).

The toxicokinetic parameters from the *in vivo* isoprenaline study were calculated manually. For this specific evaluation, the area under the curve up to the last measurable concentration (AUC_{last}), the dose-normalized AUC_{last} ($AUC_{last/dose}$), and the elimination half-life ($t_{1/2}$) were determined with the following equations (Equations 6-8). The half-life was calculated using linear interpolation.

$$AUC_{last} = \sum_{i=1}^{n} \frac{(C_{i-1}+C_i)}{2} * (t_i - t_{i-1}) \quad \text{(Eq. 6.)}$$

(Where Cn and C_{n-1} are the plasma concentrations at time points t_n and t_{n-1}, respectively.)

$$AUC_{last/dose} = AUC_{last} / \text{dose} \quad \text{(Eq. 7.)}$$

(Where dose represents the administered amount of the compound per unit of body weight.)

$$t_{1/2} = t_1 + \frac{(C_{1/2}-C_1)}{(C_2-C_1)} * (t_2 - t_1) \quad \text{(Eq. 8.)}$$

(Where $C_{1/2}$ is the half of the maximum concentration, while C_1 and C_2 are the concentrations measured at time points t_1 and t_2 between which the half-life is interpolated.)

The results were expressed as the mean ± standard deviation (SD) or mean ± standard error of the mean (SEM) or presented as box plots displaying the minimum, first quartile (Q1), median, third quartile (Q3), and maximum values.

4. RESULTS

4.1. Elaboration of a method for the toxicokinetic evaluation of isopropyl glycidyl ether

4.1.1. Method development for IPGE

The most challenging aspect of the bioanalytical method development for IPGE was the molecule's low ionisation efficiency and lack of chromophores. Initial attempts to develop an LC-ESI-MS/MS method using the ammonium adduct of the molecular ion resulted in a lower limit of quantification (LLOQ) of 5 µg/mL. In order to achieve this, 20 mM ammonium acetate in ultrapure water and acetonitrile were used as mobile phases. However, rat plasma samples obtained from the pilot toxicity study at a dose of 1000 mg/kg required higher sensitivity, as no measurable concentrations of the analyte could be detected at this LLOQ. To address this limitation, an in-source derivatisation strategy based on the gas-phase Meerwein reaction was implemented rather than performing derivatisation during sample preparation. During method development, the two most common API ionisation techniques (ESI and APCI), as well as different mobile phase modifiers (no modifier; formic acid 0.1 %; formic acid 0.5 %; formic acid 1 %; acetic acid 0.5 %, trifluoroacetic acid 0.05 %), were systematically evaluated. (T 1) The APCI source in positive ionisation mode, and using acetonitrile as both eluent and derivatising reagent modified with formic acid, provided the highest signal intensity. The optimized method resulted in a 500-fold increase in sensitivity, enabling the establishment of an LLOQ of 0.01 µg/mL for toxicokinetic studies. Representative MRM chromatograms of the final method are presented in Figure 1.

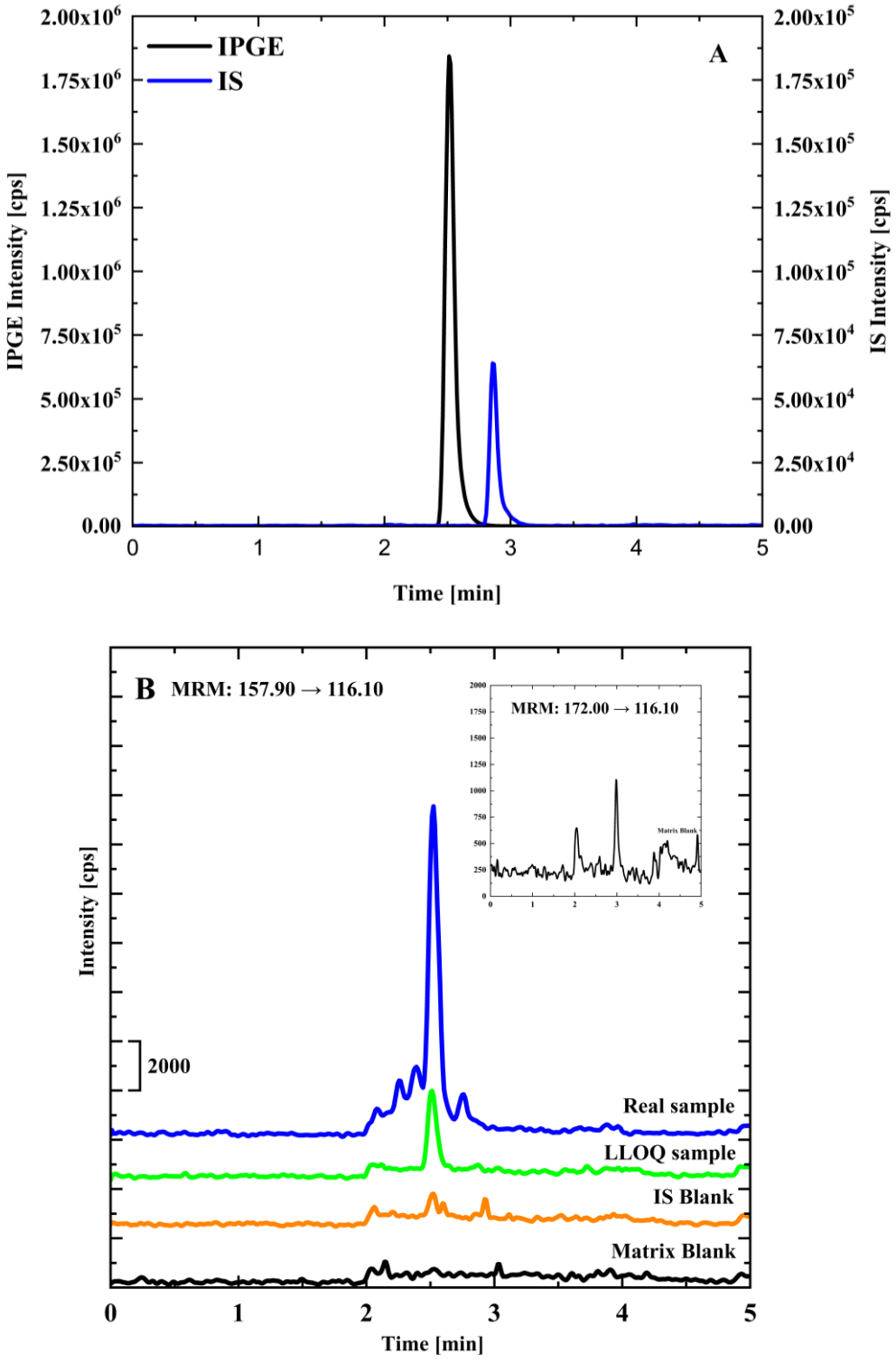

Figure 1. (T 1)

A) Representative MRM chromatograms of IPGE [157.90 → 116.10 m/z] and IS (*tert*-butyl glycidyl ether) [172.00 → 116.10 m/z] in ULOQ sample: IPGE (black), IS (blue).

B) Representative MRM chromatograms of the IPGE [157.90 → 116.10 m/z]: matrix blank (black), IS blank (orange), LLOQ sample (green) and a real study sample (blue), inset: MRM chromatogram of the corresponding IS (*tert*-butyl glycidyl ether) [172.00→ 116.10 m/z] in the matrix blank sample as proof of selectivity for IS (black)

4.1.2. Method validation for IPGE

The optimized LC-APCI-MS/MS method was validated according to the guideline established by International Council for Harmonisation of Technical Requirements for Pharmaceuticals for Human Use (ICH M10). Selectivity was confirmed by the absence of interfering peaks at the retention times of the analyte and the internal standard in blank plasma samples. The method demonstrated excellent linearity over the concentration range of 0.01 - 10 µg/mL, with the correlation coefficient (r^2) exceeding 0.99. A LLOQ of 0.01 µg/mL was established to ensure sufficient sensitivity. The method showed reliable intra-day and inter-day accuracy and precision, with coefficients of variation (CV%) within the acceptable limits of ≤15% and ≤20% at the LLOQ, respectively. Recovery values ranged between 94.6% and 106% (peak area). Stability studies indicated that IPGE remained stable in frozen plasma at -75 °C ± 10 °C and after multiple freeze-thaw cycles, but degraded when stored in rat plasma at room temperature for 24 hours. Based on these findings, appropriate sample handling procedures were established, requiring sample processing within 4 hours to ensure data accuracy. The validation results are summarized in Table S 9.

4.1.3. Toxicokinetic characterisation of IPGE

The validated method was applied to a single-dose oral toxicity study in rats. Plasma concentration-time profiles were obtained for all three dose groups (1000, 1500 and 2000 mg/kg) following oral IPGE administration. (Figure 2.) Table 1 details the toxicokinetic parameters of mean plasma concentration profiles. IPGE was rapidly absorbed, with the peak plasma concentrations (T_{max}) reached between 0.5-hour (at the doses of 1500 and 2000 mg/kg) and 1-hour post-dose (at the dose of 1000 mg/kg). The results demonstrated that C_{max} and AUC values increased more than proportionally with dose, indicating non-linear pharmacokinetic behaviour. The elimination half-life of IPGE was approximately 9 hours at the lowest dose (1000 mg/kg), and increased to 13–15 hours at higher doses (1500 and 2000 mg/kg), suggesting saturation of metabolic pathways. At the highest dose (2000 mg/kg) mortality was observed, which may be attributed to high plasma concentrations reaching up to 162 µg/mL.

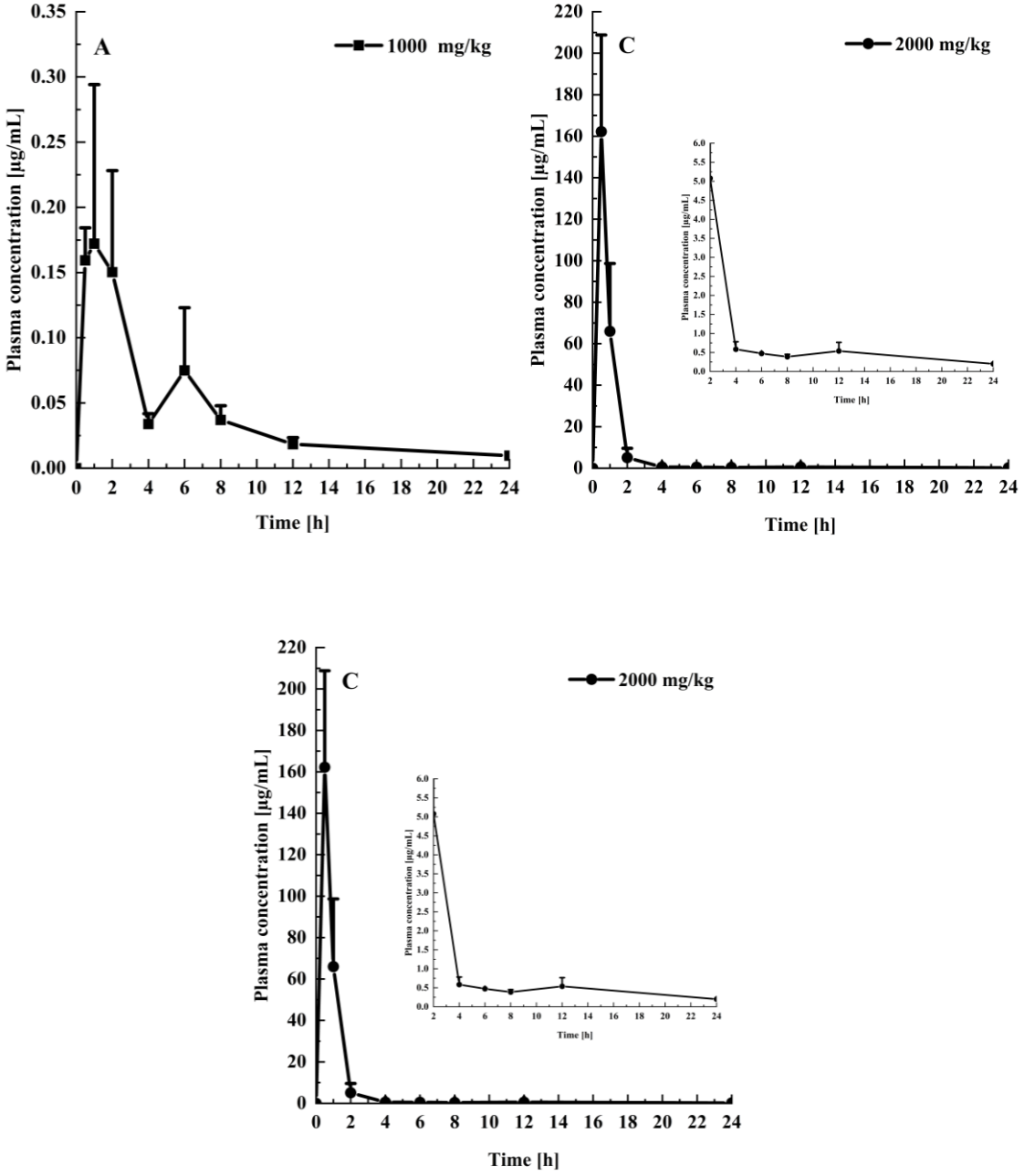

Figure 2. (T 1)

Plasma concentration - time profiles in rats after oral administration of IPGE at three dose levels (A: 1000 mg/kg; B: 1500 mg/kg; C: 2000 mg/kg). The points represent the mean plasma concentrations of 3-6 animals, whereas the whiskers are for the SEM values. Inset figures show the terminal elimination phase magnified, open symbol indicates exclusion from the terminal elimination phase fit.

Table 1. (T 1) Toxicokinetic parameters of IPGE mean plasma concentration profiles study at three dose levels (1000, 15000 and 2000 mg/kg)

Toxicokinetic parameters	Unit	Dose level		
		1000 mg/kg	**1500 mg/kg**	**2000 mg/kg**
T_{lag}	[h]	0	0	0
T_{max}	[h]	1.0	0.5	0.5
C_{max}	[µg/mL]	0.172	16.2	162
SE _C_{max}	[µg/mL]	0.0878	10.3	46.6
C_{max}/dose	[kg×µg/mL/mg]	0.000172	0.0108	0.0811
AUC_{last}	[h×µg/mL]	0.967	12.4	147
AUC_{last}/dose	[h×kg×µg/mL/mg]	0.000967	0.00827	0.0735
SE_AUC_{last}/dose	[h×kg×µg/mL/mg]	0.202	5.17	32.8
AUC_{all}	[h×µg/mL]	0.967	12.41	147.01
SE_AUC_{all}	[h×µg/mL]	0.202	5.17	32.8
MRT_{last}	[h]	6.02	4.02	1.40
No.points λ_z	-	3	3	3
Rsq	-	0.913	0.996	0.985
Rsq_{adj}	-	0.827	0.993	0.970
$t_{½\lambda}$	[h]	8.94	13.2	15.2
AUC_{inf}	[h×µg/mL]	1.09	14.5	151
AUC_{inf}/dose	[h×kg×µg/mL/mg]	0.00109	0.00969	0.0757
$AUC_{\%ext}$	[%]	11.3	14.7	2.90
MRT_{inf}	[h]	9.50	9.75	2.69

4.1.4. Identification of Possible Isopropyl Glycidyl Ether Metabolites

Qualitative analysis of plasma samples obtained from the toxicokinetic study revealed seven metabolites. The predicted metabolites were suggested based on the articles by Chen et al. (22) and Eadsforth et al (21) about the metabolism of *n*-butyl glycidyl ether, which is structurally similar to IPGE. *N*-Butyl glycidyl ether has been reported to be metabolized *via* two major pathways: 1) hydration to form a diol metabolite and 2) conjugation with glutathione. Diol metabolite underwent further metabolism to sulphate or glucuronide conjugates or *a*-hydroxy acid, which was transaminated and *N*-acetylated.

Metabolic profiling of IPGE was based on the evaluation of retention times and the detection of characteristic m/z signals in SIM mode. In the 12-minute-long LC-MS/MS method used for metabolite screening, an ESI source was utilized. Analysis was

conducted in negative ion mode for the sulphate and glucuronide conjugates, while positive ion mode was applied for the remaining metabolites. The mobile phase consisted of water and acetonitrile, both containing 0.5% formic acid. The primary metabolic pathway involved epoxide ring opening *via* hydrolysis, leading to the formation of the diol metabolite 3-isopropoxy-2-hydroxy-1-propanol (M1). This metabolite underwent further oxidation to form 3-isopropoxy-2-hydroxypropionic acid (M5). Several Phase II conjugates were also identified, indicating detoxification pathways that converted the reactive epoxide and its metabolites into less toxic forms. The glutathione pathway was represented by the direct glutathione conjugate of IPGE (M11). The hydrolysed diol metabolite (M1) underwent conjugation with sulphate and glucuronic acid forming M3, and M4 metabolites, respectively. Additionally, oxidation of the hydroxypropionic acid metabolite (M5) generated an α-keto-acid intermediate, which served as a precursor for transamination, followed by *N*-acetylation to *O*-isopropyl-*N*-acetylserine (M6) and *O*-(hydroxy-isopropyl)-*N*-acetylserine (M7). Representative SIM chromatograms of the possible metabolites (listed in Table 2 along with their names, molecular weights, mass-to-charge ratio values, and retention times) are shown in Figure 3.

Table 2. List of the possible metabolites

Metabolite	Name	molecular weight [g/mol]	mass-to-charge ratio [m/z]	retention time [min]
M1	3-isopropoxy-2-hydroxy-1-propanol	134	135	2.6
M3	Sulfate-conjugate of IPGE	214	213	3.3
M4	Glucuronide-conjugate of IPGE	310	309	2.8
M5	3-isopropoxy-2-hydroxypropionic acid	148	149	2.7
M6	*O*-isopropyl-N-acetylserine	189	190	3.2
M7	*O*-(hydroxy-isopropyl)-*N*-acetylserine	205	206	2.9
M11	Glutathione-conjugate of IPGE	423	424	3.0

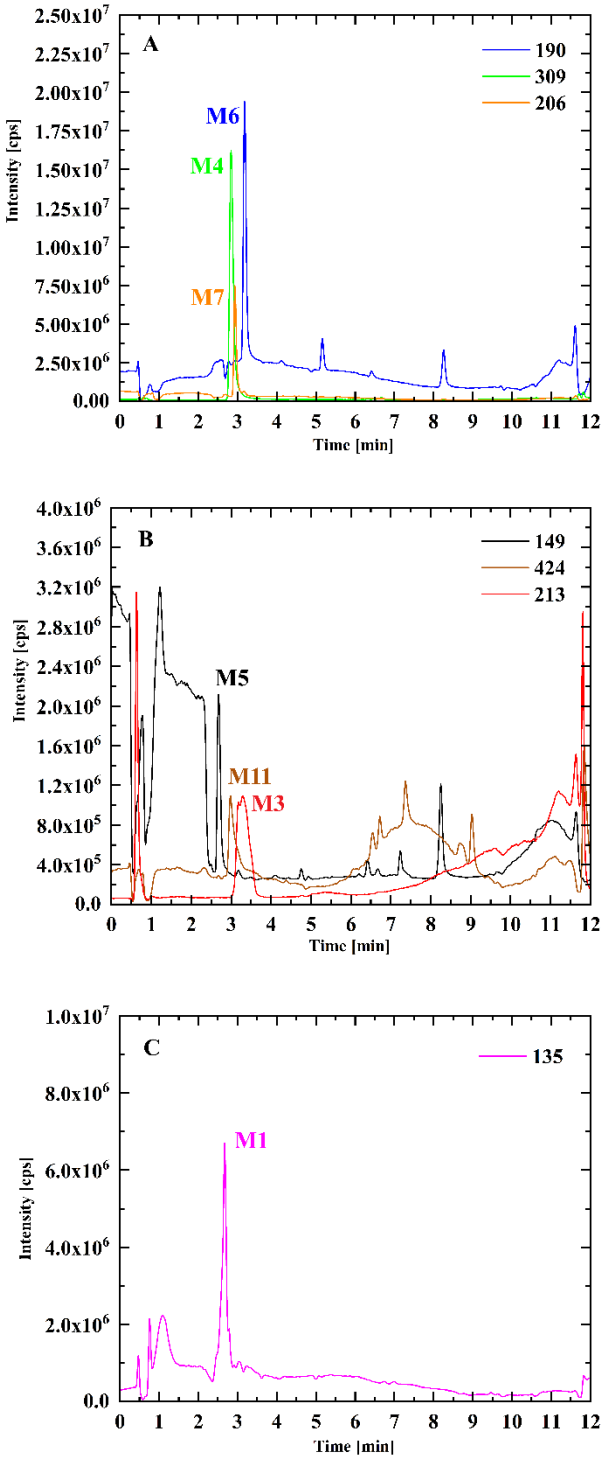

Figure 3. (T 1)
Representative SIM chromatograms of the IPGE metabolites (injection volume: 1-1-10 µL) **A**) *O*-isopropyl-*N*-acetylserine (M6) 190 *m/z* (blue), glucuronide-conjugate of IPGE (M4) 309 *m/z* (green), *O*-(hydroxy-isopropyl)-*N*-acetylserine (M7) 206 *m/z* (orange); **B**) 3-isopropoxy-2-hydroxypropionic acid (M5) 149 *m/z* (black), glutathione-conjugate of IPGE (M11) 424 *m/z* (brown), sulphate-conjugate of IPGE (M3) 213 *m/z* (red); **C**) 3-isopropoxy-2-hydroxy-1-propanol (M1) 135 *m/z* (magenta)

4.2. Challenges in the quantification of endogenous biomarker protoporphyrin IX

4.2.1. Optimization of chromatographic and detection conditions for protoporphyrin IX

To achieve optimal separation for protoporphyrin IX, several chromatographic parameters were evaluated. Based on the results of Benton et al. regarding the stationary phase, an ACE Ultracore SuperC18 column was selected for chromatographic separation. (138) Fluorescence detection wavelengths were optimized to Ex=405 nm and Em=630 nm, providing the highest signal-to-noise ratio for protoporphyrin IX while minimizing background interference from the rat plasma matrix. Carry-over was eliminated by using 2-propanol as a washing solvent. Representative HPLC-FLD chromatograms of the method are shown in Figure 4.

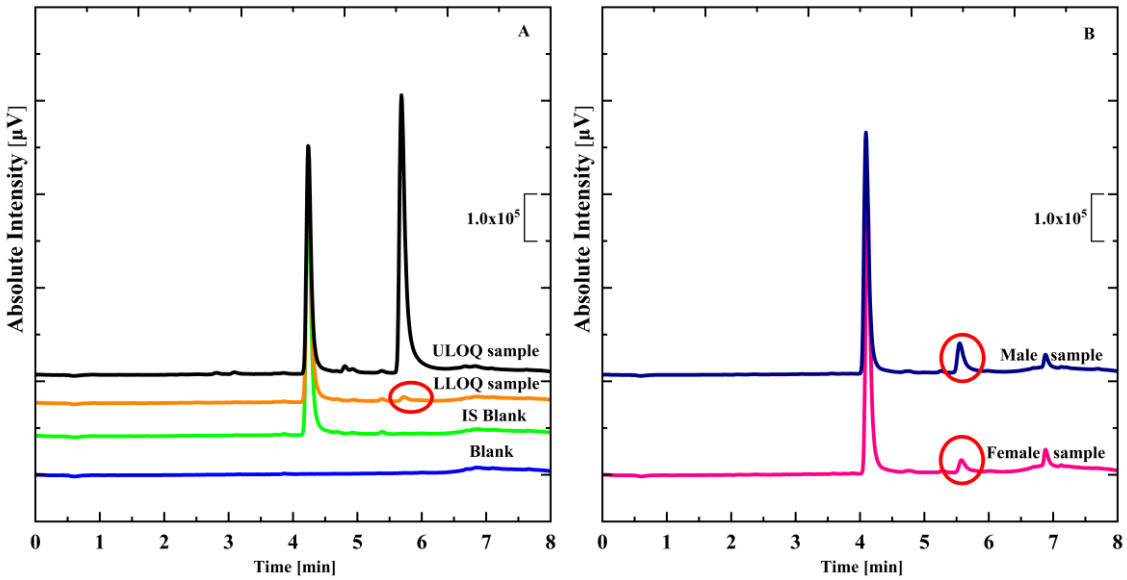

Figure 4. (T 2)
Representative HPLC-FLD chromatograms of protoporphyrin IX
HPLC-FLD Chromatograms recorded at 630 nm in surrogate and authentic matrices.

A) Blank sample in surrogate matrix (blue), IS (mesoporphyrin IX) blank sample in surrogate matrix (green), LLOQ sample (10 ng/mL) in surrogate matrix with red circle on the analyte peak (orange), ULOQ sample (700 ng/mL) in surrogate matrix (black)

B) Individual plasma sample from a female rat in authentic matrix (pink), individual plasma sample from a male rat in authentic matrix (navy blue), both with red circle on the analyte peak.

4.2.2. Characterisation of the surrogate matrix

The presence of endogenous protoporphyrin IX in rat blank plasma makes it challenging to obtain a true blank matrix, resulting in false concentration values. To address this issue, a surrogate matrix, analyte-free plasma (Figure 4 A – blue line) was produced by photodegradation. Exposure of authentic plasma (Figure 4 B) to visible light for 4 hours resulted in the complete elimination of the endogenous protoporphyrin IX content. However, the exposure to visible light for less than 4 hours did not remove protoporphyrin IX properly. The internal standard (mesoporphyrin IX) was added post-treatment; therefore, it remained unaffected by photodegradation. This process yielded a suitable "analyte-free" matrix that closely mimicked the physical and chemical properties of the authentic matrix.

4.2.3. Validation using the surrogate matrix approach

The suitability of the surrogate matrix approach was confirmed through comprehensive validation. Selectivity assessments demonstrated that the processed surrogate matrix was free from notable interference at the retention time of protoporphyrin IX, ensuring method selectivity. A critical requirement for endogenous biomarkers, parallelism, was established by comparing the two regression slopes of calibration curves prepared either by spiking in the surrogate matrix or obtained in the authentic matrix using the standard addition method. (55) The slopes were comparable, thereby verifying that the surrogate matrix is a valid substitute for the authentic biological fluid for quantification purpose. Additionally, quality control samples prepared in the authentic (low, medium, high) and surrogate matrix (LLOQ) consistently met the acceptance criteria, with accuracy within ±15% and precision below 15% (±20% and below 20% for LLOQ) across the validated calibration range of 10–700 ng/mL. Table S 10 summarizes the result of the validation process.

4.2.4. Measurement of protoporphyrin IX in rat plasma

The applicability of the method was demonstrated in a rat model treated with the protoporphyrin IX precursor, 5-aminolaevulinic acid. Following oral administration of 5-aminolaevulinic acid (100 mg/kg), a significant time-dependent increase in plasma

protoporphyrin IX levels was observed. The concentration-time profiles showed a clear accumulation of protoporphyrin IX, reaching a maximum 2 hours post-dose, followed by a gradual decline. By the 24-hour sampling point, the protoporphyrin IX levels declined to values comparable to the pre-dose and control group concentrations (Figure 5).

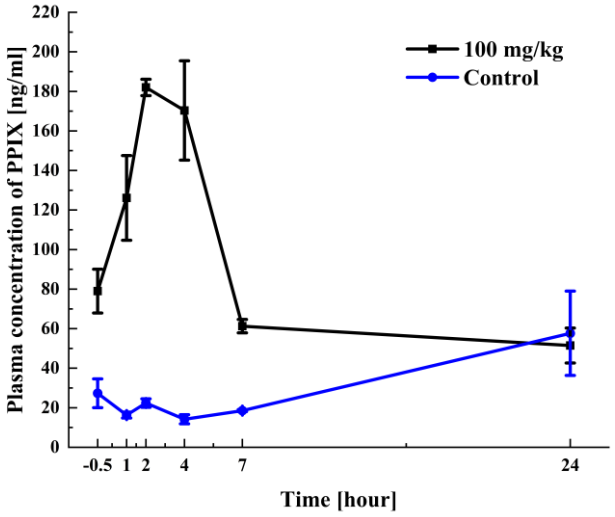

Figure 5. (T 2)

Concentration-time profiles of protoporphyrin IX in untreated and 5-aminolaevulinic acid treated rats

Time curves of protoporphyrin IX plasma concentrations in male rats following single 5-aminolaevulinic acid treatment (mean values with SEM). Black line with squares: dosed group (received 100 mg/kg 5-aminolaevulinic acid); blue line with circles: control group (received vehicle only).

4.3. Bioanalysis of pharmaceuticals

Reliable toxicity assessment of diverse chemical agents, including human and veterinary drugs as well as agrochemicals, is a fundamental requirement for regulatory compliance, commercial viability, and public safety. However, evaluating organ-specific damage, especially hepatotoxicity, nephrotoxicity, and cardiotoxicity, remains a significant challenge. Conventional biomarkers frequently lack specificity and are often unable to indicate adverse effects at an early stage. The primary aim of the joint research project between Toxi-Coop Toxicological Research Centre and HUN-REN Research Centre for Natural Sciences (2020-1.1.2-PIACI-KFI-2020-00021) was the discovery and development of innovative, extracellular vesicle-derived microRNA biomarkers for safety assessment of chemicals. Because microRNAs act as upstream regulators of

protein synthesis, they offer a promising avenue for capturing early-stage signs of toxicity.

To support the discovery of these biomarkers, a tiered experimental workflow was implemented. In accordance with the 3R (Replacement, Reduction, Refinement) principles, the study was initiated with *in vitro* test systems using rat primary hepatocytes treated with hepatotoxic model compounds (paracetamol and amoxicillin + clavulanic acid). Subsequently, the research advanced to *in vivo* rat models to induce and monitor organ-specific damage using established toxicants for the liver (paracetamol), heart (doxorubicin, isoproterenol), and kidneys (gentamicin). Accurate evaluation of the dose-response relationships in these *in vitro* and *in vivo* studies required precise determination of drug concentrations in cell culture medium, blood plasma and urine. Bioanalytical methods were established for various model toxicants to support organ-specific safety studies. Full validation was performed for the primary nephrotoxicity model compound (gentamicin), while "fit-for-purpose", qualified methods were implemented for other agents to confirm exposure.

4.3.1. Nephrotoxicity model compound: gentamicin

The LC-ESI-MS/MS method developed for the quantification of gentamicin was fully validated in both rat plasma and urine matrices. Selectivity was demonstrated by the absence of interfering peaks at the retention times of the gentamicin components (C1, C1a, C2/C2a) and the internal standard (kanamycin) in blank samples from both matrices. The method showed excellent linearity over the concentration range of 20-2000 ng/mL. The LLOQ was established at 20 ng/mL for both plasma and urine, providing sufficient sensitivity for monitoring drug levels in the nephrotoxicity study.

Precision and accuracy were evaluated at four quality control levels. Intra-day and inter-day precision (CV%) values were well within acceptable limits, remaining below 12.4% for plasma and 13.7% for urine. Accuracy was similarly robust, ranging within ±14.8% for plasma and ±13.5% for urine, thereby meeting the predefined acceptance criteria. Extraction recovery was consistent across low, medium, and high-quality control levels (ranging from 89.5% to 114%), while matrix effect assessments indicated no significant ion suppression or enhancement, with precision and accuracy deviations remaining within ±15%. The results of the validation process are in Table S 11.

Furthermore, the stability studies demonstrated that gentamicin was stable in biological matrices under various conditions. No significant degradation was observed after storage at room temperature for 24 hours, after three freeze-thaw cycles, or during long-term storage at -75 °C (validated up to 83 days for plasma and 8 days for urine). Autosampler stability was also confirmed at 5 °C, ensuring the integrity of processed samples during batch analysis. Chromatographic separation was achieved on an Supel^{TM} Carbon LC column using a rapid, 7-min gradient program. The method demonstrated good linearity and specificity, enabling reliable quantification of antibiotic concentrations in both plasma and urine matrices throughout the treatment period, despite the challenge of the complex matrix composition (Tables S 11). Representative MRM chromatograms of the method for gentamicin are depicted in Figure 6 in plasma matrix.

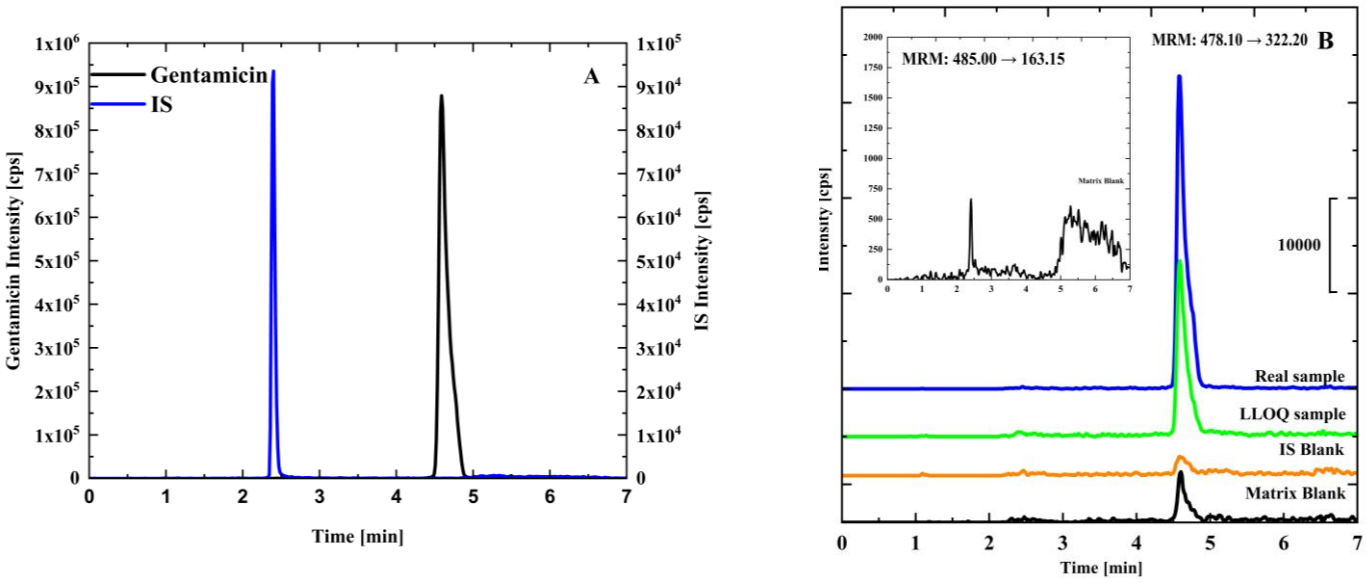

Figure 6.

A) Representative MRM chromatograms of gentamicin C1 [478.10 → 322.20 m/z] and IS (kanamycin) [485.00 → 163.15 m/z] in ULOQ plasma sample: analyte (black), IS (blue).

B) Representative MRM chromatograms of the analyte gentamicin C1 [478.10 → 322.20 m/z]: matrix blank (black), IS blank (orange), LLOQ sample (green) and a real study sample (blue), inset: MRM chromatogram of the corresponding IS (kanamycin) [485.00 → 163.15 m/z] in the matrix blank sample as proof of selectivity for IS (black) all in plasma

Daily administration of 120 mg/kg gentamicin to male Wistar rats resulted in mean plasma concentrations of 54.3±15.6 ng/mL and 72.1±22.5 ng/mL on days 5 and 10, respectively. After a 16-hour collection period, the mean urinary concentrations were

several orders of magnitude higher than those in plasma, 30,900±19,700 ng/mL and 26,200±7,761 ng/mL on days 5 and 10 (Figure 7). Furthermore, both urinary and plasma concentrations were similar on days 5 and 10.

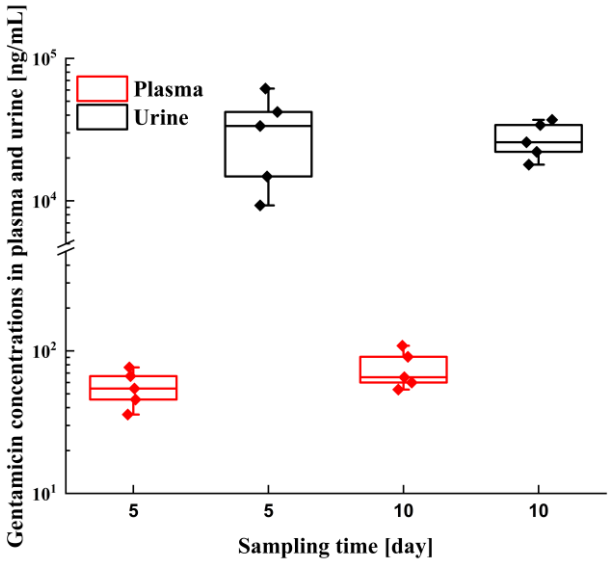

Figure 7. Gentamicin concentrations in rat plasma and urine sampled on the day 5 and 10 after intravenous administration of 120 mg/bodyweight kg daily dose) (N=5) in the nephrotoxicity study.

Gentamicin plasma (red) and urinary (black) concentrations are presented in box plots. Plasma and urine samples were collected on days 5 and 10. The box plots represent the minimum, first quartile (Q1), median, third quartile (Q3), and maximum values. Individual data points are shown as diamonds.

4.3.2. Hepatotoxicity and cardiotoxicity models

For the well-characterised model toxicants used in hepatotoxicity and cardiotoxicity studies, rapid LC-MS/MS methods were developed, focusing primarily on linearity, sensitivity (LLOQ), and specificity required for *in vitro* and *in vivo* exposure verification. Unlike the comprehensive validation performed for the nephrotoxicity model, these methods were optimized for high-throughput and immediate applicability in screening studies. To ensure data reliability, even for these rapid methods, the qualification included at least three independent analytical runs, with calibration and six replicates at each quality control level, thereby verifying the reliability of the method performance.

4.3.2.1. Hepatotoxicity model using paracetamol

To support the drug-induced liver injury model, a LC-ESI-MS/MS method was implemented for the quantification of paracetamol in cell culture medium for rat primary hepatocytes, as well as in rat plasma. Using a simple protein precipitation protocol with acetonitrile and paracetamol-d3 as the internal standard, the method provided a linear response across the wide concentration range expected in overdose scenarios. The chromatographic method (InertSustain C18 column) successfully separated the parent compound (RT: 3.1 min) from early-eluting polar matrix components. The LLOQ (0.1 µg/mL) and linearity (0.1-100 µg/mL) were sufficient to confirm systemic exposure levels corresponding to the hepatotoxic doses administered in the animal experiments. Validation results are summarized in Table S 12.

In the cell culture medium, where control (untreated) samples consistently measured 0 mM of paracetamol, the 1 mM and 10 mM dose groups yielded concentrations of 1.10 mM and 10.19 mM at 0 h and no chemical degradation was observed after 24h-incubation in cell-free culture medium. However, substantial decrease in paracetamol concentrations was detected (to 0.16 mM and 7.94 mM, respectively) after 24 h-incubation with hepatocytes.

In the *in vivo* rat model, following a single dose of 500 and 1000 mg/kg paracetamol, the intact parent compound was detectable in plasma for 8 hours at the low dose and for 24 hours at the high dose (Figure 8 A). Eight hours after administration of 500 and 1000 mg/kg dose of paracetamol, approximately twofold higher mean plasma concentrations were detected at high dose as compared to low dose (17.5 µg/mL at 500 mg/kg and 43.3 µg/mL at 1000 mg/kg). Due to the lack of available reference standards for the metabolites, their exact concentrations were not determined. Instead, relative trends were monitored by comparing chromatographic peak areas, adjusted using appropriate dilution factors. For the lower and higher doses, paracetamol sulphate was detected in plasma up to 24 and 48 hours (Figure 8 B), paracetamol glutathione up to 8 and 24 hours (Figure 8 C), and paracetamol glucuronide up to 24 and 48 hours, respectively (Figure 8 D). Although the analytical method was configured to monitor the paracetamol-cysteine and paracetamol-*N*-acetylcysteine metabolites, the concentrations of these metabolites in the analysed samples remained below the limit of detection.

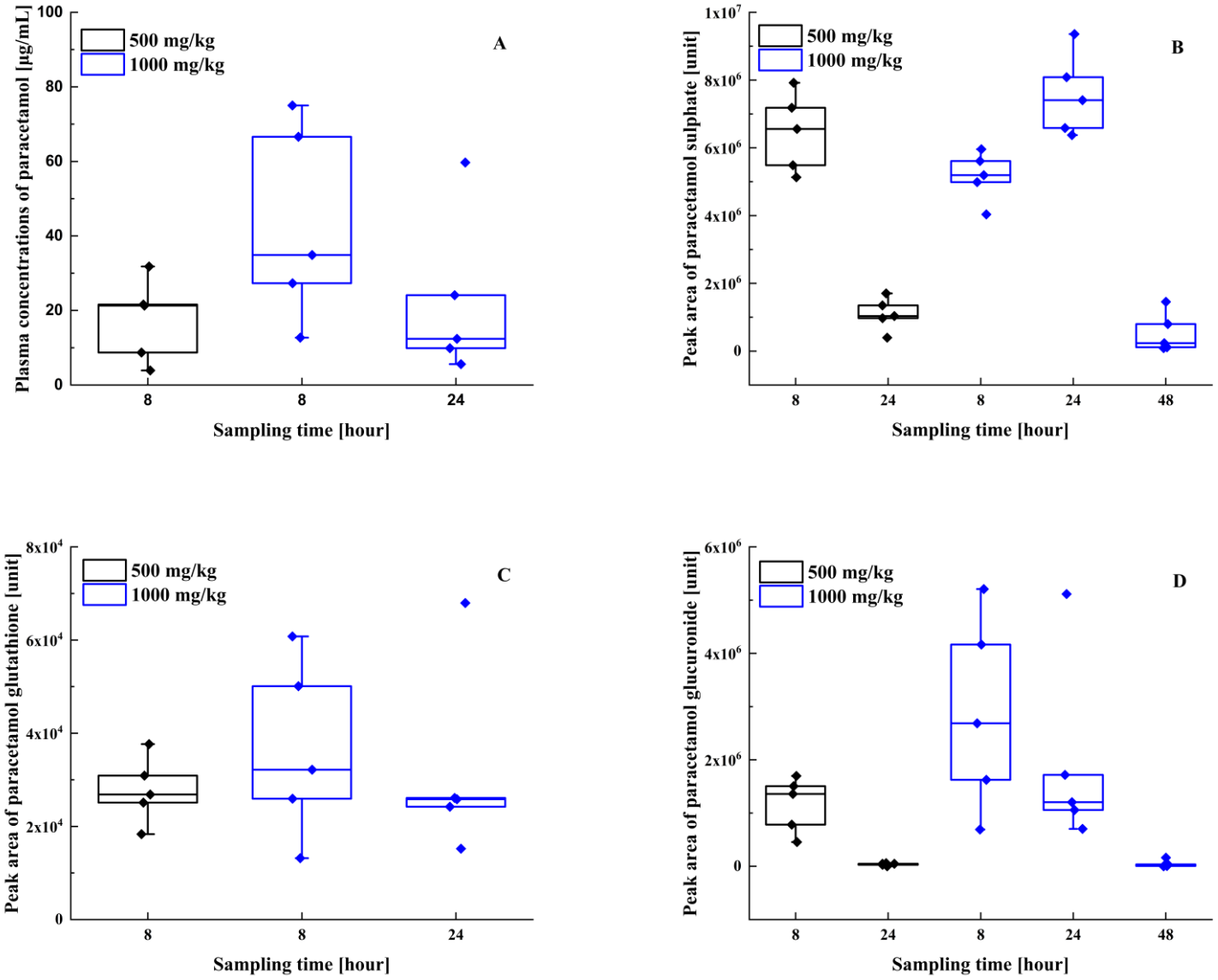

Figure 8. Concentrations of paracetamol (A) and its metabolites (B: paracetamol sulphate, C: paracetamol glutathione, D: paracetamol glucuronide) in rat plasma after oral administration of 500 and 1000 mg/kg paracetamol (N=5 per dose group).

4.3.2.2. Hepatotoxicity model using combination of amoxicillin and clavulanic acid

The combination of amoxicillin and clavulanic acid has been reported to rarely induce liver injury in patients (139, 140); therefore, we investigated the hepatotoxic potential of single administration and the combination in the *in vitro* hepatocyte model. To support hepatotoxicity screening and determine the extent of drug exposure, an LC-MS/MS

method was developed and optimized for the simultaneous quantification of amoxicillin and clavulanic acid in cell culture medium. Using the highly polar amoxicillin and the hydrolytically instable clavulanic acid, a simplified sample preparation involving a 10-fold dilution with water was applied. The method utilized positive electrospray ionisation as MS source and an InertSustain C18 (3µm, 2.1x75 mm) analytical column to achieve adequate sensitivity for both compounds. Table S 13 details the outcomes of the validation process.

In control cell culture medium, neither amoxicillin nor clavulanic acid was detected. In amoxicillin treated samples (alone or in combination with clavulanic acid), the concentrations of amoxicillin in the medium decreased by approximately 45% of the initial values during the 24-hour incubation with hepatocytes. A nearly identical decrease was observed after 24 hours of cell-free incubation. Clavulanic acid concentrations were substantially reduced to 13-16% of the initial values during the incubation with or without liver cells. Comparing the degradation profiles, clavulanic acid was more unstable in cell culture medium at 37°C than amoxicillin. The depletion for both compounds was essentially the same in the cell-free medium as in the presence of hepatocytes. The observed decreases represent chemical instability in the 37°C medium, and did not depend on enzymatic cellular metabolism. (Table 3)

Table 3. In vitro degradation of amoxicillin and clavulanic acid

	Concentration [µg/mL]		
Condition	Amoxicillin	Clavulanic acid	Amoxicillin + Clavulanic acid
0 min	15.5	6.11	15.6 + 5.96
cell-free incubation for 24 h	8.76	0.947	8.65 + 0.917
incubation with hepatocytes for 24 h	8.49	0.782	8.59 + 0.782

4.3.2.3. Cardiotoxicity model compound: doxorubicin (multiple-dose administration)

For the *in vivo* cardiotoxicity assessment following repeated administration of doxorubicin to male Wistar rats, a specific LC-MS/MS method was developed to measure doxorubicin levels in plasma. The method employed daunorubicin as an internal standard and utilized a YMC-Triart C18 column to ensure sharp peak shapes and adequate retention (RT: 1.8 min). Positive electrospray ionisation with MRM detection (544.20 → 397.05 m/z) provided high selectivity, effectively distinguishing the analyte from endogenous plasma components. The method was qualified to determine the circulating

drug levels, confirming that the administered repeated doses resulted in the expected systemic exposure associated with cardiomyopathy. The analytical validation parameters are provided in Table S 14.

Rats were treated with doxorubicin at doses of 3 and 6 mg/kg (corresponding cumulative doses of 9 and 18 mg/kg). Plasma samples were collected on day 12 (4 days after last treatment). The analytical results revealed somewhat higher plasma concentrations of doxorubicin in the high-dose group than expected based on the concentrations observed in the low-dose animals. The low- and high-dose cohorts exhibited mean plasma concentrations of 7.83±0.630 ng/mL and 22.0±3.89 ng/mL, respectively (Figure 9).

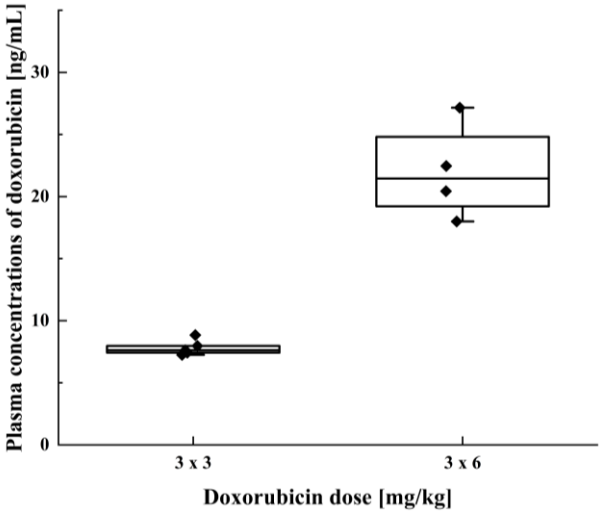

Figure 9. Doxorubicin concentrations in rat plasma cardiotoxicity study

Doxorubicin plasma concentrations in rats after repeated doses of 3 and 6 mg/kg (cumulative doses of 9 and 18 mg/kg). Plasma samples were collected on day 12 (4 days after last treatment). The box plots represent the minimum, first quartile (Q1), median, third quartile (Q3), and maximum values. Individual data points are shown as diamonds.

4.3.2.4. Cardiotoxicity Model Compound: Isoprenaline (Single-Dose Administration)

In the acute cardiotoxicity model, a single dose of isoprenaline (5 and 50 mg/kg) was administered to male Wistar rats, and blood samples were collected after 24 hours. The bioanalysis of isoprenaline presented a unique challenge due to its extreme instability and susceptibility to oxidative degradation. A specialized "rapid method" was qualified using a Kinetex-EVO C18 column and an acidified mobile phase (0.1% trifluoroacetic acid) to stabilize the catecholamine structure during analysis. Sample preparation involving

protein precipitation with trichloroacetic acid was employed instead of acetonitrile to maintain the target compound in solution. A fast 6-min method was achieved, with a 1-min retention time difference between the analyte and the internal standard (paracetamol). Despite the difficulty of analysing this hydrophilic compound, the method demonstrated sufficient linearity and sensitivity to verify the high-dose intravenous administration used to induce myocardial infarction-like injury in the rat model. The findings from the validation procedure are detailed in Table S 15.

Before initiating the main isoprenaline study, a preliminary experiment was performed using a single intravenous administration of 50 mg/kg to confirm the rapid elimination of isoprenaline. Analysis of the resulting toxicokinetic curve (Figure 10) yielded an AUC_{last} of 25,300 h×ng/mL, a dose-normalized AUC_{last} of 506 h×kg×ng/mL/mg, a clearance of 1.97 mL/h/kg, and a half-life of 3.46 min. The half-life was calculated using linear interpolation. The extremely short half-life of isoprenaline suggested that quantification of the parent compound at the main study's designated sampling times (8 and 24 hours after administration of isoprenaline dose) is unnecessary, as detectable levels are not expected in these samples.

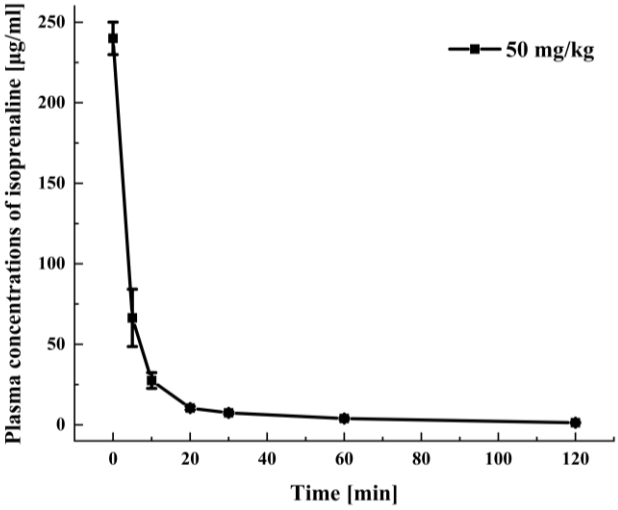

Figure 10. Concentration-time profiles of isoprenaline in male rats.

The time curve of isoprenaline plasma concentrations was determined in male rats following a single dose of 50 mg/kg (mean values with SEM).

5. DISCUSSION

The thesis highlights the role of tailored bioanalytical strategies for supporting various toxicological assessments. By successfully overcoming inherent analytical limitations, the developed methodologies provided essential kinetic data. These solutions include innovative strategies such as in-source derivatisation for IPGE, photobleaching-based surrogate matrix for protoporphyrin IX, and rapid analytical methods for pharmaceuticals. The following sections discuss the implementation and biological relevance of these analytical approaches and their application across various *in vivo* and *in vitro* toxicity models.

5.1. Challenges in the bioanalysis of IPGE

The toxicological assessment of industrial alkylating agents, such as glycidyl ethers, has long been hampered by the lack of sufficiently sensitive bioanalytical methods capable of quantifying these compounds in biological matrices. (16, 21, 22) The study presented here demonstrated that the physicochemical properties of isopropyl glycidyl ether (IPGE) — specifically its low molecular weight, high hydrophilicity, and lack of chromophores — pose substantial analytical challenges that cannot be adequately addressed by conventional approaches.

One of the pivotal findings of this research was the inadequacy of traditional electrospray ionisation for this class of compounds. As was found during method development, IPGE exhibited low proton affinity. Although formation of ammonium adduct ($[M+NH_4]^+$) could be optimized in ESI mode and yielded a stable signal, the sensitivity remained insufficient (LLOQ: 5 µg/mL). This limit rendered the method not fit-for-purpose, as the subsequent toxicokinetic study revealed that relevant plasma concentrations were several orders of magnitude below this threshold. These findings were consistent with previous reports indicating that conventional ionisation techniques often fail for small epoxides in the absence of derivatisation. (34, 35)

To address this limitation, a novel strategy based on APCI combined with an in-source derivatisation mechanism was successfully implemented. Specifically, exploitation of a gas-phase Meerwein reaction — where acetonitrile acted as a derivatising agent in the presence of formic acid —proved to be a major breakthrough (Figure 11). This reaction, occurring within the plasma corona discharge region, generated a stable cation resulting

in a 500-fold increase in sensitivity compared to the initial ESI method employing the ammonium adduct as the parent ion. This approach was inspired by the pioneering work of Wu et al. (141) and Bai et al. (32), who described this gas-phase reaction mechanism for pharmaceutical impurities based on the findings of Meurer and Eberlin (142). Moreover, the selection of APCI was further supported by its lower susceptibility to matrix effects compared to ESI, as reported by Souverain et al. (143)

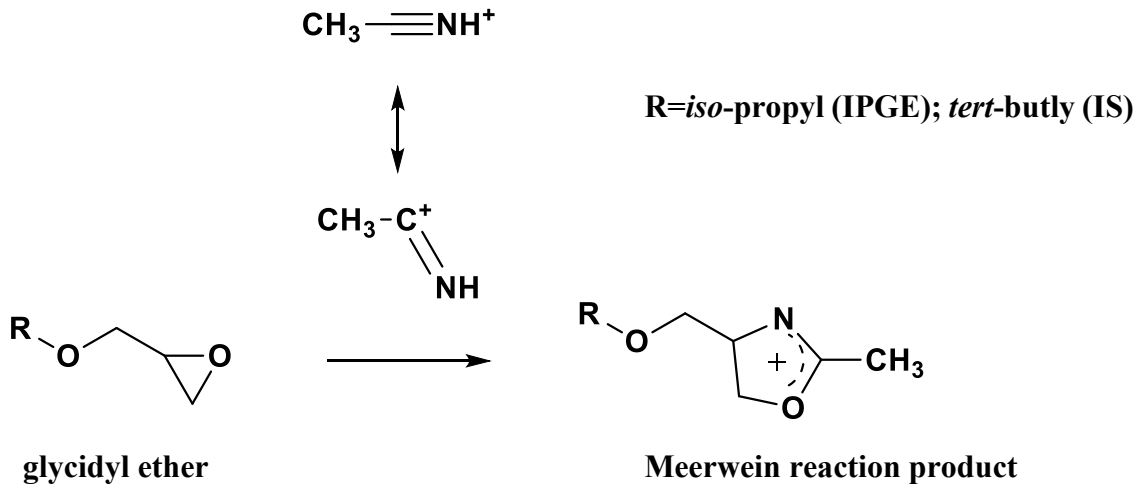

Figure 11. Reaction scheme of the Meerwein reaction taking place in the ion source

This methodological advancement was not merely a technical refinement but a prerequisite for the biological study. Without achieving LLOQ of 0.01 µg/mL, the non-linear pharmacokinetic behaviour and the saturation of metabolic pathways (Figure 12) at lower doses would have remained undetected. Based on the toxicokinetic evaluation (Table 1), IPGE was rapidly absorbed. The results demonstrated that AUC values increased more than proportionally with dose, indicating non-linear pharmacokinetic behaviour. The prolongation of the elimination half-life at higher doses further suggests saturation of metabolic pathways. The mortality observed at the highest dose (2000 mg/kg) may be attributed to high plasma concentrations (162 µg/mL), underscoring the toxicological relevance of the exposure levels.

The identification of seven putative metabolites indicated that IPGE underwent extensive biotransformation in rats. These metabolites were proposed based on the metabolic pathways of *n*-butyl glycidyl ether, as described by Chen et al. and Eadsforth

et al. for a structurally related glycidyl ether. (21, 22) Based on these findings, IPGE metabolism was proposed to proceed *via* two major pathways: 1) conjugation with glutathione, and 2) epoxide hydrolysis followed by oxidation and/or conjugation with sulphate and glucuronic acid as well as by transamination and acetylation, collectively contributing to detoxification and reduced reactivity of the parent compound. (Figure 12.) The detected Phase II conjugates suggested the involvement of detoxification pathways that convert the reactive epoxide and its intermediates into less toxic forms.

It should be noted that, in the absence of authentic analytical standards, the identification of these metabolites remained tentative and requires further confirmation using high-resolution mass spectrometry in future investigations. Nevertheless, the current findings provided a solid foundation for subsequent characterisation.

The handling of IPGE introduced an additional level of complexity due to its inherent reactivity. Stability assessments revealed that IPGE remained stable in plasma for up to 4 hours at room temperature, allowing adequate time for sample processing. However, significant degradation was observed after 24 hours, emphasizing the importance of timely analysis and appropriate storage to ensure data integrity.

Collectively, these results demonstrated that, for reactive industrial chemicals, "off-the-shelf" bioanalytical methods are often insufficient. Instead, a detailed understanding of gas-phase ion chemistry and compound-specific reactivity in the ion source may be essential for the development of robust and sensitive analytical methods.

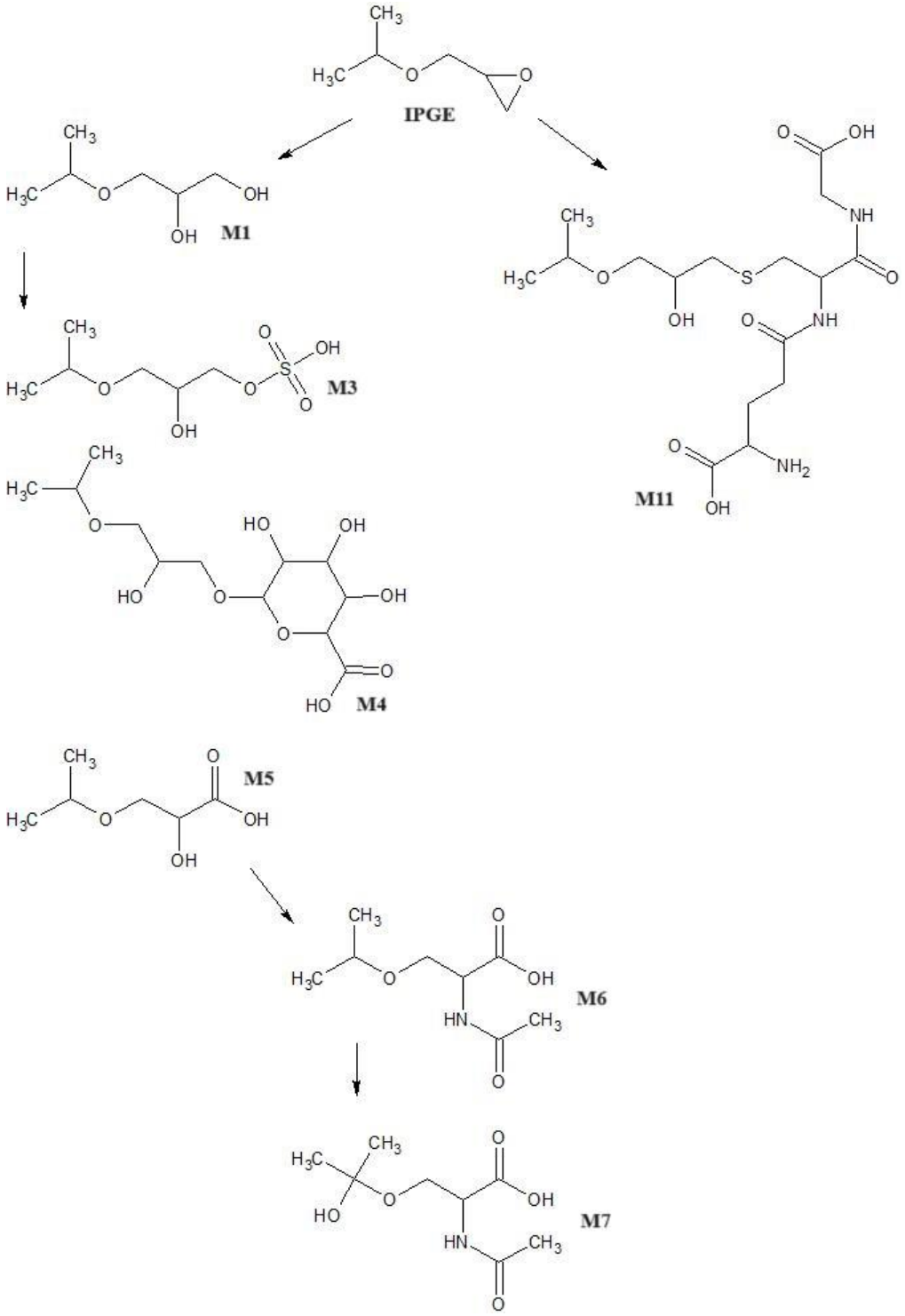

Figure 12. Proposed metabolic pathways of IPGE in rats

M1 (3-isopropoxy-2-hydroxy-1-propanol); M3 (sulfate-conjugate of IPGE); M4 (glucuronide-conjugate of IPGE); M5 (3-isopropoxy-2-hydroxypropionic acid); M6 (*O*-isopropyl-N-acetylserine); M7 (*O*-(hydroxy-isopropyl)-N-acetylserine); M11 (glutathione-conjugate of IPGE)

5.2. Implementation of surrogate matrix approach for protoporphyrin IX

The precise quantification of endogenous compounds, such as protoporphyrin IX, presents a distinct bioanalytical challenge compared to xenobiotics, primarily due to the absence of a true analyte-free blank matrix. The bioanalysis and validation of such methods are further complicated by the variable background levels in biological samples. (144, 145) In this context, rigorous validation in accordance with established bioanalytical guidelines is essential. The finalized ICH M10 guideline provides detailed and harmonized recommendations for endogenous analytes, outlining four acceptable strategies: the use of surrogate matrices, surrogate analytes, standard addition, or background subtraction. (5) In the present study, the surrogate matrix approach was selected and implemented in full compliance with these new regulatory standards.

A key innovation of the developed methodology was the in-house preparation of a surrogate matrix *via* visible light-induced analyte stripping (photobleaching). (146) To our knowledge, this represents the first reported application of photobleached plasma as a validated surrogate matrix for protoporphyrin IX quantification in alignment with the ICH M10 guideline. (5) The validity of this approach was rigorously confirmed through the assessment of parallelism, the most critical validation parameter for endogenous methods. (147) By demonstrating that the calibration slopes in the surrogate and authentic matrices were comparable — meeting the predefined slope-difference acceptance criteria described by Ji et al. — we proved that the surrogate matrix is a scientifically valid substitute for the authentic biological fluid. (55)

From a practical perspective, the developed HPLC-FLD method offered significant advantages over existing alternatives, particularly in terms of simplicity and throughput. While LC-MS/MS is often considered the gold standard for sensitivity, it typically requires costly instrumentation and complex sample preparation. For example, Walke et al. reported a highly sensitive LC-MS/MS method for serum protoporphyrin IX; however, their protocol involved a multi-step, time-consuming sample preparation procedure lasting several hours. (52) Similarly, Zhang et al. achieved high sensitivity using ultra-performance liquid chromatograph-tandem mass spectrometry, but required more elaborate extraction procedures and longer chromatographic run times compared to the present method. In contrast, our approach employed a simple protein precipitation step and a rapid 8-min gradient run, achieving an LLOQ of 10 ng/mL. (51) This sensitivity is

comparable to that reported by Macours et al. (5.63 ng/mL), while substantially reducing analysis time (8 min vs. 20 min). (148)

Furthermore, the use of gradient elution was critical for ensuring method reproducibility. Although Wakamatsu et al. successfully applied isocratic HPLC-FLD for porphyrin analysis in food matrices, such conditions are often unsuitable for complex biological samples due to the on-column accumulation of interfering matrix components. (149) The gradient approach employed here mitigated this issue, resulting in stable retention times and consistent signal responses.

The accurate quantification capability of the method was demonstrated using a 5-aminolaevulinic acid-induced protoporphyrin IX accumulation model in rats. The study confirmed that the developed HPLC-FLD method is suitable for monitoring dynamic changes in endogenous protoporphyrin IX levels in a toxicological setting. The observed plasma kinetics—characterised by a rapid increase with a peak at 2 hours post-dose followed by a gradual decline—are consistent with findings reported by Van Den Boogert et al. (1998). (46) It should be noted that, although photobleaching represents a cost-effective stripping technique, prolonged light exposure may potentially affect other light-sensitive endogenous matrix components; however, no such interference with the accurate quantification of protoporphyrin IX was observed in the present study.

In conclusion, this work demonstrated that, for the quantification of endogenous biomarkers, successful method validation critically depends on the suitability of the surrogate matrix. The photobleaching strategy presented here provided a cost-effective, ICH M10-compliant approach for generating an analyte-free matrix while preserving the complexity of the biological background. The developed HPLC-FLD method therefore represents a reliable and practical alternative to more complex MS-based workflows for routine toxicological monitoring. (150-152)

5.3. Bioanalytical support for organ-specific toxicity model experiments

5.3.1. Bioanalysis of gentamicin in the *in vivo* nephrotoxicity model

Kidney is the primary organ responsible for the excretion of many xenobiotics and is particularly susceptible to toxic injury. In our comprehensive nephrotoxicity model study gentamicin was selected as the reference compound due to its well-documented accumulation in the renal cortex. (66) Previous kinetic studies, including those by Miller

et al. (67), have demonstrated that the intrarenal accumulation of aminoglycosides is the driver of toxicity, underscoring the importance of precise monitoring of tissue and plasma levels. (153, 154)

The bioanalysis of gentamicin remained challenging due to its high polarity, lack of UV-absorbing chromophores, and complex multicomponent composition. Although alternative separation techniques, such as hydrophilic interaction chromatography (HILIC), have been proposed, the present study employed an extensive and systematic method validation strategy using a reversed-phase system with a carbon-based stationary phase. (73, 75, 155) This approach enabled accurate quantification of the principal gentamicin component, while minor components were monitored for qualitative purposes only. (63, 70) Such analytical rigor was essential to ensure that the observed nephrotoxicity biomarkers (extracellular miRNAs) correlated reliably with the systemic exposure of gentamicin, free from analytical artifacts.

Our method's applicability was confirmed through the study sample analysis of an *in vivo* model experiment. High urinary gentamicin concentrations (approximately 30,000 ng/mL) were found alongside relatively low circulating plasma levels (50–70 ng/mL). The developed method was simultaneously able to quantify gentamicin in an extremely wide concentration range exhibited in the two matrices.

5.3.2. Rapid method implementation for drug exposure in screening models

For the hepatotoxicity and cardiotoxicity screening models, the primary bioanalytical objective shifted from comprehensive validation to rapid data acquisition on sample concentrations related to the specific dose. The aim of method development was to accurately determine drug concentrations in blood plasma or cell culture media, thereby supporting parallel investigations within the research group focused on innovative, extracellular vesicle-derived biomarkers. This targeted approach reflects the need for rapid analytical support in preclinical screening, where the confirmation of administered dose levels sits in priority and does not require full regulatory validation.

To support the drug-induced liver injury model, a previously established method for paracetamol was adapted to monitor drug concentrations in both rat plasma and hepatocyte culture media. As paracetamol toxicity is driven by the saturation of metabolic pathways and the formation of reactive metabolites, the analytical method required a

broad dynamic range (0.1-100 µg/mL). Following the principles described by Kam et al., a rapid protein precipitation-based LC-MS/MS method was established. (156) Although our run time was somewhat longer (8 min vs. 3.5 min), it allowed the simultaneous detection of paracetamol and its metabolites. This approach enabled the characterisation of extensive biotransformation within the experimental systems. (61, 105) In the *in vitro* hepatocyte model, paracetamol was almost completely metabolized at the initial dose of 1 mM within 24 hours and reduced from 10 mM to ~8 mM at the high dose. Similarly, *in vivo* plasma samples showed the depletion of the parent compound alongside the formation of its major metabolites. Semi-quantitative monitoring revealed the presence of sulphate, glucuronide and glutathione conjugates. Notably, detection of the glutathione conjugate provides indirect evidence of reactive NAPQI formation, confirming that the toxicologically relevant metabolic activation occurred in the experimental models. (97) These findings verified that the applied dosing conditions achieved high exposure required to evoke drug-induced liver injury.

In hepatotoxicity model studies, amoxicillin and clavulanic acid were also investigated. The bioanalysis of these compounds presented specific stability challenges. As noted by Hoizey et al., traditional HPLC-UV methods often lack sufficient sensitivity and require complex ion-pairing reagents. (60) Although Idris and Elgorashe (157) suggested cost-effective alternatives, such as sequential injection chromatography for pharmaceutical formulations, biological matrices necessitate higher selectivity. (34, 158, 159) Therefore, an LC-MS/MS method, similar to that described by Reyns et al. was qualified; these authors demonstrated that negative electrospray ionisation enables sensitive detection of clavulanic acid (LLOQ ~ 25 ng/mL). (81) The qualified method exhibited a linear range of 0.05-2.5 µg/mL, which proved suitable for the experimental design, as the cell culture medium samples fell within this range following a 10-fold dilution. The analytical findings indicated that hepatocytes did not significantly contribute to the biotransformation of amoxicillin and clavulanic acid, as their concentrations remained stable throughout the 24-hour incubation period. This lack of hepatic metabolism was expected, as both compounds are primarily eliminated *via* renal excretion in unchanged form. (79) Nevertheless, their assessment in a liver model was essential, as this drug combination is a well-documented, albeit rare, cause of idiosyncratic drug-induced liver injury in certain patient populations. (139, 140)

In the context of cumulative cardiotoxicity, the focus was on the quantification of doxorubicin concentrations in blood plasma. Reliable monitoring of the parent drug is crucial, as its accumulation in cardiac tissue is directly linked to the development of cardiomyopathy. (108, 109) While Sottani et al. (118) and Mazzucchelli et al. (62) developed highly sensitive methods for clinical and tissue distribution studies, the present method was optimized specifically for speed and throughput in rat plasma, achieved through a simplified extraction procedure and a short run time. The qualified method demonstrated an appropriate linear range of 1-800 ng/mL, enabling quantification of all terminal plasma samples collected on day 12. The results revealed mean doxorubicin concentrations of 7.83 ng/mL and 22.0 ng/mL in the 3×3 and 3×6 mg/kg cohorts, respectively. The higher concentration observed in the high-dose group highlighted the cumulative nature of doxorubicin pharmacokinetics.

Finally, in an acute cardiotoxicity model study, isoprenaline, a non-selective β-adrenergic agonist, was investigated. The bioanalysis of isoprenaline presented a unique challenge due to its extreme instability and rapid elimination. High doses have been reported to induce infarct-like necrosis *via* complex mechanisms involving oxidative stress and apoptosis. (123, 124) To verify the intravenous doses responsible for this acute injury, a specialized rapid LC-MS/MS method was employed. As described by Zhou et al., the development of a sensitive method for isoprenaline requires careful optimization of both the mobile phase and sample handling to prevent degradation. (136) The present method utilized acidified mobile phases and fast chromatography—strategies essential for stabilizing catecholamines—to ensure reliable assessment of systemic exposure. The toxicokinetic pilot study confirmed an extremely short half-life of 3.46 min for isoprenaline in rats. This rapid elimination explains why quantification of the parent compound was unnecessary at the later sampling points (8 and 24 hours) in the main study, as detectable concentrations were not expected. Furthermore, plasma concentrations can exhibit substantial variability even under standardized dosing conditions. (127) Such variability has been reported in earlier human infusion studies and was attributed to interactions with concomitantly administered drugs. A similar degree of variability was also observed in the present pilot rat study (Figure 10, SEM values), although no concomitant medication was administered. In summary, although the rapid elimination of isoprenaline renders quantification unnecessary at later sampling points,

the developed method provided essential toxicokinetic evidence confirming the initial exposure phase required to trigger acute myocardial injury in this model.

5.4. Future perspectives

The bioanalytical strategies presented in this thesis, ranging from innovative derivatisation techniques to tailored rapid methods, provide a solid foundation for future applications in toxicological screening, occupational safety, clinical diagnostics, and the ongoing investigation of novel extracellular vesicle-derived biomarkers within our research group.

The successful implementation of in-source derivatisation *via* the gas-phase Meerwein reaction for isopropyl glycidyl ether opened new perspectives for the analysis of reactive industrial diluents. As highlighted in this work, the method has overcome the mass spectrometric ionisation limitations of small aliphatic epoxides. Future studies could extend this approach to other members of the glycidyl ether family (e.g., *n*-butyl or allyl glycidyl ether), which are widely used in the epoxy resin industry. Furthermore, the high sensitivity achieved (LLOQ 10 ng/mL) suggested that the method may be suitable for human biomonitoring applications. This would provide a valuable tool for exposure assessment in occupational health and safety studies, aligning with the principles of integrating toxicokinetics into risk assessment, as described by Terry and Hays (160). At present, data on the systemic burden of these compounds in exposed workers remain limited.

The methodology established for the bioanalysis of protoporphyrin IX in plasma supported the application of the *surrogate matrix* approach in endogenous biomarker analysis in accordance with the relatively recent ICH M10 guideline. As demonstrated, photochemical depletion of plasma provided an effective strategy to generate analyte-free matrices while preserving the biological background, particularly in cases involving light-sensitive analytes. This approach is consistent with the increasing regulatory emphasis on *parallelism* as a key criterion for method validity, as outlined by Ji et al. (55). Building on our findings, future research could extend this cost-effective photobleaching technique to other photosensitive biomarkers (e.g., vitamins or other porphyrins), thereby reducing reliance on expensive synthetic surrogate matrices in clinical laboratory settings.

The methods developed for pharmaceuticals hold significant potential for translation into clinical therapeutic drug monitoring and more sustainable analytical practices. The simplified protocols optimized for paracetamol and doxorubicin could be adapted for human plasma analysis to support applications in emergency toxicology and oncology. As emphasized by Sottani et al. and Kam et al., high-throughput LC-MS/MS methods are essential for real-time patient management. Moreover, future bioanalytical method development should increasingly incorporate "green chemistry" principles. The analytical challenges encountered with amoxicillin and clavulanic acid, highlighted the need for methods that minimize solvent consumption in routine analysis. In this context, future work should focus on integrating microsampling techniques with highly sensitive LC-MS/MS platforms. Such approaches would reduce the environmental footprint of bioanalysis while also supporting the refinement of ethical practices in animal studies. (15, 118, 156)

6. CONCLUSIONS

The present work addressed several bioanalytical challenges in chemical safety assessment through the development of novel analytical strategies. Based on the results, the following conclusions were drawn:

1. Toxicokinetic characterisation of an industrial chemical: isopropyl glycidyl ether

A sensitive LC-APCI-MS/MS method was developed and validated for the quantification of IPGE, incorporating a novel in-source derivatisation strategy (Meerwein reaction) to overcome its poor ionisation efficiency. This method enabled the first detailed characterisation of the toxicokinetic profile of IPGE in rats. In addition, qualitative profiling tentatively identified seven metabolites, suggesting that elimination was primarily driven by epoxide hydrolysis and glutathione conjugation.

2. Development of a validated bioanalytical protocol for an endogenous biomarker: protoporphyrin IX

A selective HPLC-FLD method was developed for the quantification of endogenous protoporphyrin IX using a surrogate matrix approach based on photodegraded plasma. This strategy proved to be a practical solution for managing endogenous background levels while complying with the ICH M10 guideline. The method was successfully applied to monitor 5-aminolaevulinic acid-induced protoporphyrin IX formation in an *in vivo* study, supporting its potential utility in future clinical applications.

3. Bioanalytical support for toxicity studies

Robust analytical methods were established for a range of active pharmaceutical ingredients, namely gentamicin, amoxicillin, clavulanic acid, paracetamol, doxorubicin and isoprenaline. These validated methods provided essential support for both *in vitro* and *in vivo* experiments within the research group, enabling the investigation of extracellular vesicle-associated biomarkers of drug-induced toxicity.

Overall, the present work demonstrated that “fit-for-purpose” bioanalytical strategies are critical for generating reliable data in chemical safety assessment. The approaches presented herein provided a comprehensive methodological framework for the risk assessment of industrial glycidyl ethers and some pharmaceutical agents, as well as for endogenous biomarker porphyrins.

7. SUMMARY

Accurate assessment of systemic exposure is a fundamental requirement in chemical safety studies. However, classical bioanalytical approaches are often insufficient for chemically unstable compounds, endogenous biomarkers, or complex pharmaceutical agents. Therefore, the present work focused on the development and application of tailored analytical solutions to ensure reliable data for toxicokinetic characterisation of industrial glycidyl ethers and some pharmaceuticals, as well as for endogenous biomarker porphyrins.

An LC-APCI-MS/MS method for isopropyl glycidyl ether, a reactive industrial diluent of epoxy resins, was developed using the Meerwein reaction as an in-source derivatisation strategy to overcome the poor ionisation efficiency of the analyte. The validated method, with an LLOQ of 0.01 µg/mL, enabled the first detailed characterisation of IPGE toxicokinetics in rats. Qualitative profiling tentatively identified seven metabolites, indicating that elimination is primarily driven by epoxide hydrolysis and glutathione conjugation.

The second major topic involved the quantification of protoporphyrin IX, an endogenous biomarker. To address the lack of an analyte-free blank matrix, a surrogate matrix approach was applied using photodegraded authentic rat plasma. A selective HPLC-FLD method was validated in accordance with the ICH M10 guideline, demonstrating appropriate parallelism between the surrogate and authentic matrices. This method was successfully applied to monitor the kinetics of 5-aminolaevulinic acid induced protoporphyrin IX formation in an *in vivo* rat study.

Finally, the versatility of bioanalytical support in toxicological and safety studies of pharmaceuticals was presented. Methods were established for the determination of gentamicin, amoxicillin, clavulanic acid, paracetamol, doxorubicin and isoprenaline. These methods, characterised by high sensitivity, rapid analysis, and simplified sample preparation, supported the investigation of extracellular vesicle-associated biomarkers in both *in vitro* and *in vivo* toxicity models.

In conclusion, the analytical solutions presented in this work, ranging from in-source chemical derivatisation through surrogate matrix approach to tailored rapid methods for pharmaceutical agents, provided a robust foundation for addressing complex bioanalytical challenges in safety research.

8. REFERENCES

1. Fouzi NFR, Aziz HA, Yaakub N. (2024) Systematic review of chemical safety and chemical security risk management approach. Process Safety and Environmental Protection, 183: 676-686.
2. Environment D-Gf. (2026) New rules to streamline EU chemical assessments enter into force. Vol. 2026
3. ICH Guideline M3 (R2) Non-clinical safety studies for the conduct of human clinical trials for pharmaceuticals. European Medicines Agency, Commitee for Medical Products for Human Use 2013
4. Wambaugh JF, Paul Friedman K, Beal MA, Moffat I, Hughes MF, Nong A, Dorne J-LCM, Ashraf MW, Barton-Maclaren TS, DeVito M, Ferguson SS, Judson RS, Long AS, Paini A, Sampani S, Thomas RS, Wetmore BA. (2025) Applying New Approach Methods for Toxicokinetics for Chemical Risk Assessment. Chemical Research in Toxicology, 38: 1408-1441.
5. ICH Guideline M10 on Bioanalytical Method Validation an Study Sample Analysis. European Medicines Agency, Commitee for Medical Products for Human Use2022
6. Hodiamont CJ, van den Broek AK, de Vroom SL, Prins JM, Mathôt RAA, van Hest RM. (2022) Clinical Pharmacokinetics of Gentamicin in Various Patient Populations and Consequences for Optimal Dosing for Gram-Negative Infections: An Updated Review. Clinical Pharmacokinetics, 61: 1075-1094.
7. Poole A, van Herwijnen P, Weideli H, Thomas MC, Ransbotyn G, Vance C. (2004) Review of the toxicology, human exposure and safety assessment for bisphenol A diglycidylether (BADGE). In: Food Additives and Contaminants Vol. 21 pp. 905-919
8. Pham HQ, Marks MJ. Epoxy Resins. In: Ullmann's Encyclopedia of Industrial Chemistry. Wiley, 2005.
9. Fishbein L. (1981) Carcinogenicity and Mutagenecity of Solvents - I. Glycidil Ethers, Dioxane, Nitroalkanes, Dimethylformamide and Allyl Derivatives. In: The Science of the Total Environment Vol. 17 pp. 97-110

10. Lynn HP, Darrell RB, John MW. Chapter 60 Epoxy Compounds—Olefin Oxides, Aliphatic Glycidyl Ethers,and Aromatic Monoglycidyl Ethers. In:Eula B ,Barbara C (szerk.), Patty's Toxicology. John Wiley & Sons, Inc, 2012.
11. Lv H, Liu L, Zhang Y, Song T, Lu J, Chen X. (2010) Ingenuity pathways analysis of urine metabonomics phenotypes toxicity of gentamicin in multiple organs. Molecular BioSystems, 6: 2056-2067.
12. Farouk F, Azzazy HME, Niessen WMA. (2015) Challenges in the determination of aminoglycoside antibiotics, a review. Analytica Chimica Acta, 890: 21-43.
13. Amponsah SK, Boadu JA, Dwamena DK, Opuni KFM. (2022) Bioanalysis of aminoglycosides using high-performance liquid chromatography. ADMET and DMPK, 10: 27-62.
14. Visconti G, Boccard J, Feinberg M, Rudaz S. (2023) From fundamentals in calibration to modern methodologies: A tutorial for small molecules quantification in liquid chromatography–mass spectrometry bioanalysis. Analytica Chimica Acta, 1240.
15. Delahaye L, Baerdemaeker LD, Stove CP. (2021) Determination of paracetamol and its metabolites via LC-MS/MS in dried blood volumetric absorptive microsamples: A tool for pharmacokinetic studies. Journal of Pharmaceutical and Biomedical Analysis, 206.
16. Lestido-Cardama A, Sendón R, Bustos J, Nieto MT, Paseiro-Losada P, Rodríguez-Bernaldo de Quirós A. (2022) Food and beverage can coatings: A review on chemical analysis, migration, and risk assessment. Comprehensive Reviews in Food Science and Food Safety, 21: 3558-3611.
17. Pottenger LH, Boverhof DR, Waechter JM. Epoxy Compounds-Olefin Oxides, Aliphatic Glycidyl Ethers, and Aromatic Monoglycidyl Ethers. In: Patty's Toxicology. John Wiley & Sons, Inc.
18. Anderson HH, Dunlap MK, Hine CH, Kodama JK, Wellington JS. (1956) The toxicology of glycidol and some glycidyl ethers. A.M.A. archives of industrial health, 14: 250-264.
19. Program NT. (1990) NTP Toxicology and Carcinogenesis Studies of Allyl Glycidyl Ether (CAS No. 106-92-3) in Osborne-Mendel Rats and B6C3F1 Mice

(Inhalation Studies). Vol. 376 pp. 1-219, National Toxicology Program technical report series

20. Echa. (2024) Registration, Evaluation, Authorisation and Restriction of Chemicals (REACH) Dossier. 2,3-epoxypropyl isopropyl ether (CAS No 4016-14-2). In: https://echa.europa.eu/hu/registration-dossier/-/registered-dossier/23504/7/1,
21. Eadsforth CV, Hutson DH, Logan CJ, Morrison BJ. (1985) The metabolism of n-butyl glycidyl ether in the rat and rabbit. Xenobiotica, 15: 579-589.
22. Chen L-J, Lebetkin EH, Nwakpuda EI, Burka LT. (2007) Metabolism and disposition of n-butyl glycidyl ether in F344 rats and B6C3F1 mice. Drug Metabolism and Disposition, 35: 2218-2224.
23. Pérez HL, Plná K, Osterman-Golkar S. (1997) Dosimetry of glycidyl ethers in mice by quantification of haemoglobin adducts. Chemico-Biological Interactions, 103: 1-16.
24. Xue J, Liu Y, Yang D, Zhao Y, Cai Y, Zhang T, Kannan K. (2022) A review of properties, production, human exposure, biomonitoring, toxicity, and regulation of bisphenol A diglycidyl ethers and novolac glycidyl ethers. In: Environmental Chemistry and Ecotoxicology Vol. 4 pp. 216-230, KeAi Communications Co.
25. Wang D, Zhao H, Fei X, Synder SA, Fang M, Liu M. (2021) A comprehensive review on the analytical method, occurrence, transformation and toxicity of a reactive pollutant: BADGE. Environment International, 155: 106701-106701.
26. OECD. Test No. 422: Combined Repeated Dose Toxicity Study with the Reproduction/Developmental Toxicity Screening Test, doi:10.1787/9789264264403-en. OECD2016
27. Hanaoka T, Kawamura N, Hara K, Tsugane S. (2002) Urinary bisphenol A and plasma hormone concentrations in male workers exposed to bisphenol A diglycidyl ether and mixed organic solvents. Occupational and Environmental Medicine, 59: 625-628.
28. Chang Y, Nguyen C, Paranjpe VR, Gilliland F, Zhang J. (2014) Analysis of bisphenol A diglycidyl ether (BADGE) and its hydrolytic metabolites in biological specimens by high-performance liquid chromatography and tandem

mass spectrometry. Journal of Chromatography B: Analytical Technologies in the Biomedical and Life Sciences, 965: 33-38.

29. Gallart-Ayala H, Moyano E, Galceran MT. (2010) Multiple-stage mass spectrometry analysis of bisphenol A diglycidyl ether, bisphenol F diglycidyl ether and their derivatives. Rapid Communications in Mass Spectrometry, 24: 3469-3477.
30. Míguez J, Herrero C, Quintás I, Rodríguez C, Gigosos PG, Mariz OC. (2012) A LC–MS/MS method for the determination of BADGE-related and BFDGE-related compounds in canned fish food samples based on the formation of [M+NH4]+ aducts. Food Chemistry, 135: 1310-1315.
31. Newman JW, Hammock BD. (2001) Optimized thiol derivatizing reagent for the mass spectral analysis of disubstituted epoxy fatty acids. In: Journal of Chromatography A, pp. 223-240
32. Bai L, Sun M, An J, Liu DQ, Chen TK, Kord AS. (2010) Enhancing the detection sensitivity of trace analysis of pharmaceutical genotoxic impurities by chemical derivatization and coordination ion spray-mass spectrometry. Journal of Chromatography A, 1217: 302-306.
33. Liu J, Chen X, Zhang Y, Miao H, Liu K, Li L, Zhong D. (2011) Derivatization of (5R)-hydroxytriptolide from benzylamine to enhance mass spectrometric detection: Application to a Phase I pharmacokinetic study in humans. Analytica Chimica Acta, 689: 69-76.
34. Sun L, Wu H, Ren L, Cong J, Qin X, Wang X, Qi X, Kang L, Zhang J, Wu C. (2018) Development and validation of a highly sensitive LC-MS/MS method for determination of brain active agent dianhydrogalactitol in mouse plasma and tissues: Application to a pharmacokinetic study. Journal of Chromatography B: Analytical Technologies in the Biomedical and Life Sciences, 1087-1088: 90-97.
35. Główka FK, Romański M, Tezyk A, zaba C, Wróbel T. (2012) HPLC method for determination of biologically active epoxy-transformers of treosulfan in human plasma: Pharmacokinetic application. Journal of Pharmaceutical and Biomedical Analysis, 62: 105-113.
36. Califf RM. (2018) Biomarker definitions and their applications. Experimental Biology and Medicine, 243: 213-221.

37. Group F-NBW. BEST (Biomarkers, EndpointS, and other Tools) Resource. Food and Drug Administration (US); National Institutes of Health (US), Silver Spring (MD), 2016
38. Kim BF, Bohandy J. Spectroscopy of Porphyrins. Johns Hopkins APL Technical Digest, 2: 153-163.
39. Giménez-Campillo C, Montoya-Méndez I, Campillo N, Arroyo-Manzanares N, del Val Oliver B, Zarauz-García J, Sáenz L, Viñas P. (2024) Evaluation of the potential use of protoporphyrins as biomarkers of anemic disease in human urine from inflammatory bowel disease patients. Journal of Pharmaceutical and Biomedical Analysis, 251.
40. Giménez-Campillo C, Hernández JdD, Guillén I, Campillo N, Arroyo-Manzanares N, Torre-Minguela Cd, Viñas P. (2022) Reddish Colour in Cooked Ham Is Developed by a Mixture of Protoporphyrins Including Zn-Protoporphyrin and Protoporphyrin IX. Foods, 11.
41. Hindmarsh JT, Oliveras L, Greenway DC. (1999) Plasma Porphyrins in the Porphyrias. Clinical Chemistry, 45: 1070-1076.
42. Brun A, Sandberg S. (1991) New Trends in Photobiology (Invited Review) Mechanisms of photosensitivity in porphyric patients with special emphasis on erythropoietic protoporphyria. J. Photochem. Photobiol. B: Biol, 10: 285-285.
43. Gerscher S, Connelly JP, Beijersbergen Van Henegouwen GMJ, Macrobert AJ, Watt P, Rhodes LE. (2001) A quantitative assessment of protoporphyrin IX metabolism and phototoxicity in human skin following dose-controlled delivery of the prodrugs 5-aminolaevulinic acid and 5-aminolaevulinic acid-n-pentylester. British Journal of Dermatology, 144: 983-990.
44. Marcus SL, de Souza MP. (2024) Theranostic Uses of the Heme Pathway in Neuro-Oncology: Protoporphyrin IX (PpIX) and Its Journey from Photodynamic Therapy (PDT) through Photodynamic Diagnosis (PDD) to Sonodynamic Therapy (SDT). Cancers, 16.
45. Fukuda H, Casas A, Batlle A. (2005) Aminolevulinic acid: From its unique biological function to its star role in photodynamic therapy. International Journal of Biochemistry and Cell Biology, 37: 272-276.

46. Van Den Boogert J, Van Hillegersberg R, De Rooij FWM, De Bruin RWF, Edixhoven-Bosdijk A, Houtsmuller AB, Siersema PD, Wilson JHP, Tilanus HW. (1998) Aminolaevulinic acid-induced protoporphyrin IX accumulation in tissues: pharrnacokinetics after oral or intravenous administration. Journal of Photochemistry and Photobiology B: Biology, 44: 29-38.
47. Knipps J, Fischer I, Neumann LM, Rapp M, Dibué-Adjei M, Freiin von Saß C, Placke JM, Mijderwijk HJ, Steiger HJ, Sabel M, Cornelius JF, Kamp MA. (2019) Quantification of PpIX-fluorescence of cerebral metastases: a pilot study. Clinical and Experimental Metastasis, 36: 467-475.
48. Croizat G, Gregor A, Joniova J, Gerelli E, Wagnières G. (2022) Identification of excimer delayed fluorescence by Protoporphyrin IX: A novel access to local chromophore concentration? Journal of Photochemistry and Photobiology B: Biology, 229.
49. Fyrestam J, Östman C. (2017) Determination of heme in microorganisms using HPLC-MS/MS and cobalt(III) protoporphyrin IX inhibition of heme acquisition in Escherichia coli. Analytical and Bioanalytical Chemistry, 409: 6999-7010.
50. Gu L, Yue X, Zhong H, Mei K, Wang D. (2022) A new technique of quantifying protoporphyrin IX in microbial cells in seawater. Frontiers in Marine Science, 9.
51. Zhang C, Ma C, Zhu L, Yao M. (2023) Simultaneous determination of protoporphyrin IX and magnesium protoporphyrin IX in Arabidopsis thaliana and Camellia sinensis using UPLC-MS/MS. Plant Methods, 19.
52. Walke A, Krone C, Stummer W, König S, Suero Molina E. (2024) Protoporphyrin IX in serum of high-grade glioma patients: A novel target for disease monitoring via liquid biopsy. Scientific Reports, 14.
53. Danton M, Lim CK, Danton M, Lim CK. (2006) Porphyrin profiles in blood, urine and faeces by HPLC/ electrospray ionization tandem mass spectrometry. Biomed. Chromatogr, 20: 612-621.
54. Santos NR, Bandeira MdJ, Bah HAF, Rodrigues JLG, Cardoso MS, Rocha AR, Menezes-Filho JA. (2021) Zinc-protoporphyrin determination by HPLC with fluorescence detection as a biomarker of lead effect in artisanal pottery workers. Biomedical Chromatography, 35.

55. Ji AJ, Xu G, Tao L, Jiao HJ, Palmer RE. (2022) Criteria of slope and endogenous level for selection of matrix in the quantitation of endogenous compounds by LC-MS/MS. Bioanalysis, 14: 807-816.
56. Otsuka S, Matsumoto K, Nakajima M, Tanaka T, Ogura S. (2015) Oxygen availability for porphyrin biosynthesis enzymes determines the production of protoporphyrin IX (PpIX) during hypoxia. PLoS ONE, 10.
57. Yamamoto J, Ogura SI, Shimajiri S, Nakano Y, Akiba D, Kitagawa T, Ueta K, Tanaka T, Nishizawa S. (2015) 5-Aminolevulinic acid-induced protoporphyrin IX with multi-doseionizing irradiation enhances host antitumor response and strongly inhibits tumor growth in experimental glioma in vivo. Molecular Medicine Reports, 11: 1813-1819.
58. Yoshioka E, Chelakkot VS, Licursi M, Rutihinda SG, Som J, Derwish L, King JJ, Pongnopparat T, Mearow K, Larijani M, Dorward AM, Hirasawa K. (2018) Enhancement of cancer-specific protoporphyrin ix fluorescence by targeting oncogenic ras/MEK pathway. Theranostics, 8: 2134-2146.
59. Ota U, Fukuhara H, Ishizuka M, Abe F, Kawada C, Tamura K, Tanaka T, Inoue K, Ogura S-I, Shuin T. (2015) Plasma protoporphyrin IX following administration of 5-aminolevulinic acid as a potential tumor marker. Molecular and Clinical Oncology, 3: 797-801.
60. Hoizey G, Lamiable D, Frances C, Trenque T, Kaltenbach M, Denis J, Millart H. (2002) Simultaneous determination of amoxicillin and clavulanic acid in human plasma by HPLC with UV detection. Journal of Pharmaceutical and Biomedical Analysis, 30: 661-666.
61. Dargue R, Grant I, Nye LC, Nicholls A, Dare T, Stahl SH, Plumb RS, Lee K, Jalan R, Coen M, Wilson ID. (2020) The analysis of acetaminophen (paracetamol) and seven metabolites in rat, pig and human plasma by U(H)PLC-MS. Bioanalysis, 12: 485-500.
62. Mazzucchelli S, Ravelli A, Gigli F, Minoli M, Corsi F, Ciuffreda P, Ottria R. (2017) LC–MS/MS method development for quantification of doxorubicin and its metabolite 13-hydroxy doxorubicin in mice biological matrices: Application to a pharmaco-delivery study. Biomedical Chromatography, 31.

63. Isoherranen N, Soback S. (2000) Determination of gentamicins C(1), C(1a), and C(2) in plasma and urine by HPLC. Clinical chemistry, 46: 837-842.
64. Marre R, Tarara N, Louton T, Sack K. (1980) Age-Dependent Nephrotoxicity and the Pharmacokinetics of Gentamicin in Rats. European journal of pediatrics, 133: 25-29.
65. Peng GW, Gadalia MAF, Peng A, Smith V, Chiou WL. (1977) High-PressureLiquid-Chromatographic Methodfor Determinationof Gentamicinin Plasma. In: Clinical Chemistry Vol. 23 pp. 1838-1838
66. Luft FC, K1eit SA. (1974) Renal Parenchymal Accumulation of Aminoglycoside Antibiotics in Rats. The Journal of Infectious Diseases, 130.
67. Miller T, Phillips S, North D. (1979) Pharmacokinetics of gentamicin in the treatment of renal infection: A therapeutic anomaly explained. Kidney International, 15: 160-166.
68. Trnovec T, Navarova J, Kettner M, Greguskova M, Bezek S, Gajdomik A, Kyselova A. (1978) Pharmacokinetics of Gentamicin Administered Intratracheally to Rats. Antimicrob Agents Chemother, 14: 166-167.
69. Lenz EM, Bright J, Knight R, Westwood FR, Davies D, Major H, Wilson ID. (2005) Metabonomics with 1H-NMR spectroscopy and liquid chromatography-mass spectrometry applied to the investigation of metabolic changes caused by gentamicin-induced nephrotoxicity in the rat. Biomarkers, 10: 173-187.
70. Nakano Y, Sakamaki H, Tasaki-Handa Y, Saito S. (2024) High-pH mobile phase in reversed-phase liquid chromatography-tandem mass spectrometry to improve the separation efficiency of aminoglycoside isomers. Analytical Sciences, 40: 375-384.
71. Lecároz C, Campanero MA, Gamazo C, Blanco-Prieto MJ. (2006) Determination of gentamicin in different matrices by a new sensitive high-performance liquid chromatography-mass spectrometric method. Journal of Antimicrobial Chemotherapy, 58: 557-563.
72. Buszewski B, Noga S. (2012) Hydrophilic interaction liquid chromatography (HILIC)—a powerful separation technique. Analytical and Bioanalytical Chemistry, 402: 231-247.

73. Kahsay G, Song H, Van Schepdael A, Cabooter D, Adams E. (2014) Hydrophilic interaction chromatography (HILIC) in the analysis of antibiotics. Journal of Pharmaceutical and Biomedical Analysis, 87: 142-154.
74. Oertel R, Neumeister V, Kirch W. (2004) Hydrophilic interaction chromatography combined with tandem-mass spectrometry to determine six aminoglycosides in serum. Journal of Chromatography A, 1058: 197-201.
75. Sun X, Yang Y, Tian Q, Shang D, Xing J, Zhai Y. (2018) Determination of gentamicin C components in fish tissues through SPE-Hypercarb-HPLC-MS/MS. Journal of Chromatography B: Analytical Technologies in the Biomedical and Life Sciences, 1093-1094: 167-173.
76. Zhang C, Hu J, Sun F, Jia M, Chen G, Wu C, Zheng L. (2018) Determination of four main components of gentamicin in animal tissues after solid-phase extraction by high-performance liquid chromatography/tandem mass spectrometry. Rapid Communications in Mass Spectrometry, 32: 1766-1772.
77. Heller DN, Peggins JO, Nochetto CB, Smith ML, Chiesa OA, Moulton K. (2005) LC/MS/MS measurement of gentamicin in bovine plasma, urine, milk, and biopsy samples taken from kidneys of standing animals. Journal of Chromatography B: Analytical Technologies in the Biomedical and Life Sciences, 821: 22-30.
78. Ibrahim F, Elgawish MS, Mehana E, El-Adl SM, Baraka MM, Ibrahim SM, Sebaiy MM. (2020) Toxicity Profile and Pharmacokinetic Study of Antibiotic Mixtures, Gentamicin and Vancomycin, in Rat Plasma by Ecofriendly Liquid Chromatography Coupled Tandem Mass Spectrometry. Chemical Research in Toxicology, 33: 2647-2658.
79. Yaxin F, Xiaojie W, Miao Z, Beining G, Guoying C, Jicheng Y, Youancheng C, Jing Z. (2016) Rapid and Simultaneous Quantification of Amoxicillin and Clavuanic Acid in Human Plasma and Urine by Ultra-Performance Liquid Chromatography Tandem Mass Spectrometry and Its Application to a Pharmacokinetic Study. Analytical Sciences, 32: 1269-1276.
80. Tsou T-L, Wu J-R, Young C-D, Wang T-M. (1997) Simultaneous determination of amoxycillin and clavulanic acid in pharmaceutical products by HPLC with fl-cyclodextrin stationary phase. Journal of Pharmaceutical and Biomedical Analysis, 15: 1205-1205.

81. Reyns T, De Baere S, Croubels S, De Backer P. (2006) Determination of clavulanic acid in calf plasma by liquid chromatography tandem mass spectrometry. Journal of Mass Spectrometry, 41: 1414-1420.
82. Foulstone M, Reading C. (1982) Assay of Amoxicillin and Clavulanic Acid, the Components of Augmentin, in Biological Fluids with High-Performance Liquid Chromatography. ANTIMICROBIAL AGENTS AND CHEMOTHERAPY, 22: 753-762.
83. de Marco BA, Natori JSH, Fanelli S, Tótoli EG, Salgado HRN. (2017) Characteristics, Properties and Analytical Methods of Amoxicillin: A Review with Green Approach. Critical Reviews in Analytical Chemistry, 47: 267-277.
84. Buszewski B, Noga S. (2012) Hydrophilic interaction liquid chromatography (HILIC)-a powerful separation technique. Analytical and Bioanalytical Chemistry, 402: 231-247.
85. Fawaz S, Merzouk M, Barton S, Nabhani-Gebara S. (2021) Stability of Amoxicillin and Clavulanic Acid in Separate Containers for Administration via a Y-Site. Drug Design, Development and Therapy, Volume 15: 3979-3984.
86. Bellur Atici E, Yazar Y, Ağtaş Ç, Ridvanoğlu N, Karlığa B. (2017) Development and validation of stability indicating HPLC methods for related substances and assay analyses of amoxicillin and potassium clavulanate mixtures. Journal of Pharmaceutical and Biomedical Analysis, 136: 1-9.
87. Matar KM. (2006) Simple and rapid LC method for the determination of amoxicillin in plasma. Chromatographia, 64: 255-260.
88. Matar KM, Nazi EM, El-Sayed YM, Al-Yamani MJ, Al-Suwayeh SA, Al-Khamis KI. (2005) Quantitative determination of clavulanic acid in plasma by HPLC: Application to a pharmacokinetic study. Journal of Liquid Chromatography and Related Technologies, 28: 97-107.
89. Foroutan SM, Zarghi A, Shafaati A, Khoddam A, Movahed H. (2007) Simultaneous determination of amoxicillin and clavulanic acid in human plasma by isocratic reversed-phase HPLC using UV detection. Journal of Pharmaceutical and Biomedical Analysis, 45: 531-534.

90. Xi W, He L, Guo C, Cai Q, Zeng Z. (2012) Simultaneous Determination of Amoxicillin and Clavulanic Acid in Dog Plasma by High-Performance Liquid Chromatography Tandem Mass Spectrometry. Analytical Letters, 45: 1764-1776.
91. Yoon KH, Lee SY, Kim W, Park JS, Kim HJ. (2004) Simultaneous determination of amoxicillin and clavulanic acid in human plasma by HPLC-ESI mass spectrometry. Journal of Chromatography B: Analytical Technologies in the Biomedical and Life Sciences, 813: 121-127.
92. Dear JW, Clarke JI, Francis B, Allen L, Wraight J, Shen J, Dargan PI, Wood D, Cooper J, Thomas SHL, Jorgensen AL, Pirmohamed M, Park BK, Antoine DJ. (2018) Risk stratification after paracetamol overdose using mechanistic biomarkers: results from two prospective cohort studies. The Lancet Gastroenterology and Hepatology, 3: 104-113.
93. Vliegenthart ADB, Antoine DJ, Dear JW. (2015) Target biomarker profile for the clinical management of paracetamol overdose. British Journal of Clinical Pharmacology, 80: 351-362.
94. Gulmez SE, Larrey D, Pageaux GP, Lignot S, Lassalle R, Jové J, Gatta A, McCormick PA, Metselaar HJ, Monteiro E, Thorburn D, Bernal W, Zouboulis-Vafiadis I, De Vries C, Perez-Gutthann S, Sturkenboom M, Bénichou J, Montastruc JL, Horsmans Y, Salvo F, Hamoud F, Micon S, Droz-Perroteau C, Blin P, Moore N. (2013) Transplantation for acute liver failure in patients exposed to NSAIDs or paracetamol (Acetaminophen): The multinational case-population SALT study. Drug Safety, 36: 135-144.
95. Ramachandran A, Jaeschke H. (2023) Mitochondria in Acetaminophen-Induced Liver Injury and Recovery: A Concise Review. In: Livers Vol. 3 pp. 219-231, Multidisciplinary Digital Publishing Institute (MDPI)
96. Liao J, Lu Q, Li Z, Li J, Zhao Q, Li J. (2023) Acetaminophen-induced liver injury: Molecular mechanism and treatments from natural products. Frontiers in Pharmacology, 14.
97. Jaeschke H, Ramachandran A. (2024) Acetaminophen Hepatotoxicity: Paradigm for Understanding Mechanisms of Drug-Induced Liver Injury. Annual Review of Pathology: Mechanisms of Disease, 19: 453-478.

98. Akakpo JY, Ramachandran A, Duan L, Schaich MA, Jaeschke MW, Freudenthal BD, Ding W-X, Rumack BH, Jaeschke H. Delayed Treatment with 4-Methylpyrazole Protects against Acetaminophen Hepatotoxicity in Mice by Inhibition of c-Jun N-Terminal Kinase. Toxicological Sciences, 170: 57-68.
99. Brunner LJ, Bai S. (1999) Simple and rapid assay for acetaminophen and conjugated metabolites in low-volume serum samples. Journal of Chromatography B, 732: 323-329.
100. Pereira FJ, Rodríguez-Cordero A, López R, Robles LC, Aller AJ. (2021) Development and validation of an rp-hplc-pda method for determination of paracetamol, caffeine and tramadol hydrochloride in pharmaceutical formulations. Pharmaceuticals, 14.
101. An JH, Lee HJ, Jung BH. (2012) Quantitative analysis of acetaminophen and its six metabolites in rat plasma using liquid chromatography/tandem mass spectrometry. Biomedical Chromatography, 26: 1596-1604.
102. Tan Qy, Zhu Rh, Li Hd, Wang F, Yan M, Dai Lb. (2012) Simultaneous quantitative determination of paracetamol and its glucuronide conjugate in human plasma and urine by liquid chromatography coupled to electrospray tandem mass spectrometry: Application to a clinical pharmacokinetic study. Journal of Chromatography B: Analytical Technologies in the Biomedical and Life Sciences, 893-894: 162-167.
103. Cook SF, King AD, van den Anker JN, Wilkins DG. (2015) Simultaneous quantification of acetaminophen and five acetaminophen metabolites in human plasma and urine by high-performance liquid chromatography-electrospray ionization-tandem mass spectrometry: Method validation and application to a neonatal pharmacokinetic study. Journal of Chromatography B: Analytical Technologies in the Biomedical and Life Sciences, 1007: 30-42.
104. Gicquel T, Aubert J, Lepage S, Fromenty B, Morel I. (2013) Quantitative Analysis of Acetaminophen and its Primary Metabolites in Small Plasma Volumes by Liquid Chromatography-Tandem Mass Spectrometry. Journal of Analytical Toxicology, 37: 110-116.
105. Pietruk K, Gbylik-Sikorska M, Łebkowska-Wieruszewska B, Gajda A, Giorgi M, Sartini I, Jedziniak P. (2021) Development of a multimatrix UHPLC-MS/MS

method for the determination of paracetamol and its metabolites in animal tissues. Molecules, 26.

106. Harahap Y, Ardiningsih P, Winarti AC, Purwanto DJ. (2020) Analysis of the doxorubicin and doxorubicinol in the plasma of breast cancer patients for monitoring the toxicity of doxorubicin. Drug Design, Development and Therapy, 14: 3469-3475.

107. Arnold RD, Slack JE, Straubinger RM. (2004) Quantification of Doxorubicin and metabolites in rat plasma and small volume tissue samples by liquid chromatography/electrospray tandem mass spectroscopy. Journal of Chromatography B: Analytical Technologies in the Biomedical and Life Sciences, 808: 141-152.

108. Zeng X, Cai H, Yang J, Qiu H, Cheng Y, Liu M. (2019) Pharmacokinetics and cardiotoxicity of doxorubicin and its secondary alcohol metabolite in rats. Biomedicine and Pharmacotherapy, 116.

109. Mross K, Maessen P, Van Der Vijgh WJF, Gall H, Boven E, Pinedo HM. (1988) Pharmacokinetics and metabolism of epidoxorubicin and doxorubicin in humans. Journal of Clinical Oncology, 6: 517-526.

110. Wang X, Hui R, Chen Y, Wang W, Chen Y, Gong X, Jin J. (2019) Discovery of novel doxorubicin metabolites in MCF7 doxorubicin-resistant cells. Frontiers in Pharmacology, 10.

111. Beijnen JH, Underbergii WJM. (1991) HPLC determination of doxorubicin, doxorubicinol and four aglycone metabolites in plasma of AIDS patients*. Journal of Pharmaceutical & Biomedical Analysis, 9: 995-1002.

112. Licata S, Saponiero A, Mordente A, Minotti G. (2000) Doxorubicin metabolism and toxicity in human myocardium: Role of cytoplasmic deglycosidation and carbonyl reduction. Chemical Research in Toxicology, 13: 414-420.

113. Van Asperen J, Van Tellingen O, Beijnen JH. (1998) Determination of doxorubicin and metabolites in murine specimens by high-performance liquid chromatography. Journal of Chromatography B, 712: 129-143.

114. Maliszewska O, Treder N, Roszkowska A, Olędzka I, Kowalski P, Bączek T, Plenis A. (2022) Comparative Study of Various Procedures for Extracting Doxorubicin from Animal Tissue Samples. Separations, 10: 6-6.

115. Liu Y, Yang Y, Liu X, Jiang T. (2008) Quantification of pegylated liposomal doxorubicin and doxorubicinol in rat plasma by liquid chromatography/electrospray tandem mass spectroscopy: Application to preclinical pharmacokinetic studies. Talanta, 74: 887-895.
116. Zhou Q, Meng P, Zhang Y, Chen P, Wang H, Tan G. (2020) The compatibility effects of sini decoction against doxorubicin-induced heart failure in rats revealed by mass spectrometry-based serum metabolite profiling and computational analysis. Journal of Ethnopharmacology, 252.
117. Xu J, Liu Y, Yu Y, Ni Q, Chen Y. (2012) Subcellular Quantification of Doxorubicin and Its Metabolite in Cultured Human Leukemia Cells Using Liquid Chromatography-Tandem Mass Spectrometry. Analytical Letters, 45: 1980-1994.
118. Sottani C, Poggi G, Melchiorre F, Montagna B, Minoia C. (2013) Simultaneous measurement of doxorubicin and reduced metabolite doxorubicinol by UHPLC-MS/MS in human plasma of HCC patients treated with TACE. Journal of Chromatography B: Analytical Technologies in the Biomedical and Life Sciences, 915-916: 71-78.
119. Semreen MH, Alniss HY, Mousa MK, El-Awady R, Khan F, Al-Rub KA. (2018) Quantitative determination of doxorubicin in the exosomes of A549/MCF-7 cancer cells and human plasma using ultra performance liquid chromatography-tandem mass spectrometry. Saudi Pharmaceutical Journal, 26: 1027-1034.
120. Tariq M, Al-Badr AA. Isoproterenol Vol. 14. The Squibb Institute for Medical Research 1985
121. Stein SW, Thiel CG. (2017) The History of Therapeutic Aerosols: A Chronological Review. Journal of Aerosol Medicine and Pulmonary Drug Delivery, 30: 20-41.
122. G Rona, C I Chappel, T Balazs, Gaurdy R. (1959) An infarct-like myocardial lesion and other toxic manifestations produced by isoproterenol in the rat. AMA Arch Pathol., 67: 443-455.
123. Gyongyosi A, Zilinyi R, Czegledi A, Tosaki A, Tosaki A, Lekli I. (2019) The Role of Autophagy and Death Pathways in Dose-dependent Isoproterenolinduced Cardiotoxicity. Current Pharmaceutical Design, 25: 2192-2198.

124. Liu YT, Jia HM, Chang X, Ding G, Zhang HW, Zou ZM. (2013) The metabolic disturbances of isoproterenol induced myocardial infarction in rats based on a tissue targeted metabonomics. Molecular BioSystems, 9: 2823-2834.
125. Conway WD, Minatoya H, Lands AM, Shekosky JM, Piontek MRW, Jensen MA, Selheris MS, Gosztyla MM. (1968) Absorption and elimination profile of isoproterenol. 3. The metabolic fate of dl-isoproterenol-7-3H in the dog. Journal of pharmaceutical sciences, 57: 1135–1141.
126. Kadar D, Tang HY, Conn AW, Toronto C. (1974) Isoproterenol metabolism in children after intravenous administration. Clinical pharmacology and therapeutics, 16: 789–795.
127. Hjemdahl P, Martinsson A, Larsson K. (1986) Improvement of the isoprenaline infusion test by plasma concentration measurements. In: Life Sciences Vol. 39 pp. 629-635
128. Kumar N, Devineni SR, Gajjala PR, Dubey SK, Kumar P. (2017) Synthesis, isolation, identification and characterization of new process-related impurity in isoproterenol hydrochloride by HPLC, LC/ESI-MS and NMR. Journal of Pharmaceutical Analysis, 7: 394-400.
129. Shahrokhian S, Panahi S, Salimian R. (2019) An electrochemical sensing platform based on nitrogen-doped hollow carbon spheres for sensitive and selective isoprenaline detection. Journal of Electroanalytical Chemistry, 847.
130. Lupetti KO, Vieira IC, Fatibello-Filho O. (2002) Flow injection spectrophotometric determination of isoproterenol using an avocado (Persea americana) crude extract immobilized on controlled-pore silica reactor. In: Talanta Vol. 57 pp. 135-143
131. Hadwiger ME, Park S, Torchia SR, Lunte CE. (1997) Simultaneous determination of the elimination profiles of the individual enantiomers of racemic isoproterenol using capillary electrophoresis and microdialysis sampling. In: Journal of Pharmaceutical and Biomedical Analysis Vol. 15 pp. 621-621
132. Yao H, Sun YY, Lin X, Cheng J, Huang L. (2006) Flow-injection chemiluminescence determination of catecholamines based on their enhancing effects on the luminol-potassium periodate system. Luminescence, 21: 112-117.

133. Liu YM, Wang CQ, Mu HB, Cao JT, Zheng YL. (2007) Determination of catecholamines by CE with direct chemiluminiscence detection. Electrophoresis, 28: 1937-1941.
134. Reid JJ, Stitzel RE, Head RJ. (1985) HPLC-ECD Procedure for the Measurement of O-Methylation of Catechol Estrogens by Vascular Tissue. Journal of pharmacological methods, 1: 25-39.
135. Maio M, Di Fiore C, Iannone A, Carriera F, Notardonato I, Avino P. (2022) Review of the Analytical Methods Based on HPLC-Electrochemical Detection Coupling for the Evaluation of Organic Compounds of Nutritional and Environmental Interest. Analytica, 3: 54-78.
136. Zhou J, Yin H, Ma H, Wei S, Wen E, Zhang W, Dang H. (2017) Efficient and selective analytical method for the quantification of a β-adrenoceptor agonist, isoproterenol, by LC–MS/MS and its application to pharmacokinetics studies. Journal of Liquid Chromatography and Related Technologies, 40: 699-705.
137. Shi N, Bu X, Zhang M, Wang B, Xu X, Shi X, Hussain D, Xu X, Chen D. (2022) Current Sample Preparation Methodologies for Determination of Catecholamines and Their Metabolites. In: Molecules Vol. 27, MDPI
138. Benton CM, Lim CK, Moniz C, Jones DJ. (2012) Ultra high-performance liquid chromatography of porphyrins in clinical materials: Column and mobile phase selection and optimisation. Biomedical Chromatography, 26: 714-719.
139. deLemos AS, Ghabril M, Rockey DC, Gu J, Barnhart HX, Fontana RJ, Kleiner DE, Bonkovsky HL. (2016) Amoxicillin–Clavulanate-Induced Liver Injury. Digestive Diseases and Sciences, 61: 2406-2416.
140. Björnsson E. (2016) Hepatotoxicity by Drugs: The Most Common Implicated Agents. International Journal of Molecular Sciences, 17: 224-224.
141. Wu L, Liu DQ, Kord AS. (2010) Gas-Phase Meerwein Reaction of Epoxides with Protonated Acetonitrile Generated by Atmospheric Pressure Ionizations. Journal of the American Society for Mass Spectrometry, 21: 1802-1813.
142. Meurer EC, Eberlin MN. (2006) The atmospheric pressure Meerwein reaction. Journal of Mass Spectrometry, 41: 470-476.

143. Souverain S, Rudaz S, Veuthey JL. (2004) Protein precipitation for the analysis of a drug cocktail in plasma by LC-ESI-MS. Journal of Pharmaceutical and Biomedical Analysis, 35: 913-920.
144. Uher M, Mičuda S, Kacerovský M, Hroch M. (2023) An alternative approach to validation of liquid chromatography-mass spectrometry methods for the quantification of endogenous compounds. Journal of Chromatography A, 1705.
145. Khamis MM, Adamko DJ, El-Aneed A. (2021) Strategies and Challenges in Method Development and Validation for the Absolute Quantification of Endogenous Biomarker Metabolites Using Liquid CHROMATOGRAPHY-TANDEM Mass Spectrometry. Mass Spectrometry Reviews, 40: 31-52.
146. Boere IA, Robinson DJ, De Bruijn HS, Kluin J, Tilanus HW, Sterenborg HJCM, De Bruin RWF. (2006) Protoporphyrin IX Fluorescence Photobleaching and the Response of Rat Barrett's Esophagus Following 5-aminolevulinic Acid Photodynamic Therapy. Photochemistry and Photobiology, 82: 1638-1639.
147. Agrawal K, Voggu RR, Pisek D, Becht S, Chudnovskiy R, Dufour GM, Arfvidsson C, Thomas CE. (2021) A validated surrogate analyte LC-MS/MS assay for quantification of endogenous cortisol in human whole blood. Journal of Pharmaceutical and Biomedical Analysis, 198.
148. Macours P, Cotton F. (2006) Improvement in HPLC separation of porphyrin isomers and application to biochemical diagnosis of porphyrias. Clinical Chemistry and Laboratory Medicine, 44: 1433-1440.
149. Wakamatsu Ji, Okui J, Hayashi N, Nishimura T, Hattori A. (2007) Zn protoporphyrin IX is formed not from heme but from protoporphyrin IX. Meat Science, 77: 580-586.
150. Gabeler EEE, Sluiter W, Van Hillegersberg R, Edixhoven A, Schoonderwoerd K, Statius Van Eps RG, Van Urk H. (2003) Aminolaevulinic Acid-induced Protoporphyrin IX Pharmacokinetics in Central and Peripheral Arteries of the Rat. Photochemistry and Photobiology, 78: 82-87.
151. Gabeler EEE, Sluiter W, Hillegersberg R, Edixhoven A, Schoonderwoerd K, Eps RGS, Urk H. (2003) Aminolaevulinic Acid-induced Protoporphyrin IX Pharmacokinetics in Central and Peripheral Arteries of the Rat¶. Photochemistry and Photobiology, 78: 82-87.

152. Nakanishi T, Ogawa T, Yanagihara C, Tamai I. (2015) Kinetic Evaluation of Determinant Factors for Cellular Accumulation of Protoporphyrin IX Induced by External 5-Aminolevulinic Acid for Photodynamic Cancer Therapy. Journal of Pharmaceutical Sciences, 104: 3092-3100.
153. Zhang TY, Li S, Zhu QF, Wang Q, Hussain D, Feng YQ. (2019) Derivatization for liquid chromatography-electrospray ionization-mass spectrometry analysis of small-molecular weight compounds. TrAC - Trends in Analytical Chemistry, 119.
154. Zhang X, Wang J, Wu Q, Li L, Wang Y, Yang H. (2019) Determination of kanamycin by high performance liquid chromatography. Molecules, 24.
155. Chang C. (2011) Applications of hyphenated analytical techniques in pharmaceutical industry. The University of Oklahoma
156. Kam RKT, Chan MHM, Wong HT, Ghose A, Dondorp AM, Plewes K, Tarning J. (2018) Quantitation of paracetamol by liquid chromatography-mass spectrometry in human plasma in support of clinical trial. Future Science OA, 4.
157. Idris AM, Elgorashe REE. (2011) Sequential injection chromatography against HPLC and CE: Application to separation and quantification of amoxicillin and clavulanic acid. Microchemical Journal, 99: 174-179.
158. Baietto L, D'Avolio A, De Rosa FG, Garazzino S, Michelazzo M, Ventimiglia G, Siccardi M, Simiele M, Sciandra M, Di Perri G. (2010) Development and validation of a simultaneous extraction procedure for HPLC-MS quantification of daptomycin, amikacin, gentamicin, and rifampicin in human plasma. Analytical and Bioanalytical Chemistry, 396: 791-798.
159. Bijleveld Y, de Haan T, Toersche J, Jorjani S, van der Lee J, Groenendaal F, Dijk P, van Heijst A, Gavilanes AWD, de Jonge R, Dijkman KP, van Straaten H, Rijken M, Zonnenberg I, Cools F, Nuytemans D, Mathôt R. (2014) A simple quantitative method analysing amikacin, gentamicin, and vancomycin levels in human newborn plasma using ion-pair liquid chromatography/tandem mass spectrometry and its applicability to a clinical study. Journal of Chromatography B: Analytical Technologies in the Biomedical and Life Sciences, 951-952: 110-118.
160. Terry C, Hays S. (2022) Integrating toxicokinetics into toxicology studies and the human health risk assessment process for chemicals: Reduced uncertainty, better

health protection. In: Regulatory Toxicology and Pharmacology Vol. 128, Academic Press Inc.

9. BIBLIOGRAPHY OF PUBLICATIONS

9.1. Publications related to the thesis:

[T 1]
Authors: Aliz Széles, Károly Schöll, Gábor Hirka, Katalin Monostory, Tibor Renkecz
Title: Toxicokinetic Characterization of Isopropyl Glycidyl Ether in Rat by a Validated LC-APCI-MS/MS Method Using In-Source Derivatization
Journal: Chemical Research in Toxicology
Date: Available online 5 March 2025 (Volume 38 / Issue 3, 380-391, 17 March 2025)
DOI: https://doi.org/10.1021/acs.chemrestox.4c00376
IF: 4.1

[T 2]
Authors: Aliz Széles, Károly Schöll, Gábor Hirka, Katalin Monostory, Tibor Renkecz
Title: Validation and sample bioanalysis of protoporphyrin IX in rat plasma by the surrogate matrix approach
Journal: Journal of Chromatography B
Date: Available online 22 September 2025 (Volume 1267, 15 December 2025)
DOI: https://doi.org/10.1016/j.jchromb.2025.124799
IF: 2.5

9.2. Publications not related to the thesis:

[N 1]
Authors: Csaba Kirchkeszner, Noémi Petrovics, Aliz Széles, Yelena Koshman, Bálint Sámuel Szabó, Zoltán Nyiri, Márton Novák, Tamás Rikker, Zsuzsanna Eke
Title: Comprehensive study of retention influencing gas chromatographic parameters affecting linear retention indices
Journal: Journal of Chromatography A
Date: Available online 5 June 2024 (Volume 1729, 16 August 2024)
DOI: https://doi.org/10.1016/j.chroma.2024.465052
IF: 4.0

∑IF: 10.6

9.3. Patent Applications related to the thesis:

[P 1]

Title: Identification of glycidyl ethers in biological and environmental samples using LC-APCI-MS/MS

Inventors: Aliz Széles, Katalin Monostory, Tibor Renkecz, Károly Schöll, Gábor Hirka

Hungarian patent application case number: P2500018(receipt number: 311174000-20250115-0800-000953)

PCT patent application interlocutory application number: PCT/HU2026/050002

10. ACKNOWLEDGEMENTS

I would like to express my sincere gratitude to my supervisor, Katalin Monostory, and my corporate consultant, Tibor Renkecz, for their continuous support, valuable advice, and constructive comments, which greatly contributed to the successful completion of my thesis.

I am also thankful to the managing director of Toxi-Coop Zrt., Gábor Hirka, for providing me with the opportunity for carry out the experimental work.

I would like to express my gratitude to the former and current members of the analytical laboratory at the Budapest site of Toxi-Coop Zrt., namely Tamás Péter Báldi, Gergely Becskereki, Evelin Girincsi, Lili Knyazoviczki, Tiborné Németh, Gáborné Szeker, Judit Sárszegi, and Angelika Turi for their assistance and support.

I am grateful to the members of the animal house at the Budapest site of Toxi-Coop Zrt., Tímea Csörge, Marcell Madár, Sára Sárdi and Károly Schöll, for their professional help.

I would also like to thank the members of the research group at HUN-REN Research Centre for Natural Sciences, Sámuel Balázs, Ferenc Fekete, and Károly Hegedűs, for their collaboration and support.

I am deeply thankful to my family for their constant encouragement, their loving and calm home environment, and their always positive and motivating words, which helped me greatly throughout my work.

Last but not least, I would like to express my heartfelt gratitude to my husband for everything.

11. FUNDING

This project was implemented with the support of the Ministry of Culture and Innovation from the National Research, Development and Innovation Fund, financed by the 2020-1.1.2-PIACI-KFI -2020-00021 application program.

This work was supported by the 2024–2.1.2-EKÖP-KDP2024-00002 University Research Scholarship Programme of the Ministry for Culture and Innovation from the source of the National Research, Development and Innovation Fund.

Additional funding was secured through the Semmelweis 250+ Excellence Grant.

12. APPENDIX - SUPPLEMENTARY MATERIAL

Table S 1. Chemical structures and formulas of the examined compounds.

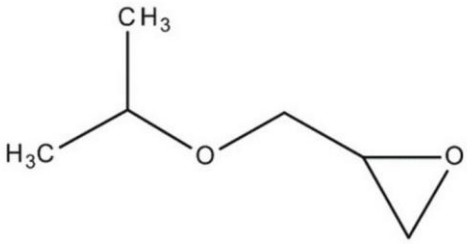	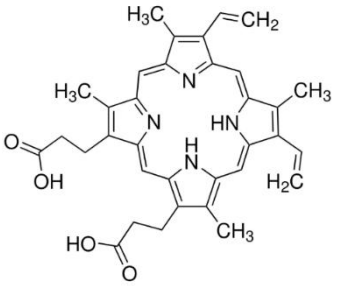
2,3-Epoxypropyl isopropyl ether $C_6H_{12}O_2$	Protoporphyrin IX $C_{34}H_{34}N_4O_4$
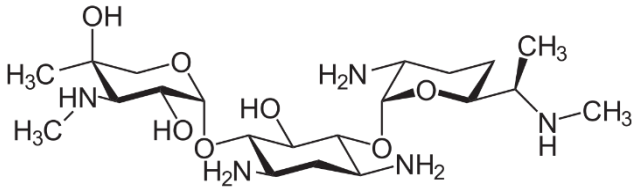	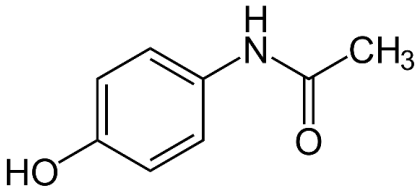
Gentamicin (C1) $C_{21}H_{43}N_5O_7$	Paracetamol [acetaminophen] $C_8H_9NO_2$
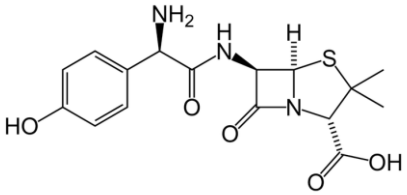	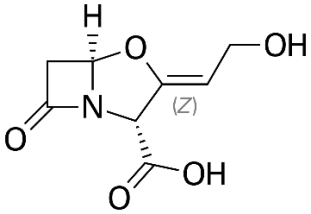
Amoxicillin $C_{16}H_{19}N_3O_5S$	Clavulanic acid $C_8H_9NO_5$
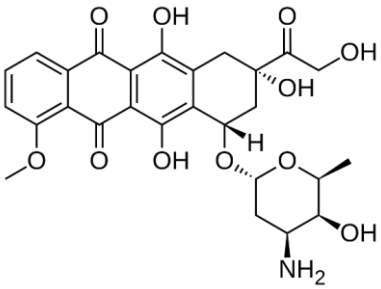	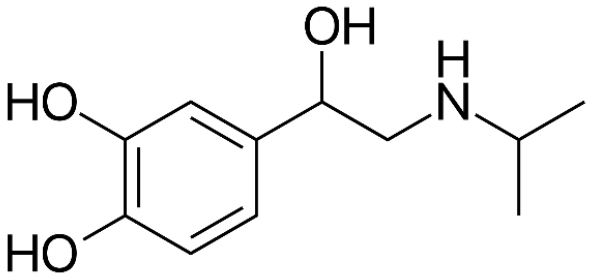
Doxorubicin $C_{27}H_{29}NO_{11}$	Isoprenaline [Isoproterenol] $C_{11}H_{17}NO_3$

Table S 2. (T 1) LC-APCI-MS/MS method for determination of IPGE in rat plasma

L C - A P C I - M S / M S c o n d i t i o n s					
Apparatus	MS: LCMS-8060 (Shimadzu, Japan) UHPLC: NexeraX2 (Shimadzu, Japan)				
Data Acquisition System	LabSolutions				
Column	YMC-Triart C18 3µm, 2.1x75 mm (Japan) with YMC-Triart C18 3µm, 2.1x10 mm guard column (Japan)				
Column temperature	30 °C		**Autosampler temperature**		10 °C
Injection volume	10 µL		**Washing solvent**		2-propanol
Run time (+ Waiting time)	5.0 min (+ 2.0 min)		**Flow rate**		0.4 mL/min
Mobile phase (Eluent)	A: 0.5% formic acid in ultrapure water B: 0.5% formic acid in acetonitrile				
Retention times [t_R]	isopropyl glycidyl ether (analyte): **2.5 min** *tert*-butyl glycidyl ether (IS): **3.2 min**				

Gradient program	**Time [min]**	**Eluent A [%]**	**Eluent B [%]**
	0.00	90	10
	0.50	90	10
	3.50	10	90
	4.00	10	90
	4.50	90	10
	5.00	90	10

Diverter valve program	**Time [min]**	**Valve position**	**Event**
	0.00	Waste	Washing
	2.00	Detector	Column effluent in-line
	4.00	Waste	Washing

Parameters for MS/MS detection	**Compounds to be monitored**	**Q1 (m/z)**	**Q3 (m/z)**	**Dwell time (ms)**	**Collision Energy (V)**
	Analyte Meerwein reaction product	157.90	116.10	100	-14.0
		157.90	74.10	100	-15.0
		157.90	57.15	100	-19.0
	IS Meerwein reaction product	172.00	57.25	100	-14.0
		172.00	74.15	100	-15.0
		172.00	116.10	100	-19.0

Scan Type:	MRM
Polarity:	Positive
Ion Source:	APCI
Interface Voltage:	4 kV
Interface Temperature:	350 °C
Desolvation Line (DL) Temperature:	300 °C

Sample Preparation
1 50 µL of rat plasma
2 10 µL of methanol
3 150 µL of 1 µg/mL IS working solution in acetonitrile
4 Vortexing
5 Centrifuging
6 Supernatant pipetting into autoinjector vials

Table S 3. (T 2) HPLC-FLD method for determination of protoporphyrin IX in rat plasma

HPLC-FLD conditions				
Apparatus	FLD: RF-20AXS (Shimadzu, Japan) HPLC: LC-20 Prominence (Shimadzu, Japan)			
Data Acquisition System	LabSolutions			
Column	ACE Ultracore SuperC18 column 2.5µm, 2.1×75 mm (UK) with Inertsil ODS-4 3µm, 1.5×10 mm guard column (Japan)			
Column temperature	30 °C		**Autosampler temperature**	10 °C
Injection volume	1 µL		**Washing solvent**	2-propanol
Run time (+ Waiting time)	8.0 min		**Flow rate**	0.5 mL/min
Mobile phase (Eluent)	A: ultrapure water containing 0.05% v/v trifluoroacetic acid B: acetonitrile containing 0.05% v/v trifluoroacetic acid			
Retention times [t_R]	Protoporphyrin IX (analyte): **5.7 min** Mesoporphyrin IX (IS): **4.2 min**			
Gradient program	**Time [min]**	**Eluent A [%]**	**Eluent B [%]**	
	0.00	60	40	
	0.50	60	40	
	5.00	30	70	
	5.50	0	100	
	6.50	0	100	
	7.00	60	40	
	8.00	60	40	
Parameters for fluorescence detection	Excitation wavelength: 405 nm Emission wavelength: 630 nm Data acquisition rate: 2 Hz Detector Temperature: 30 °C			
Sample preparation	1 50 µL of rat plasma 2 10 µL of dimethylformamide: methanol (1:1) 3 10 µL of 2 µg/mL IS working solution 4 150 µL acetonitrile 5 Vortexing 6 Centrifuging 7 Supernatant pipetting into autoinjector vials Samples are protected from light during preparation (amber vial).			
				

Table S 4. LC-ESI-MS/MS method for determination of gentamicin in rat plasma and urine

LC-ESI-MS/MS conditions					
Apparatus	MS: LCMS-8060 (Shimadzu, Japan) UHPLC: NexeraX2 (Shimadzu, Japan)				
Data Acquisition System	LabSolutions				
Column	Supel™ Carbon LC 2.7µm, 2.1 x 100 mm, column with Supel™ Carbon LC 2.7µm, 2.1 x 20 mm, guard column				
Column temperature	60 °C		**Autosampler temperature**	5 °C	
Injection volume	1 µL*		**Washing solvent**	A:B (1:1)	
Run time	7.0 min		**Flow rate**	0.35 mL/min	
Mobile phase (Eluent)	A: 5% ammonium solution in ultrapure water B: acetonitrile				
Retention times [t_R]	Gentamicin C1 (analyte): **4.6 min** Gentamicin C2 and C2a: **3.6 min** Gentamicin C1a: **3.2 min** Kanamycin (IS): **2.4 min**				
Gradient program	**Time [min]**	**Eluent A [%]**	**Eluent B [%]**		
	0.00	95	5		
	0.50	95	5		
	1.00	60	40		
	3.50	60	40		
	4.00	10	90		
	5.00	10	90		
	6.00	95	5		
	7.00	95	5		
No diverter valve program was used.					
Parameters for MS/MS detection	**Compounds to be monitored**	**Q1 (m/z)**	**Q3 (m/z)**	**Dwell time (ms)**	**Collision Energy (V)**
	Gentamicin C1 (analyte)	478.10	322.20	100	-14.0
		478.10	160.30	100	-21.0
	Gentamicin C2 and C2a	464.10	322.30	100	-15.0
		464.20	160.20	100	-22.0
	Gentamicin C1a	450.10	322.10	100	-15.0
		450.20	160.30	100	-23.0
	Kanamycin (IS)	485.00	163.15	100	-25.0
		485.00	324.20	100	-17.0
	Scan Type: MRM Polarity: Positive Ion Source: ESI Interface Voltage: 4 kV Interface Temperature: 300 °C Desolvation Line (DL) Temperature: 200 °C				
Sample Preparation	1 50 µL of rat plasma/urine 2 10 µL of ultrapure water 3 150 µL 0.1 g/mL trichloroacetic acid solution 4 10 µL of IS1µg working solution 5 Vortexing 6 1. Centrifuging 7 Supernatant pipetting into Eppendorf tubes (only plasma) 8 2. Centrifuging (only plasma) 9 Supernatant pipetting into autoinjector vials Samples are protected from light during preparation (amber vial).				

* Injection volume may be slightly modified depending on the actual sensitivity of LC-MS/MS system.

Table S 5. LC-ESI-MS/MS method for the determination amoxicillin and clavulanic acid in cell culture medium

L C - E S I - M S / M S c o n d i t i o n s						
Apparatus	MS: LCMS-8060 (Shimadzu, Japan) UHPLC: NexeraX2 (Shimadzu, Japan)					
Data Acquisition System	LabSolutions					
Column	InertSustain C18 3µm, 2.1x75 mm with Inertsil ODS-4 3µm, 1.5x10 mm guard column					
Column temperature	25 °C		**Autosampler temperature**		10 °C	
Injection volume	2 µL*		**Washing solvent**		methanol	
Run time	4.0 min		**Flow rate**		0.4 mL/min	
Mobile phase (Eluent)	A: 0.1% formic acid in ultrapure water B: 0.1% formic acid in acetonitrile					
Retention times [t_R]	Amoxicillin (analyte 1): **2.0 min** Clavulanic acid (analyte 2): **1.7 min**					
Gradient program	**Time [min]**	**Eluent A [%]**	**Eluent B [%]**			
	0.00	95	5			
	0.75	95	5			
	2.00	0	100			
	3.00	0	100			
	3.10	95	5			
	4.00	95	5			
Diverter valve program	**Time [min]**	**Valve position**	**Event**			
	0.00	Waste	Washing			
	1.20	Detector	Column effluent in-line			
	3.00	Waste	Washing			
Parameters for MS/MS detection	**Compounds to be monitored**	**Q1 (m/z)**	**Q3 (m/z)**	**Dwell time (ms)**	**Collision Energy (V)**	
	Amoxicillin (analyte 1)	363.90	223.10	100	11.0	
		363.90	206.15	100	22.0	
		636.90	320.10	100	22.0	
	Clavulanic acid (analyte 2)	197.90	82.10	100	15.0	
		197.90	108.15	100	10.0	
		197.90	136.15	100	9.0	
	Scan Type: MRM Polarity: Negative Ion Source: ESI Interface Voltage: 4 kV Interface Temperature: 300 °C Desolvation Line (DL) Temperature: 200 °C					
Sample Preparation	1 100 µL of medium sample 2 900 µL of ultrapure water 3 Vortexing					

* Injection volume may be slightly modified depending on the actual sensitivity of LC-MS/MS system.

Table S 6. LC-ESI-MS/MS method for determination of paracetamol in rat plasma

L C - E S I - M S / M S c o n d i t i o n s					
Apparatus	MS: LCMS-8060 (Shimadzu, Japan) UHPLC: NexeraX2 (Shimadzu, Japan)				
Data Acquisition System	LabSolutions				
Column	InertSustain C18 3µm, 2.1x75 mm with Inertsil ODS-4 3µm, 1.5x10 mm guard column				
Column temperature	30 °C		**Autosampler temperature**	10 °C	
Injection volume	1 µL*		**Washing solvent**	2-propanol	
Run time (+ Waiting time)	8.0 min		**Flow rate**	0.4 mL/min	
Mobile phase (Eluent)	A: 0.1% formic acid in ultrapure water B: 0.1% formic acid in methanol				
Retention times [t_R]	Paracetamol (analyte): **3.1 min** Paracetamol-d3 (IS): **3.1 min**				
Gradient program	**Time [min]**	**Eluent A [%]**	**Eluent B [%]**		
	0.00	95	5		
	4.50	60	40		
	5.00	5	95		
	6.00	5	95		
	6.50	95	5		
	8.00	95	5		
Diverter valve program	**Time [min]**	**Valve position**	**Event**		
	0.00	Waste	Washing		
	1.50	Detector	Column effluent in-line		
	5.00	Waste	Washing		
Parameters for MS/MS detection	**Compounds to be monitored**	**Q1 (m/z)**	**Q3 (m/z)**	**Dwell time (ms)**	**Collision Energy (V)**
	Paracetamol (analyte)	152.10	110.15	50	-17.0
		152.10	65.05	50	-29.0
		152.10	93.05	50	-25.0
	Paracetamol-d3 (IS)	155.10	110.15	50	-17.0
		155.10	65.05	50	-29.0
		155.10	93.05	50	-25.0
	Scan Type: MRM Polarity: Positive Ion Source: ESI Interface Voltage: 4 kV Interface Temperature: 300 °C Desolvation Line (DL) Temperature: 200 °C				
Sample Preparation	1 50 µL of rat plasma 2 10 µL of methanol 3 150 µL of 1 µg/mL IS working solution in acetonitrile 4 Vortexing 5 Centrifuging 6 Supernatant pipetting into autoinjector vials				
					

* Injection volume may be slightly modified depending on the actual sensitivity of LC-MS/MS system.

Table S 7. LC-ESI-MS/MS method for determination of doxorubicin in rat plasma

L C - E S I - M S / M S c o n d i t i o n s					
Apparatus	MS: LCMS-8060 (Shimadzu, Japan) UHPLC: NexeraX2 (Shimadzu, Japan)				
Data Acquisition System	LabSolutions				
Column	YMC-Triart C18 3µm, 2.1x75 mm with YMC-Triart C18 3µm, 2.1x10 mm guard column				
Column temperature	30 °C		**Autosampler temperature**	10 °C	
Injection volume	10 µL*		**Washing solvent**	2-propanol	
Run time (+ Waiting time)	5.0 min		**Flow rate**	0.4 mL/min	
Mobile phase (Eluent)	A: 10mM ammonium acetate 0.1% formic acid in ultrapure water B: acetonitrile				
Retention times [t_R]	Doxorubicin (analyte): **1.8 min** Daunorubicin (IS): **2.4 min**				

Gradient program	**Time [min]**	**Eluent A [%]**	**Eluent B [%]**
	0.00	70	30
	1.25	70	30
	2.00	10	90
	3.50	10	90
	4.00	70	30
	5.00	70	30

Diverter valve program	**Time [min]**	**Valve position**	**Event**
	0.00	Waste	Washing
	1.00	Detector	Column effluent in-line
	3.00	Waste	Washing

Parameters for MS/MS detection	**Compounds to be monitored**	**Q1 (m/z)**	**Q3 (m/z)**	**Dwell time (ms)**	**Collision Energy (V)**
	Doxorubicin (analyte)	544.20	397.05	100	-13.0
		544.20	379.00	100	-20.0
	Daunorubicin (IS)	528.30	321.05	100	-25.0
		528.30	381.15	100	-11.0
	Scan Type: MRM Polarity: Positive Ion Source: ESI Interface Voltage: 4 kV Interface Temperature: 300 °C Desolvation Line (DL) Temperature: 200 °C				

Sample Preparation
1 50 µL of rat plasma 2 10 µL of ultrapure water 3 150 µL of 1 µg/mL IS working solution in methanol 4 Vortexing 5 Centrifuging 6 Supernatant pipetting into autoinjector vials

* Injection volume may be slightly modified depending on the actual sensitivity of LC-MS/MS system.

Table S 8. LC-ESI-MS/MS method for determination of isoprenaline in rat plasma

L C - E S I - M S / M S c o n d i t i o n s					
Apparatus	MS: LCMS-8060 (Shimadzu, Japan) UHPLC: NexeraX2 (Shimadzu, Japan)				
Data Acquisition System	LabSolutions				
Column	Kinetex-EVO C18 2.6µm, 3x50 mm with InertSustain C18 3µm, 1.5x10 mm guard column				
Column temperature	30 °C or 25 °C		**Autosampler temperature**	4 °C	
Injection volume	3 µL*		**Washing solvent**	acetonitrile	
Run time (+ Waiting time)	6.0 min		**Flow rate**	0.4 mL/min	
Mobile phase (Eluent)	A: 0.1% trifluoroacetic acid in ultrapure water B: methanol				
Retention times [t_R]	Isoprenaline (analyte): **1.4 min** Paracetamol (IS): **2.4 min**				

Gradient program	**Time [min]**	**Eluent A [%]**	**Eluent B [%]**
	0.00	95	5
	1.50	95	5
	2.50	70	30
	3.50	10	90
	4.00	10	90
	4.50	95	5
	6.00	95	5

Diverter valve program	**Time [min]**	**Valve position**	**Event**
	0.00	Waste	Washing
	0.50	Detector	Column effluent in-line
	4.00	Waste	Washing

Parameters for MS/MS detection	**Compounds to be monitored**	**Q1 (m/z)**	**Q3 (m/z)**	**Dwell time (ms)**	**Collision Energy (V)**
	Isoprenaline (analyte)	211.90	194.20	100	-11.0
		211.90	152.10	100	-17.0
	Paracetamol (IS)	151.90	110.10	100	-12.0
		151.90	65.15	100	-26.0
		151.90	93.15	100	-21.0

Scan Type:	MRM
Polarity:	Positive
Ion Source:	ESI
Interface Voltage:	4 kV
Interface Temperature:	400 °C
Desolvation Line (DL) Temperature:	200 °C

Sample Preparation
1 50 µL of rat plasma 2 10 µL of ultrapure water 3 20 µL of 0.1 g/mL trichloroacetic acid solution 4 400 µL of 3 µg/mL IS working solution in ultrapure water 5 Vortexing 6 Centrifuging 7 Supernatant pipetting into autoinjector vials Samples are protected from light during preparation.

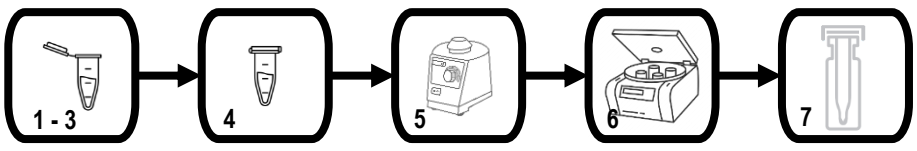

* Injection volume may be slightly modified depending on the actual sensitivity of LC-MS/MS system.

Table S 9. (T 1) LC-APCI-MS/MS method validation results of IPGE

Results of the bioanalytical method validation			
Selectivity	No interfering component was detected in the blank sample	**Stability in rat plasma stored for 4 hours at room temperature**	88.9 % (8 µg/mL) 95.7 % (0.03 µg/mL)
Linear range **Limit of quantification (LLOQ)**	0.01 – 10 µg/mL 0.01 µg/mL	**Stability in rat plasma stored for 24 hours at room temperature**	67.4 % (8 µg/mL) 45.0 % (0.03 µg/mL)
Precision of QC samples	intra-day: ≤ 10.9 % inter-day: ≤ 9.74 %	**Stability in rat plasma 3 freeze-thaw cycles**	96.6 % (8 µg/mL) 90.3 % (0.03 µg/mL)
Accuracy of QC samples	intra-day: ≤ ±12.3 % inter-day: ≤ ±6.67 %	**Stability in rat plasma at -75°C ± 10°C stored for 26 days**	91.5 % (8 µg/mL) 86.0 % (0.03 µg/mL)
Recovery (peak area)	106 % (8 µg/mL) 94.6 % (0.03 µg/mL)	**Autosampler stability after storage for 2 days (+10°C)**	≤ 5.13% [Precision] ≤ +14.0% [Accuracy]
Recovery **(peak area ratio)**	111 % (8 µg/mL) 114 % (0.03 µg/mL)	**Processed sample re-injection after storage for 3 days (+10°C)**	≤13.0 % [Precision] ≤ -13.3% [Accuracy]
Rat plasma 5× diluted QC samples **Rat plasma 15× diluted QC samples**	3.06 % [Precision] +4.2 % [Accuracy] 2.30 % [Precision] -13.3 % [Accuracy]	**Internal Standard stability (at -30 to -15°C for 49 days)**	Stock Solution ≤±8.66 % Working Solution ≤±7.01 %
Matrix effect (8 µg/mL) **Matrix effect** (0.03 µg/mL)	12.3 % [Precision] +13.7 % [Accuracy] 10.3 % [Precision] -13.0 % [Accuracy]	**Analyte stability (at -30 to -15°C for 49 days)**	Stock Solution ≤±6.25 % Working Solution ≤±2.95 %
Solutions			
Internal Standard stability (-15 to -30°C) 49 days **	Stock Solution -8.66 % Working Solution -7.01 %	**Internal Standard stability 4 hours (RT) ****	Working Solution -3.85 %
Analyte stability (-15 to -30°C) 49 days **	Stock Solution ≤ ±5.27 % Working Solution ≤ ±3.82 %	**Analyte stability 4 hours (RT) ****	Working Solution ≤ ±14.4 %

* Recovery = Processed peak area/post-spiked peak area*100

** Deviation = (Stored peak area /freshly prepared peak area*100)-100

Table S 10. (T 2) HPLC-FLD method validation results overview for protoporphyrin IX

Results of the bioanalytical method validation			
Surrogate matrix		**Authentic matrix**	
Selectivity in plasma (normal, hemolyzed, lipemic)	No interfering component was detected in the blank sample for analyte and IS.	**Selectivity in plasma (normal, hemolyzed, lipemic)**	No interfering component was detected in the blank sample for IS.
Linear range **Limit of quantification (LLOQ)**	10 – 700 ng/mL 10 ng/mL	**Parallelism**	Parallelism was verified for the surrogate matrix.
Precision of LLOQ QC samples	intra-day: ≤ 14.8 % inter-day: 10.0 %	**Precision of QC samples (low, medium, high)**	intra-day: ≤ 11.1 % inter-day: 9.29 %
Accuracy of LLOQ QC samples	intra-day: ≤ ±8.50 % inter-day: -3.43 %	**Accuracy of QC samples (low, medium, high)**	intra-day: ≤ ±10.5 % inter-day: +4.34 %
Recovery QC * *	High 93.5 % Medium 94.9 % Low 94.4 % IS 104 %	**Recovery QC** * *	High 93.1 % Medium 104 % Low 102 % IS 111 %
Matrix effect (high qc) **Matrix effect** (low qc) CV %	≤ 1.08 % [Precision] ≤ ±3.83 % [Accuracy] ≤ 8.38 % [Precision] ≤ ±5.33 % [Accuracy]	**Matrix effect** (high QC) **Matrix effect** (low QC) CV %	≤ 4.43 % [Precision] ≤ ±3.67 % [Accuracy] ≤ 4.50 % [Precision] ≤ ±3.29 % [Accuracy]
Stability in rat plasma stored for 4 hours (RT) % of the nominal concentration	90.0 % (550 ng/mL) 89.7 % (30 ng/mL)	**Stability in rat plasma stored for 4 hours (RT)** % of the nominal concentration	101 % (550 ng/mL) 88.7 % (30 ng/mL)
Stability in rat plasma stored for 24 hours (RT) % of the nominal concentration	94.0 % (550 ng/mL) 88.7 % (30 ng/mL)	**Stability in rat plasma stored for 24 hours (RT)** % of the nominal concentration	93.6 % (550 ng/mL) 98.0 % (30 ng/mL)
Stability in rat plasma 3 freeze-thaw cycle % of the nominal concentration	90.7 % (550 ng/mL) 93.9 % (30 ng/mL)	**Stability in rat plasma 3 freeze-thaw cycle** % of the nominal concentration	102 % (550 ng/mL) 102 % (30 ng/mL)
Stability in rat plasma (-75°C ± 10°C) 14 days % of the nominal concentration	99.3 % (550 ng/mL) 90.7 % (30 ng/mL)	**Stability in rat plasma (-75°C ± 10°C) 14 days** % of the nominal concentration	107 % (550 ng/mL) 95.0 % (30 ng/mL)
Autosampler stability (+10°C) 4 days LLOQ QC samples % of the nominal concentration	93.5 % (10 ng/mL)	**Autosampler stability (+10°C) 4 days QC samples** % of the nominal concentration	91.1 % (550 ng/mL) 89.7 % (30 ng/mL)
Processed LLOQ QC samples re-injection after storage for 4 days (+10°C)	4.26 % [Precision] -6.00 % [Accuracy]	**Processed QC samples re-injection after storage for 4 days (+10°C)**	≤ 8.64 % [Precision] ≤ ±6.10 % [Accuracy]
Rat plasma 2× diluted QC samples (final concentration 550 ng/mL)	4.32 % [Precision] ±0.667 % [Accuracy]	-	-
Solutions			
Internal Standard stability (-15 to -30°C) 7 days **	Stock Solution +6.21 % Working Solution +2.76 %	**Internal Standard stability 4 hours (RT)** **	Working Solution +3.23 %
Analyte stability (-15 to -30°C) 7 days **	Stock Solution ≤ ±2.58 % Working Solution ≤ ±0.573 %	**Analyte stability 4 hours (RT)** **	Working Solution ≤ ±14.0 %

* Recovery = Processed peak area/post-spiked peak area*100

** Deviation = (Stored peak area /freshly prepared peak area*100)-100

Table S 11. LC-ESI-MS/MS method validation for gentamicin

Results of the bioanalytical method validation			
Plasma matrix		**Urine matrix**	
Selectivity in plasma (normal, hemolyzed, lipemic)	No interfering component was detected in the blank sample for analyte and IS.	**Selectivity in urine (normal)**	No interfering component was detected in the blank sample for analyte and IS.
Linear range **Limit of quantification (LLOQ)**	20 – 2000 ng/mL 20 ng/mL	**Linear range** **Limit of quantification (LLOQ)**	20 – 2000 ng/mL 20 ng/mL
Precision of QC samples	intra-day: ≤ 8.95 % inter-day: 12.4 %	**Precision of QC samples**	intra-day: ≤ 13.7% inter-day: 9.31 %
Accuracy of QC samples	intra-day: ≤ ±14.8 % inter-day: -7.50 %	**Accuracy of QC samples**	intra-day: ≤ ±13.5 % inter-day: -11.0 %
Recovery QC *	High 114 % Medium 109 % Low 111 % IS 110 %	**Recovery QC** *	High 89.5 % Medium 106 % Low 91.9 % IS 102 %
Matrix effect (high qc) **Matrix effect** (low qc) CV %	≤ 2.77 % [Precision] ≤ ±8.50 % [Accuracy] ≤ 4.66 % [Precision] ≤ ±15.0 % [Accuracy]	**Matrix effect** (high qc) **Matrix effect** (low qc) CV %	≤ 4.52 % [Precision] ≤ ± 8.75% [Accuracy] ≤ 6.48 % [Precision] ≤ ±11.0 % [Accuracy]
Stability in rat plasma stored for 4 hours (RT) % of the nominal concentration	95.6 % (1600 ng/mL) 98.5 % (60 ng/mL)	**Stability in rat urine stored for 4 hours (RT)** % of the nominal concentration	106 % (1600 ng/mL) 111 % (60 ng/mL)
Stability in rat plasma stored for 24 hours (RT) % of the nominal concentration	**124 % (1600 ng/mL)** **137 % (60 ng/mL)**	**Stability in rat urine stored for 24 hours (RT)** % of the nominal concentration	102 % (1600 ng/mL) **119 % (60 ng/mL)**
Stability in rat plasma 3 freeze-thaw cycle % of the nominal concentration	95.6 % (1600 ng/mL) 109 % (60 ng/mL)	**Stability in rat urine 3 freeze-thaw cycle** % of the nominal concentration	93.1 % (1600 ng/mL) 109 % (60 ng/mL)
Stability in rat plasma (-75°C ± 5°C) 83 days % of the nominal concentration	91.3 % (1600 ng/mL) 93.5 % (60 ng/mL)	**Stability in rat urine (-75°C ± 5°C) 8 days** % of the nominal concentration	96.3 % (1600 ng/mL) 94.8 % (60 ng/mL)
Autosampler stability (+5°C) 1 day QC samples % of the nominal concentration	High 88.1 % Medium 86.8 % Low 91.3 %	**Autosampler stability (+5°C) 1 day QC samples** % of the nominal concentration	High 113 % Medium 104 % Low 95.0 %
Processed QC samples re-injection after storage for 2 days (+5°C)	9.67 % [Precision] -14.4 % [Accuracy]	**Processed QC samples re-injection after storage for 2 days (+5°C)**	10.4 % [Precision] -8.83 % [Accuracy]
Rat plasma 10× diluted QC samples (final concentration 1600 ng/mL)	6.63 % [Precision] ±6.88 % [Accuracy]	**Rat urine 10× diluted QC samples** (final concentration 1600 ng/mL)	7.74 % [Precision] ±1.25 % [Accuracy]
Solutions			
Internal Standard stability (-15 to -30°C) 7 days **	Stock Solution -1.37% Working Solution +13.7 %	**Internal Standard stability 4 hours (RT)** **	Working Solution -4.12 %
Analyte stability (-15 to -30°C) 7 days **	Stock Solution ≤ ±7.29 % Working Solution ≤ ±14.1 %	**Analyte stability 4 hours (RT)** **	Working Solution ≤ ±14.9 %

* Recovery = Processed peak area/post-spiked peak area*100

** Deviation = (Stored peak area /freshly prepared peak area*100)-100

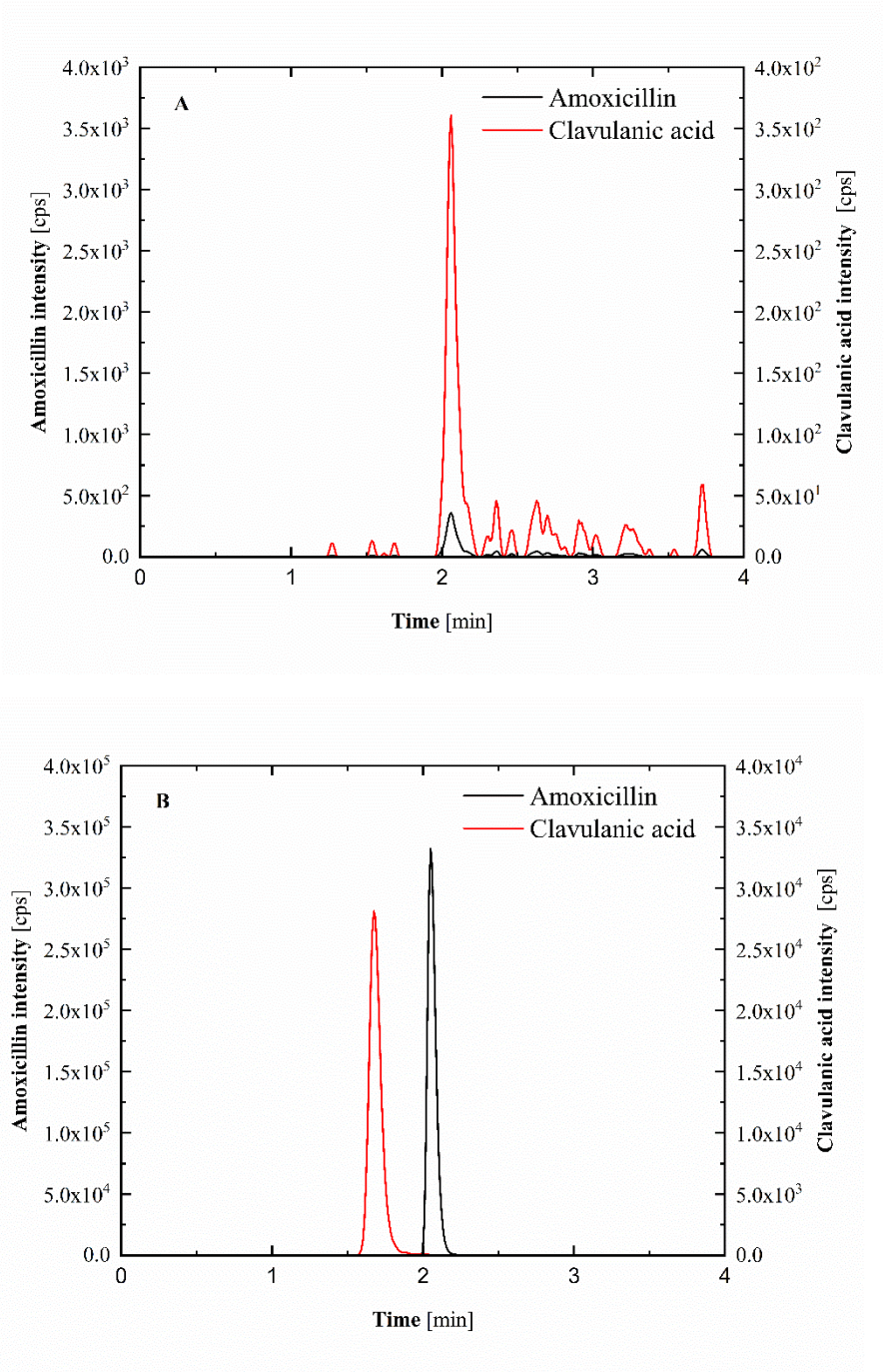

Figure S 1.

A) Representative MRM chromatograms of amoxicillin [363.90 → 223.10 m/z] and clavulanic acid [197.90 → 82.10 m/z] in blank sample: amoxicillin (black), clavulanic acid (red).

B) Representative MRM chromatograms of amoxicillin [363.90 → 223.10 m/z] and clavulanic acid [197.90 → 82.10 m/z] in medium QC sample: amoxicillin (black), clavulanic acid (red).

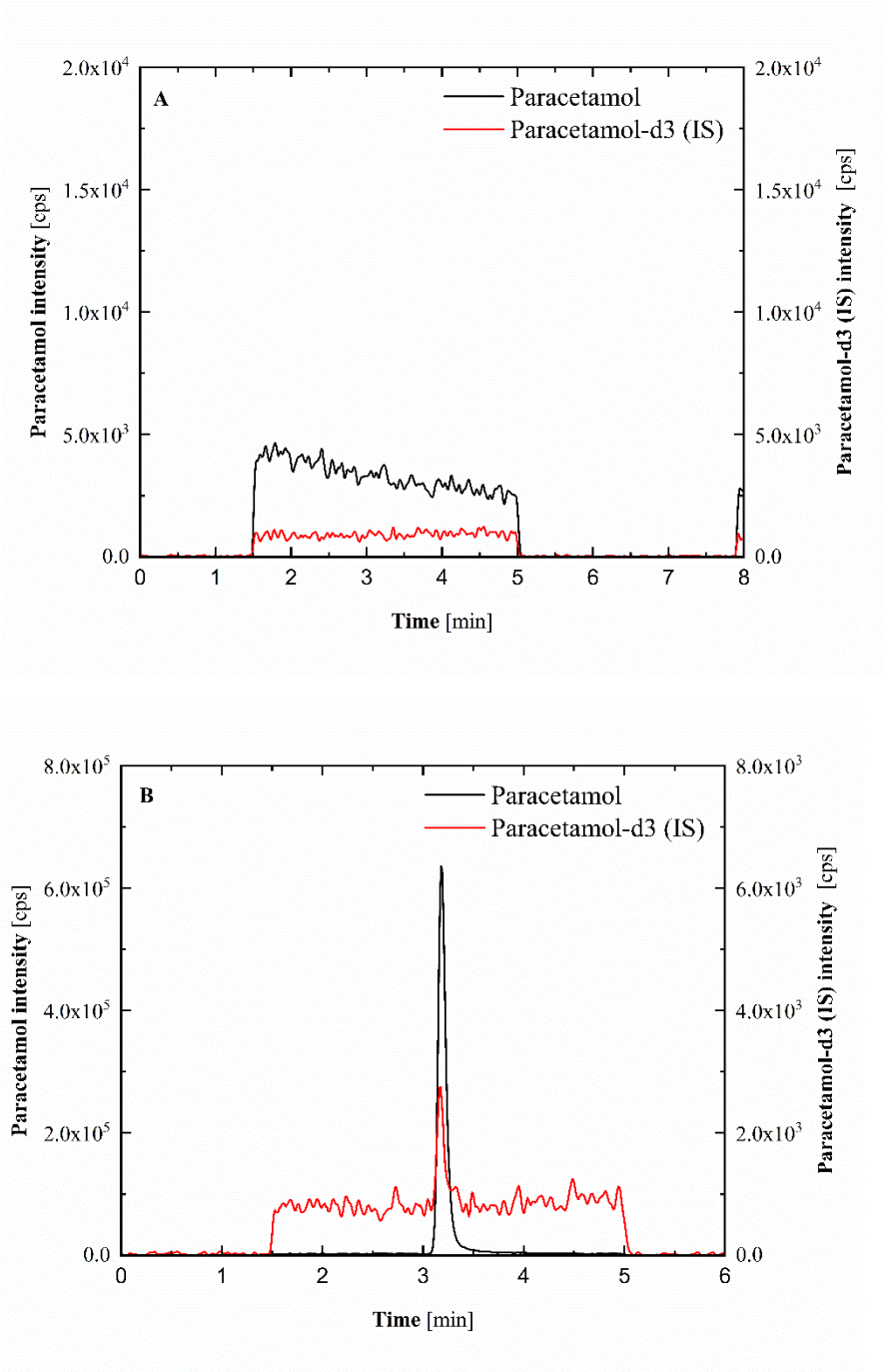

Figure S 2.

A) Representative MRM chromatograms of paracetamol [152.10 → 110.15 m/z] and IS [155.10 → 110.15 m/z] in blank sample: paracetamol (black), IS (red).

B) Representative MRM chromatograms of paracetamol [152.10 → 110.15 m/z] and IS [155.10 → 110.15 m/z] in medium QC sample: paracetamol (black), IS (red).

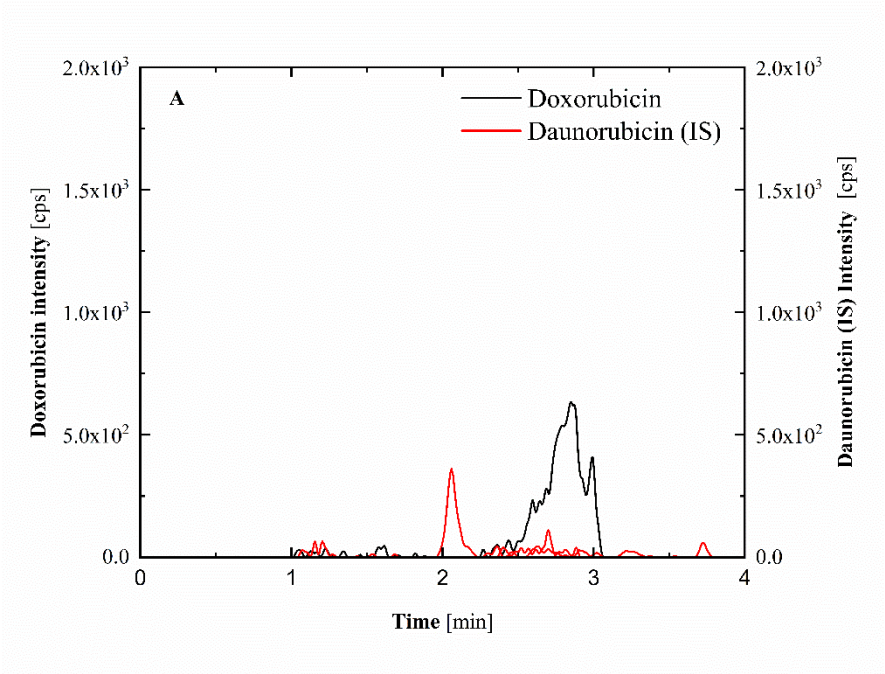

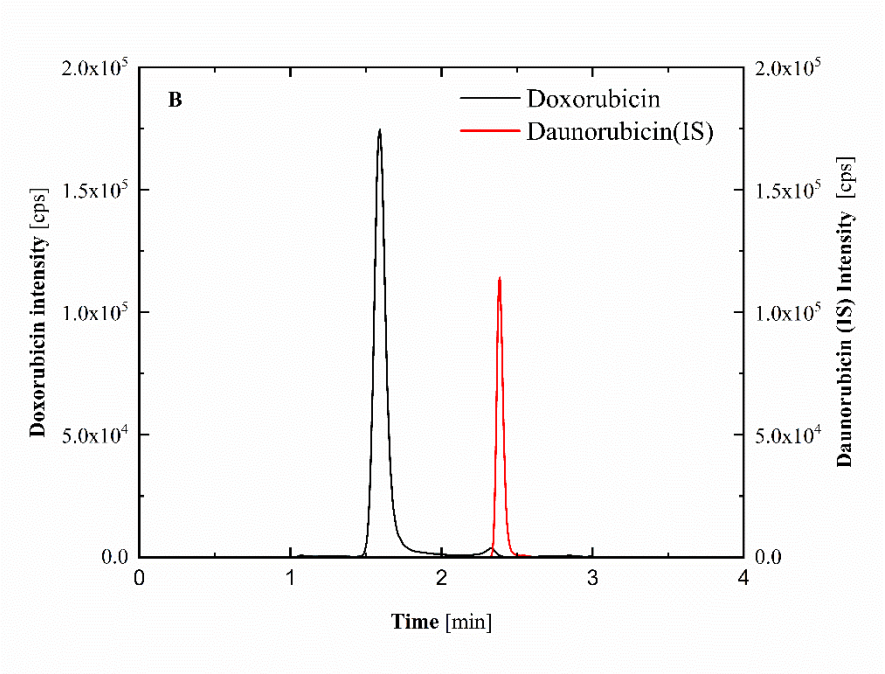

Figure S 3.

A) Representative MRM chromatograms of doxorubicin [544.20 → 397.05 m/z] and IS [528.30 → 321.05 m/z] in blank sample: doxorubicin (black), IS (red).

B) Representative MRM chromatograms of doxorubicin [544.20 → 397.05 m/z] and IS [528.30 → 321.05 m/z] in medium QC sample: doxorubicin (black), IS (red).

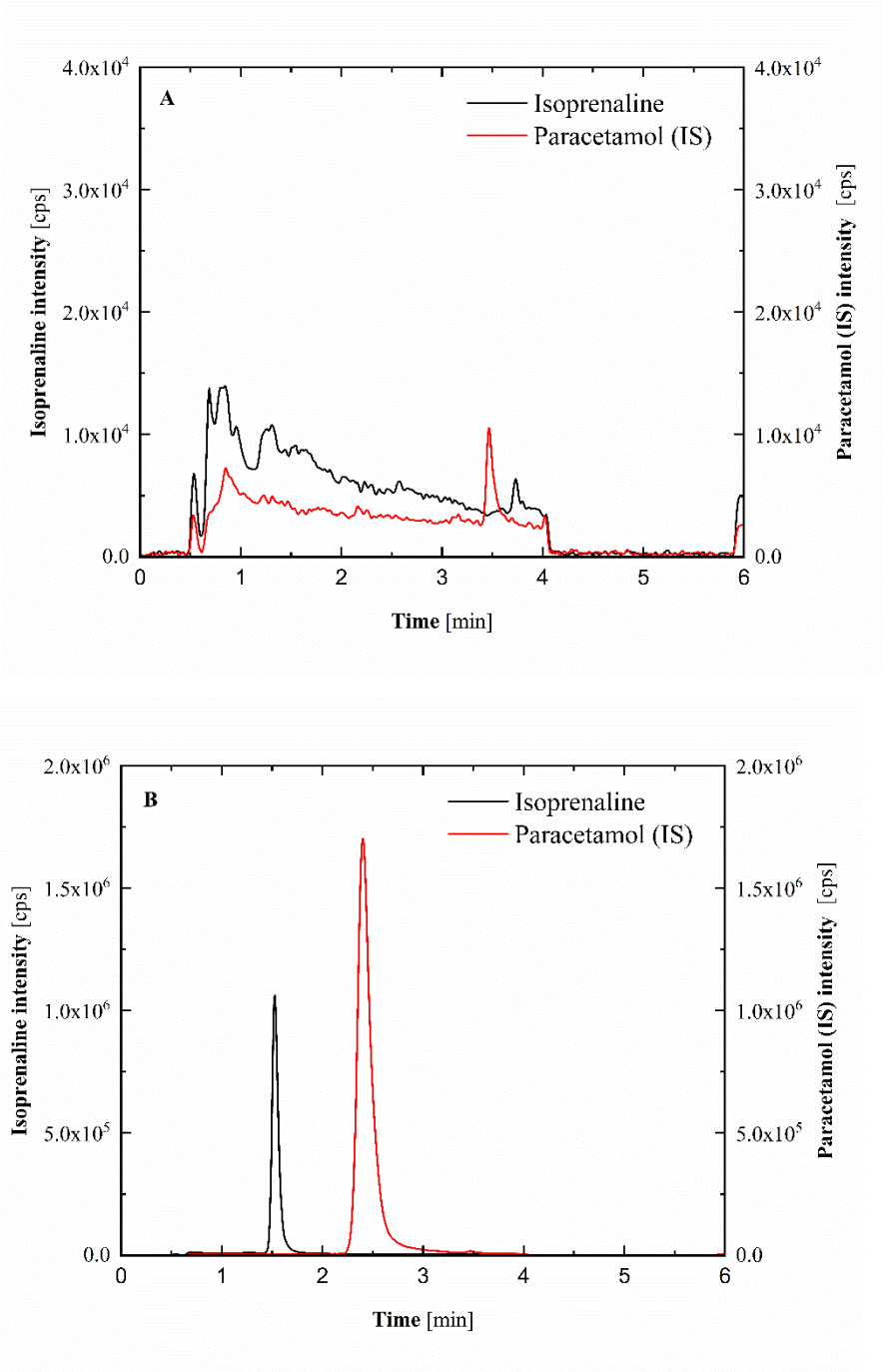

Figure S 4.

A) Representative MRM chromatograms of isoprenaline [211.90 → 194.20 m/z] and IS [151.90 → 110.10 m/z] in blank sample: isoprenaline (black), IS (red).

B) Representative MRM chromatograms of isoprenaline [211.90 → 194.20 m/z] and IS [151.90 → 110.10 m/z] in medium QC sample: isoprenaline (black), IS (red).

Table S 12. Inter- and intra-day accuracy and precision results of paracetamol in plasma

Nominal concentration of paracetamol [µg/mL]	Intra-day *(n = 6)*		Inter-day *(n = 18)*	
	Accuracy (%)	Precision (CV%)	Accuracy (%)	Precision (CV%)
80 (QCH)	3.80	11.7	1.25	6.80
16 (QCM)	6.30	13.4	0.0	8.85
0.3 (QCL)	10.0	8.60	6.67	6.95
0.1 (QCLLOQ)	-19.0	17.3	0.0	8.09

Mean accuracy: within ±20% for the LLOQ and within ±15% for all other concentrations

Precision: ≤20 CV% for the LLOQ and ≤15 CV% for all other concentrations

Table S 13. Inter- and intra-day accuracy and precision results of amoxicillin and clavulanic acid in medium

Nominal concentration of amoxicillin [mg/mL]	Intra-day *(n = 6)*		Inter-day *(n = 18)*	
	Accuracy (%)	Precision (CV%)	Accuracy (%)	Precision (CV%)
4 (QCH)	-10.8	1.12	-8.00	2.50
0.4 (QCM)	-2.00	1.38	-.0750	1.63
0.15 (QCL)	-2.00	1.45	-1.33	1.61
Nominal concentration of clavulanic acid [mg/mL]	Intra-day *(n = 6)*		Inter-day *(n = 18)*	
	Accuracy (%)	Precision (CV%)	Accuracy (%)	Precision (CV%)
4 (QCH)	-10.3	0.809	-7.75	2.20
0.4 (QCM)	1.03	1.60	1.25	1.88
0.15 (QCL)	2.22	2.30	-0.667	2.42

Mean accuracy: within ±20% for the LLOQ and within ±15% for all other concentrations

Precision: ≤20 CV% for the LLOQ and ≤15 CV% for all other concentrations

Table S 14. Inter- and intra-day accuracy and precision results of doxorubicin in plasma

Nominal concentration of doxorubicin [ng/mL]	Intra-day *(n = 6)*		Inter-day *(n = 18)*	
	Accuracy (%)	Precision (CV%)	Accuracy (%)	Precision (CV%)
800 (QCH)	-14.5	2.30	-6.86	6.21
300 (QCM)	-13.5	2.85	-4.59	7.20
3 (QCL)	-2.54	12.4	0.190	10.4
1 (QCLLOQ)	-8.66	8.77	-2.27	9.84

Mean accuracy: within ±20% for the LLOQ and within ±15% for all other concentrations

Precision: ≤20 CV% for the LLOQ and ≤15 CV% for all other concentrations

Table S 15. Inter- and intra-day accuracy and precision results of isoprenaline in plasma

Nominal concentration of isoprenaline [ng/mL]	Intra-day *(n = 6)*		Inter-day *(n = 18)*	
	Accuracy (%)	Precision (CV%)	Accuracy (%)	Precision (CV%)
800 (QCH)	-6.75	9.45	-2.25	7.82
80(QCM)	-3.75	7.96	1.25	6.32
15 (QCL)	-7.80	11.3	-4.73	8.17
5 (QCLLOQ)	10.5	8.49	1.50	10.0

Mean accuracy: within ±20% for the LLOQ and within ±15% for all other concentrations

Precision: ≤20 CV% for the LLOQ and ≤15 CV% for all other concentrations